

การหาค่าเหมาะที่สุดของกระบวนการพ่นแห้งในการเตรียมยาผงสำหรับสูดของพอลิ (ดี,แอล-แล็ก
ไทด์-โค-กลัยโคไลด์) ที่บรรจุยาไรแฟมพิซิน



นางสาวเพ็ญภา เสาร์คำ

ศูนย์วิทยทรัพยากร
จุฬาลงกรณ์มหาวิทยาลัย

วิทยานิพนธ์นี้เป็นส่วนหนึ่งของการศึกษาตามหลักสูตรปริญญาเภสัชศาสตรมหาบัณฑิต

สาขาวิชาเภสัชอุตสาหกรรม ภาควิชาวิทยาการเภสัชกรรมและเภสัชอุตสาหกรรม

คณะเภสัชศาสตร์ จุฬาลงกรณ์มหาวิทยาลัย

ปีการศึกษา 2553

ลิขสิทธิ์ของจุฬาลงกรณ์มหาวิทยาลัย

OPTIMIZATION OF SPRAY-DRYING PROCESS FOR
PREPARATION OF INHALABLE RIFAMPICIN-LOADED POLY(d,l-
LACTIDE-CO-GLYCOLIDE) POWDER

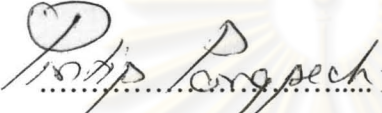
Miss Phennapha Saokham



A Thesis Submitted in Partial Fulfillment of the Requirements
for the Degree of Master of Science in Pharmacy Program in Industrial Pharmacy
Department of Pharmaceutics and Industrial Pharmacy
Faculty of Pharmaceutical Sciences
Chulalongkorn University
Academic Year 2010
Copyright of Chulalongkorn University

Thesis Title OPTIMIZATION OF SPRAY-DRYING PROCESS FOR
PREPARATION OF INHALABLE RIFAMPICIN-LOADED
POLY(D,L-LACTIDE-CO-GLYCOLIDE) POWDER
By Miss Phennapha Saokham
Field of Study Industrial Pharmacy
Thesis Advisor Associate Professor Poj Kulvanich, Ph.D.
Thesis Co-advisor Jittima Chatchawalsaisin, Ph.D.


Accepted by the Faculty of Pharmaceutical Sciences, Chulalongkorn
University in Partial Fulfillment of the Requirements for the Master's Degree



..... Dean of the Faculty of Pharmaceutical Sciences
(Associate Professor Pintip Pongpech, Ph.D.)

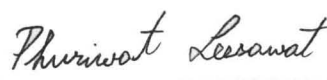
THESIS COMMITTEE


..... Chairman
(Associate Professor Kraisi Umprayn, Ph.D.)


..... Thesis Advisor
(Associate Professor Poj Kulvanich, Ph.D.)


..... Thesis Co-advisor
(Jittima Chatchawalsaisin, Ph.D.)


..... Examiner
(Narueporn Sutanthavibul, Ph.D.)


..... Examiner
(Associate Professor Phuriwat Leesawat, Ph.D.)

เพ็ญญา เสาร์คำ : การหาค่าเหมาะที่สุดของกระบวนการพ่นแห้งในการเตรียมผงสำหรับสูดของพอลิ (ดี,แอล-แล็กไทด์-โค-กลัยโคไลด์) ที่บรรจุยาไรแฟมพิซิน. (OPTIMIZATION OF SPRAY-DRYING PROCESS FOR PREPARATION OF INHALABLE RIFAMPICIN-LOADED POLY(D,L-LACTIDE-CO-GLYCOLIDE) POWDER) อ.ที่ปรึกษาวิทยานิพนธ์หลัก : รศ.ภก.ดร.พจน์ กุลวานิช, อ.ที่ปรึกษาวิทยานิพนธ์ร่วม : อ.ภญ.ดร.จิตติมา ชัชวาลย์สายสิทธิ์ 120 หน้า.

งานวิจัยนี้ใช้การออกแบบการทดลองแบบแฟกตอเรียลในการศึกษาอิทธิพลของปัจจัยทางกระบวนการพ่นแห้งที่มีผลต่อคุณสมบัติของผงสำหรับสูดของพอลิ (ดี,แอล-แล็กไทด์-โค-กลัยโคไลด์) ที่บรรจุยาไรแฟมพิซิน โดยศึกษาผลของ inlet drying temperature, aspirator control, pump setting และ nozzle gas flow setting ที่มีต่อปริมาณผงแห้งที่ได้, ขนาดอนุภาค, ปริมาณไรแฟมพิซินที่ถูกกักเก็บในผงแห้ง และ เปอร์เซ็นต์การละลายของไรแฟมพิซินในผงแห้งที่ 20 นาทีแรก พบว่า ปัจจัยที่มีผลต่อผงสำหรับสูดของพอลิ(ดี,แอล-แล็กไทด์-โค-กลัยโคไลด์) ที่บรรจุยาไรแฟมพิซินมากที่สุด คือ nozzle gas flow setting และพบว่า การเปลี่ยนแปลงปัจจัยทางกระบวนการพ่นแห้งที่ศึกษาไม่ส่งผลต่อปริมาณไรแฟมพิซินที่ถูกกักเก็บในผงแห้งและเปอร์เซ็นต์การละลายของไรแฟมพิซินในผงแห้งที่ 20 นาทีของผงพอลิ (ดี,แอล-แล็กไทด์-โค-กลัยโคไลด์) ที่บรรจุยาไรแฟมพิซิน จากนั้นทำการหาค่าเหมาะที่สุดของกระบวนการพ่นแห้งในการเตรียมผงพอลิ (ดี,แอล-แล็กไทด์-โค-กลัยโคไลด์) ที่บรรจุยาไรแฟมพิซิน โดยใช้การศึกษาพื้นผิวคอบสอง ในการศึกษาค้นคว้าใช้การทดลองแบบ central composite face centered (CCF) ในการสร้างสมการที่ใช้การทำนายและสร้างพื้นผิวคอบสอง พบว่า สภาวะในการเตรียมผงพอลิ (ดี,แอล-แล็กไทด์-โค-กลัยโคไลด์) ที่บรรจุยาไรแฟมพิซินที่เหมาะสมในการเตรียมในผงพอลิ (ดี,แอล-แล็กไทด์-โค-กลัยโคไลด์) ที่บรรจุยาไรแฟมพิซินเป็นผงแห้งสำหรับสูด คือ inlet temperature 55 องศาเซลเซียส, aspirator control 100 เปอร์เซ็นต์, pump setting 10 เปอร์เซ็นต์ และ nozzle gas flow setting 33 มิลลิเมตร ซึ่งทำให้ได้ผงแห้งพอลิ (ดี,แอล-แล็กไทด์-โค-กลัยโคไลด์) ที่บรรจุยาไรแฟมพิซินที่มีขนาดอนุภาค 3.1997 ไมครอนและปริมาณผงแห้งที่ได้เป็น 33.4517 เปอร์เซ็นต์โดยน้ำหนัก จากนั้นนำข้อมูลความสัมพันธ์ของกระบวนการพ่นแห้งที่มีต่อปริมาณผงแห้งพอลิ (ดี,แอล-แล็กไทด์-โค-กลัยโคไลด์) ที่บรรจุยาไรแฟมพิซินที่ได้และขนาดอนุภาคของพอลิ (ดี,แอล-แล็กไทด์-โค-กลัยโคไลด์) ที่บรรจุยาไรแฟมพิซินมาศึกษา design space ของกระบวนการพ่นแห้ง โดยกำหนดให้ปริมาณผงแห้งที่ได้ต้องไม่น้อยกว่า 30 เปอร์เซ็นต์และขนาดอนุภาคของผงแห้งอยู่ระหว่าง 3-5 ไมครอนซึ่งเป็นขนาดอนุภาคที่สามารถนำส่งผงแห้งเข้าสู่ปอดได้ พบว่า กระบวนการพ่นแห้งที่ศึกษานี้สามารถผลิตผงแห้งพอลิ (ดี,แอล-แล็กไทด์-โค-กลัยโคไลด์) ที่บรรจุยาไรแฟมพิซินเพื่อนำไปใช้เป็นยาสูดพ่นได้

ภาควิชา.....วิทยาการเกษตรกรรมและเกษตรอุตสาหกรรม
สาขาวิชา.....เกษตรอุตสาหกรรม
ปีการศึกษา.....2553

ลายมือชื่อนิสิต เพ็ญญา เสาร์คำ
ลายมือชื่อ อ.ที่ปรึกษาวิทยานิพนธ์หลัก พจน์
ลายมือชื่อ อ.ที่ปรึกษาวิทยานิพนธ์ร่วม จิตติมา

5076582933 : MAJOR INDUSTRIAL PHARMACY

KEYWORDS: RIFAMPICIN/ INHALATION/ DESIGN OF EXPERIMENT/
SPRAY DRYING/ DESIGN SPACE

PHENNAPHA SAOKHAM: OPTIMIZATION OF SPRAY-DRYING
PROCESS FOR PREPARATION OF INHALABLE RIFAMPICIN-
LOADED POLY(D,L-LACTIDE-CO-GLYCOLIDE) POWDER. THESIS
ADVISOR: ASSOCIATE PROFESSOR POJ KULVANICH, Ph.D.,
THESIS CO-ADVISOR: JITTIMA CHATCHAWALSAISIN, Ph.D., 120
pp.

In this study, a 2⁴ full factorial design with center points was performed to investigate the influence of the following independent spray drying process parameters: inlet drying temperature (°C), aspirator control (%), pump setting (%) and nozzle gas flow setting (mm) on the properties of poly(D,L-lactide-co-glycolide) (PLGA) microparticles loaded with rifampicin. The rifampicin-PLGA microparticles were obtained from spraying the mixed solution in a mini spray dryer. The process yield, mass median diameter, entrapment efficiency and dissolution at first 20 min were evaluated. First, the nozzle gas flow setting was found to be a main effect on the studied responses followed by inlet drying temperature, aspirator control, and pump setting. Full factorial design with center points revealed all process parameters did not effect on entrapment efficiency and dissolution at 20 min. This study aims to optimize the operating conditions to maximize process yield of inhalable rifampicin-PLGA microparticles. The optimal operation conditions thus were evaluated by response surface methodology. Central composite face centered (CCF) design showed quadratic model were adequate. A statistical optimization of the spray drying process parameters gave recommended conditions by using inlet drying temperature 55 °C, aspirator control 100%, pump setting 10% and nozzle gas flow setting 33 mm. This experiment would to generate a process yield of 33.4517 % by weigh of microparticles with a mass median diameter of 3.1997 µm. Finally, the data form design experiment was used in defining the process design space. The design space has been evaluated considering the significant process parameters and the relative influence of each variable on the desired characteristics of PLGA microparticles loaded rifampicin: process yield not less than 30% and mass median diameter between 3 and 5 µm. It is shown that spray drying method can produce rifampicin-PLGA microparticles that high productivity and compliance of inhalable powder specifications.

Department: Pharmaceutics and Industrial Pharmacy

Field of study: Industrial Pharmacy

Academic year: 2010

Student's signature: พัทธนา

Advisor's signature: [Signature]

Co-advisor's signature: [Signature]

ACKNOWLEDGEMENTS

I would like to express my deep and sincere gratitude to my thesis advisor for his meaningful advice, invaluable guidance helpfulness, and warmest encouragement throughout my investigation. His patience, kindness and understanding are also deeply appreciated.

My deep appreciation is to Jittima Chatchawalsaisin, Ph.D., my thesis co-advisor, her kind assistance, helpful consultation and everlasting support.

I wish to acknowledge The Thailand Research Fund (TFR) and Graduate School of Chulalongkorn University for the financial support on this research project.

In addition, I would like to acknowledge the friendship, assistance and encouragement of my friends, colleagues and the staff of the Department of Pharmaceutics and Industrial Pharmacy and other person whose names have not been mentioned.

Ultimately, I would like to express my heartfelt and truly thank to my beloved parents and family for their care, endless love, cheerfulness, understanding and encouragement throughout my life.

ศูนย์วิทยทรัพยากร
จุฬาลงกรณ์มหาวิทยาลัย

CONTENTS

	Page
ABSTRACT (THAI).....	iv
ABSTRACT (ENGLISH).....	v
ACKNOWLEDGEMENTS.....	vi
CONTENTS.....	vii
LIST OF TABLES.....	ix
LIST OF FIGURES.....	xi
LIST OF ABBREVIATIONS.....	xiii
CHAPTER I INTRODUCTION.....	1
CHAPTER II LITERATURE REVIEW.....	4
Spray dried powder for inhalation.....	4
Experimental design and Response surface methodology.....	14
Design space.....	23
CHAPTER III EXPERIMENTAL.....	27
Materials.....	27
Equipments.....	28
Methods.....	28
Preparation of PLGA microspheres loaded with rifampicin.....	28
Characterization of rifampicin-PLGA microparticles.....	29
Design of experiment (DOE).....	36
Statistical analysis.....	40
Optimization.....	42
Design space.....	42
CHAPTER IV RESULTS AND DISCUSSION.....	44
Morphology of the rifampicin-PLGA loaded microparticles.....	44
Full factorial design.....	45

	Page
Central composite face centered (CCF) design	71
Optimization of spray drying condition	87
Design space	91
CHAPTER V CONCLUSIONS	97
REFERENCES	99
APPENDICES	103
Appendix A	104
Appendix B	105
Appendix C	107
Appendix D	111
BIOGRAPHY	115



ศูนย์วิทยทรัพยากร
จุฬาลงกรณ์มหาวิทยาลัย

LIST OF TABLES

Table		Page
1	Particle properties and their effects on respiratory drug delivery..	5
2	The deposition mechanism of various particle size ranges.....	7
3	The measurement of aerodynamic properties.....	13
4	Full factorial designs of two, three and four factors.....	19
5	Analysis of variance table for the least squares fit of a model that is in its parameters.....	21
6	Experimental factors and their level in full factorial design.....	37
7	Experiment design of two-level full factorial design.....	38
8	Experimental factors and their level in central composite face centered design.....	38
9	Experiment design of central composite face centered design.....	39
10	The factor effect estimate of linear model for process yield.....	45
11	ANOVA table for the linear model for process yield.....	46
12	The factor effect estimate of mass median diameter.....	53
13	ANOVA table for the linear model for mass median diameter.....	54
14	The factor effect estimate of entrapment efficiency from a 2 ⁴ factorial design.....	61
15	The factor effect estimate of entrapment efficiency from a 2 ³ factorial design.....	62
16	ANOVA table for the selected linear model of entrapment efficiency.....	62
17	The factor effect estimate of dissolution at 20 min.....	67
18	ANOVA table for the selected factorial model of dissolution at 20 min.....	68
19	ANOVA table for the reduced quadratic model of process yield.....	72
20	ANOVA table for the reduced quadratic model of mass median diameter.....	79
21	Criteria for optimization of spray drying parameters.....	87

Table		Page
22	Optimum spray drying parameters and their predicted response variables.....	88
23	Predicted values and their 95% prediction interval of responses for the optimum condition number 1.....	90
24	Actual response value and their bias for optimum condition number 1.....	91
25	Summary of design space for rifampicin-PLGA microparticles.....	92
26	Accuracy data of percentage of analytical recovery of rifampicin in entrapment efficiency.....	108
27	Precision data of rifampicin in entrapment efficiency.....	109
28	Accuracy data of percentage of analytical recovery of rifampicin in dissolution condition.....	112
29	Precision data of rifampicin in dissolution condition.....	113

LIST OF FIGURES

Figure		Page
1	The steps of spray drying process.....	8
2	Effect of leucine on fine particle fraction (FPF).....	10
3	The guideline for designing an experiment.....	15
4	The key steps in design space identification.....	23
5	Contour plot of dissolution and friability for granulation process.....	25
6	Proposed designs space which comprised of the overlap region of ranges for friability and or dissolution.....	26
7	A schematic diagram of modified flow through dissolution apparatus.....	33
8	Scanning electron microphotographs of rifampicin-PLGA microspheres.....	44
9	Main effect plot of nozzle gas flow rate for process yield on the linear model.....	48
10	Interaction plots of linear model for process yield.....	49
11	Residual analysis of the linear model for process yield.....	50
12	Contour plots and surface plots of linear model for process yield.....	51
13	Main effect plots of linear model for mass median diameter.....	56
14	Interaction plots of linear model for mass median diameter.....	57
15	Residual analysis of linear model for mass median diameter.....	58
16	Contour plots and surface plots of linear model for mass median diameter.....	59
17	Main effect plots of first-model for entrapment efficiency.....	64
18	Interaction plot between inlet drying temperature and aspirator control of first-model for entrapment efficiency.....	64
19	Residual analysis of linear model for entrapment efficiency.....	65
20	Contour plot and surface plot between inlet drying temperature and aspirator control interaction of linear model for entrapment efficiency.....	66
21	Interaction plot between inlet drying temperature and pump setting of linear model for dissolution at 20 min.....	69
22	Residual analysis of linear model for dissolution at 20 min.....	69

Figure		Page
23	Contour plot and surface plot between inlet drying temperature and pump setting interaction of linear model for dissolution at 20 min.....	79
24	Main effect plot of nozzle gas flow rate for process yield on quadratic model.....	74
25	Residual analysis of the quadratic model for process yield.....	74
26	Interaction plots of quadratic model for process yield.....	75
27	Contour plots and surface plots of quadratic model for the process yield.....	76
28	Residual analysis of quadratic model for mass median diameter.....	81
29	Main effect plots of quadratic model for mass median diameter.....	82
30	Interaction plots of quadratic model for mass median diameter.....	83
31	Contour plots and surface plots of quadratic model for mass median diameter.....	84
32	Design spaces of inhalable rifampicin-PLGA microparticles when inlet drying temperature is at low level.....	92
33	Design spaces of inhalable rifampicin-PLGA microparticles when inlet drying temperature is at medium level.....	94
34	Design spaces of inhalable rifampicin-PLGA microparticles when inlet drying temperature is at high level.....	95
35	The chromatogram of standard rifampicin in entrapment efficiency.....	107
36	The chromatogram of PLGA in chloroform.....	107
37	Calibration curve for entrapment efficiency condition.....	110
38	The chromatogram of standard rifampicin in dissolution condition.....	111
39	The chromatogram of phosphate buffer saline pH 7.4.....	111
40	Calibration curve for dissolution condition.....	114

List of abbreviations

%	Percentage
µm	Micrometer (s)
µl	Microliter (s)
°C	Degree celcius (centrigrade)
CV	Coefficient of variation
CCF	Central composite face centered
DOE	Design of experiment
et al.	<i>et alii</i> , 'and others'
HPLC	High performance liquid chromatographic
mg	Milligram (s)
min	Minute (s)
ml	Milliliter (s)
mm	Millimeter (s)
MMD	Mass median diameter
pH	The negative logarithm of the hydrogen ion concentration
PLGA	Poly(d,l-lactide-co-glycolide)
RSD	Relative standard deviation
SD	Standard deviation
SEM	Scanning electron microscopy

CHAPTER I

INTRODUCTION

Tuberculosis (TB) is a chronic infectious disease caused by *Mycobacterium tuberculosis* (MTB). The primary target site of infection is the lung in the respiratory tract and finally hides in alveolar macrophages. According to the World Health Organization (WHO), in 2009, there were an estimated 8.9-9.9 million incident cases of TB, 9.6-13.3 million prevalent cases of TB, 1.1-1.7 million deaths from TB among HIV-negative people and an additional 0.45-0.62 million TB deaths among HIV-positive people (*Global Tuberculosis Control: a short update to the 2009 report*, 2009).

Rifampicin is the first choice drug in the treatment guideline of tuberculosis. But the long term oral administration and combination with other antibiotics cause the increasing toxic side effect especially hepatotoxicity when use with pyrazinamide, one of the first choice drug for TB treatment. Thus, the new administration route which increase local therapeutic effect and reduce systemic side effect is required (Suarez et al., 2001b, Suarez et al., 2001a).

Recently, the inhalable rifampicin loaded microspheres were produced for the new drug delivery system which is directly target to alveolar macrophages. The particles will deposit in the periphery of the lung due to their aerodynamic size, where they will be ingested by alveolar macrophages, and slow dissolution will occur (Suarez et al., 2001b). Poly (d,l-lactide-co-glycolide), PLGA, is used as a carrier for delivery to alveolar macrophages because it is a biocompatible and biodegradable polymer, which is hydrolytically degraded into the non-toxic oligomers or monomers; lactic acid and glycolic acid (Tomoda and Makino, 2007).

In previous paper, there are two techniques that used to produce PLGA microparticles loaded with rifampicin, solvent evaporation and spray drying method. Compare with solvent evaporation method, spray drying technique is a one step

continuous process that is an attractive manufacturing process in the industry (Maltesen et al., 2008). Since the late 1970's, the solvent evaporation method was fully developed. Many studies have been conducted to evaluate the process and to understand the effect of individual formulation parameters on the final product (Suarez et al., 2001b). But, on the other hand, the effect of spray drying process on the powder has not been investigated.

Design of experiment (DOE) is a well-known method for understanding the effect of formulation or process parameters on the interested product properties. Traditional development of pharmaceutical formulation is based on a time and energy consuming approach of changing one variable at a time while keeping other variables constant. DOE technique allows testing of a large number of variables in a few experimental runs. Many studies have used DOE to investigate the effect of the spray drying process parameters on particle characteristics (Maltesen et al., 2008, Zidan et al., 2007). However, these studies have not studied the effect of process parameters on rifampicin-loaded PLGA microparticles preparation.

Nowadays, the role of design spaces has become very important for pharmaceutical industries. To define the design space, the process characterization studies are performed. One of the tools that evaluate the influence of process parameters is design of experiment. Sundaram et al., 2010 demonstrated the utility of DOE approach for development of lyophilization process but there is no publication that shows the DOE approach for spray drying process.

The aim of this study was to investigate the influence of spray drying process parameters on properties of PLGA microspheres loaded with rifampicin through DOE through full factorial design and identify a design space of the spray drying parameters.

Objectives of this study were:

1. To study the effect of spray drying process parameters for preparation of PLGA microspheres loaded with rifampicin powder.

2. To evaluate the optimum values of spray drying process parameters for inhalable rifampicin-PLGA microparticle through design of experiment (DOE).
3. To identify a design space of spray drying parameters in order to get the inhalable rifampicin-PLGA microparticles.



ศูนย์วิทยทรัพยากร
จุฬาลงกรณ์มหาวิทยาลัย

CHAPTER II

LITERATURE REVIEW

Spray dried powder for inhalation

Spray drying is widely used manufacturing process which uses the solution or suspension to dry particles. The technology has been applied in many areas, including pharmaceutical industries. In this field, spray drying is used to produce particles that form the dry dosage forms for parenteral, nasal, or pulmonary delivery, and are administered as suspensions, powders or aerosols.

In recent years, the inhalation dosage technology has been focused on 2 parallel development pathways that are development of novel inhaler devices and improvement of existing inhalation formulation. One of the improvements is about particle engineering. It has been used to design complex particles which meet the requirement of respiratory particles. Those particles must be able to stabilize the active pharmaceutical ingredient and provide physical stability for the dosage form on storage. They must have adequate powder flow properties and dispersibility and suitable aerodynamic properties. Moreover narrow particle size distribution, optimal bioavailability and sustained release may be concern.

Requirements of respiratory particles

For pulmonary delivery, the requirements of respiratory particles are very important because the lower micron-size range, solid particles can exhibit different aerosolization behaviors. These properties depend on the complex nature of interparticulate interactions, type of formulation and inhalation device, inhalation flow rate and breathing pattern (Chow et al., 2007). Table 1 lists the physical parameters influencing the therapeutic performance of respiratory formulations.

The desirable powder characteristics include high fine particle fraction (FPF) and emitted dose (ED), high dose consistency and uniformity, and independence of the type of device and inhalation flow rate. Thus, the suitable aerodynamic particles

should have a narrow particle size distribution and should be aerosolizable at low aerodynamic dispersion forces. In addition, the requirement of physical and chemical stability implies that storage must not have a significant effect on the drug's physical form (such as polymorphism), particle size distribution and/or dose content uniformity.

Table 1 Particle properties and their effects on respiratory drug delivery (Chow et al., 2007)

Particle Characteristics	Effects on Formulation
Solid state	Physical and chemical stability, bioavailability, toxicity
Particle size distribution, shape, porosity/density	Aerosolization behavior, in vitro and in vivo deposition profiles, bioavailability
Surface morphology, energetics and electrostatics, powder bulk density, agglomeration, cohesiveness, flow properties	Powder handling, inhaler filling, dose metering, storage stability, shelf-life, dose uniformity and consistency
Co-formulation/blending	Dose uniformity, modified or extended release, toxicity

1. Particle aerodynamic diameter (Chow et al., 2007)

The aerodynamic diameter, d_A , is defined as the diameter of a unit density sphere which settles through air with a velocity equal to the particle in question. This diameter defines the mechanism of particle deposition in the respiratory system. In previous review, it has been that the aerodynamic diameter (d_A) depends on the particle Reynolds number, Re , as well as the particulate properties (geometric size, shape and density) and can be calculated by semi-empirical models. The well-known relationship depicted by equation below, through applicable at the Stokes flow regime of $Re < 0.1$, can be used to estimate the aerodynamic diameter:

$$d_A \cong d_V \sqrt{\frac{\rho}{x\rho_0}} \quad (1)$$

where d_V is the volume-equivalent diameter, ρ_0 is the unit density of spherical calibration spheres, ρ is the particle density and x is the dynamic shape factor, defined as the ratio of the drag force on a particle to the drag force on the particle volume-equivalent sphere at the same velocity. Thus d_A can be reduced by decreasing the volume-equivalent particle diameter (d_V), reducing the particle density (ρ) and/or increasing the particle dynamic shape factor (x).

Traditionally, reduction of d_V has been effected by micronization, usually by jet-milling but spray drying decrease of both particle density and size. Theoretically, a smaller d_A can also be obtained with non-spherical shape particles, such as platelets, rods or fibers because the x value can be as high as 10.

2. Interparticulate interactions

The principal adhesive forces between particles consist of van der Waals forces, electrostatic forces, and the surface tension of adsorbed liquid layers. These forces are influenced by physicochemical properties, including particle density and size distribution, particle morphology (shape, habit, surface texture), and surface composition (including adsorbed moisture) (Hickey, 2004). In addition, interparticulate forces effects aggregation, flowability, and dispersibility (defined by the balance of the aerodynamic stress and the aggregate strength) of the particles. Thus, it can be concluded that the aggregation strength (Chow et al., 2007), flow properties, and disperse properties are influenced by physicochemical properties of the inhalation particles. For example, it has been shown that irregular particle produced by spray drying can significantly lower the interparticulate interaction and increase the FPF (Chow et al., 2007). Because the irregular particles have a smaller contact area than the smooth particles of the same d_V and the interparticulate forces are also reduced.

3. Particle deposition, uptake and dissolution

The particle size and morphology effect on aspects of drug delivery to lung, including deposition, dissolution and clearance mechanism (Chow et al., 2007). Different size of particle show differ deposition mechanism.

Particle size below 5 μm can be distributed into smaller airways and the diameter range between 3 to 5 μm is used for local treatment by gravitational sedimentation mechanism. With the same mechanism, the particle size range between 0.5 to 3 μm can be deposited into capillary-rich alveolar airspace for systemic action and local effect. Moreover, submicron particles (aerodynamic diameter < 0.5 μm) can be exhaled, if they are not aggregated and/or if insufficient time is available for their migration to the lung walls. Therefore slow deep breathing and breath holding help deposition, too. It has been suggested that fiber shape particles can be more efficiently deposited on the respiratory wall because of the particle interception. The particle that are not solubilized immediately may adhere to the epithelial lining and be cleared more slowly so large volume diameter particles such as porous particles show a better bioavailability than solid particles (of the same volume diameter) because of their improved dissolution rate or their size-related delaying effect on the phagocytic clearance. Compared with micron particles, nanoparticles are deposited in much greater number concentration than microparticles so their phagocytic clearance can be delayed. In addition, poor water-soluble nanoparticles have higher overall dissolution rate, so the dissolution rate and phagocytic clearance may lead to improve bioavailability for nanosize range drug particle.

Table 2 The deposition mechanism of various particle size ranges

Aerodynamic diameter (μm)	Deposition Mechanism
> 5	Inertial impaction
3 - 5	Gravitational sedimentation
0.5 - 3	Gravitational sedimentation
< 0.5	Brownian diffusion

4. Solid-state form and structure

The aerodynamic performance and dissolution behavior also affect the physical stability and solid-state structure. As a rule, crystalline particles are required because they are the most stable form to avoid solid-state transitions. Moreover, their non-spherical shapes have low interparticulate interaction and thermodynamic stable.

For therapeutic effect of inhaled particles, amorphous form may be considerable for rapid dissolution and absorption, stabilizing biological molecules and/or formulating drugs into sustained-release biodegradable polymeric microspheres or microcapsules (Chow et al., 2007). Some drugs, especially therapeutic protein, cannot be prepared in crystalline forms. Large porous particles are normally amorphous. Many composite particles, containing drugs and other excipients, are also amorphous or partly crystalline.

Following from the above discussion, optimal physicochemical properties for efficient pulmonary drug delivery particles should be have aerodynamic particle size below 5 μm with narrow size distribution, low surface energy and charge, non-spherical morphology, low density (or high porosity) and high physical and chemical stability.

Spray dried powder process and control

Spray drying technology is a common practice of powder preparation for a wide range of drugs. It can be used to deliver particles to the lung via a dry powder inhaler (DPI). A typical spray drying process consists of 4 steps that show in figure 1.

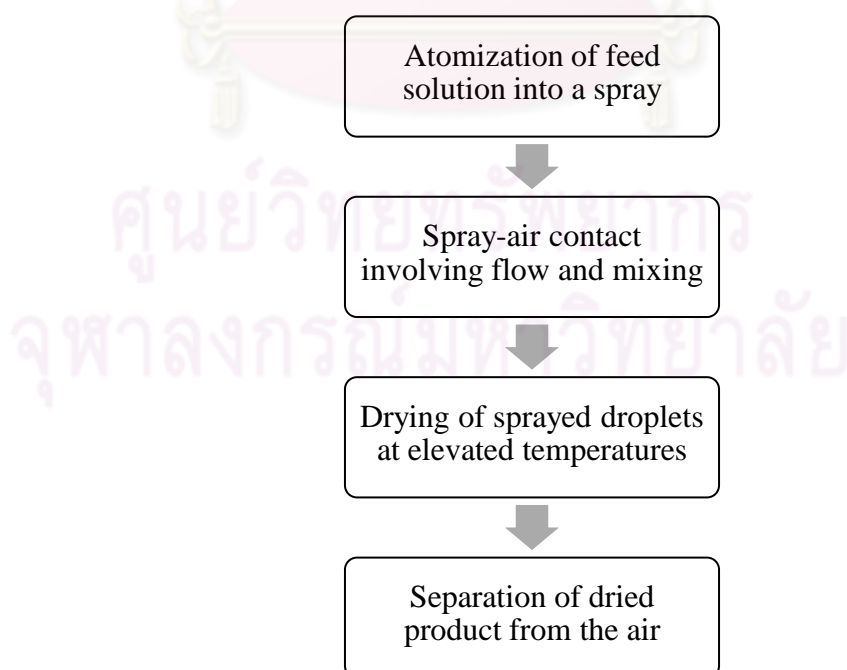


Figure 1 The steps of spray drying process

The benefits of this technology are simple technique, easy to scale up and operate, and able to produce composite materials. However, particle production for inhalation using this technology is a relatively new field with only a single marketed (Exubera® — mannitol-stabilized insulin)(Chow et al., 2007). One reason is the suitable size for inhalation (below 5 μm) is very limit to reduce and intensive process optimization is required. Moreover, the physical instability and thermal degradation must be concerned.

The properties of the spray dried powders are controlled by both spray drying process parameter and formulation parameters (Chougule et al., 2007). The operating parameters such as atomization pressure, atomization nozzle type, powder collection technique, droplet drying time and rate, feed rate, airflow, and drying temperature including inlet temperature and outlet temperature. For example, it has been that plain-jet air-blast atomizers shows smaller initial droplet size than ultrasonic atomizer. Larger particles can be prepared by using a larger nozzle orifice, smaller atomization airflow and a higher feed concentration (Elversson and Fureby., 2005). Particle shape and morphology can be controlled by varying the feed solution or adjusting the outlet drying temperature (Gilani et al., 2005). Varying feed concentration and atomization rate show the different degrees of particle surface corrugation (Chow et al., 2007). The spray drying parameters, feed rate and pressure of the compressed air had little impact on spray dried powder properties but the inlet temperature tended to make the heavier powder (Bosquillon et al., 2001). In certain case, optimal humidity of drying gas can afford desirable densities or aerodynamic diameters of particles. Too high or too low moisture content of drying gas tend to obtain higher tapped density, higher mass median aerodynamic diameter (MMAD), and lower volume median geometric diameter of the particles (Chen et al., 2005).

Another factor that affects the spray dried powder properties is formulation parameter. The powder composition and solution properties most greatly affected particle characteristics (Bosquillon et al., 2001). Such adding albumin charged particle morphology and varying its concentration had little impact on size and density but removing from the formulation led to heavier powders as well as to a important decrease in fine particle fraction (FPF) and emitted dose (ED)(Bosquillon et al., 2001). The type of sugar or polyol such as mannitol incorporated did not affect the

particle size, density and overall morphology of the resultant powders (Bosquillon et al., 2001). Blending spray dried powders with suitable excipients (lactose, mannitol or sodium chloride) can also improve aerodynamic behavior of those powders. Adding common excipients such as lactose and tween 20 into the feed solution can cause the formulation of rougher surface particle (Chow et al., 2007). Adding leucine led to increase on FPF shown in figure 2. Moreover, the proportion of solvent system and its viscosity influenced the aerodynamic properties. It has been shown that decreasing the concentration of the excipients and ethanol in the feed solution decreased powder density but did not affect particle size (Bosquillon et al., 2001, Rabbani and Se, 2005). High viscosity of the feed solution showed low yield, high density and small particle size (Rabbani and Se, 2005). Chitosan, hyaluronic acid and starch are natural polymer of choice for pulmonary sustained release formulation (Chow et al., 2007) so incorporation of those polymers into feed solution affect the drug release properties. For example, increasing molecular weight of chitosan increased duration of turbutaline sulfate spray dried powders (Learoyd et al., 2008). In addition, synthetic polymer such as poly L-lactic acid (PLA) and poly D,L-lactic/glycolic acid (PLGA) are also used (Takashima et al., 2007).

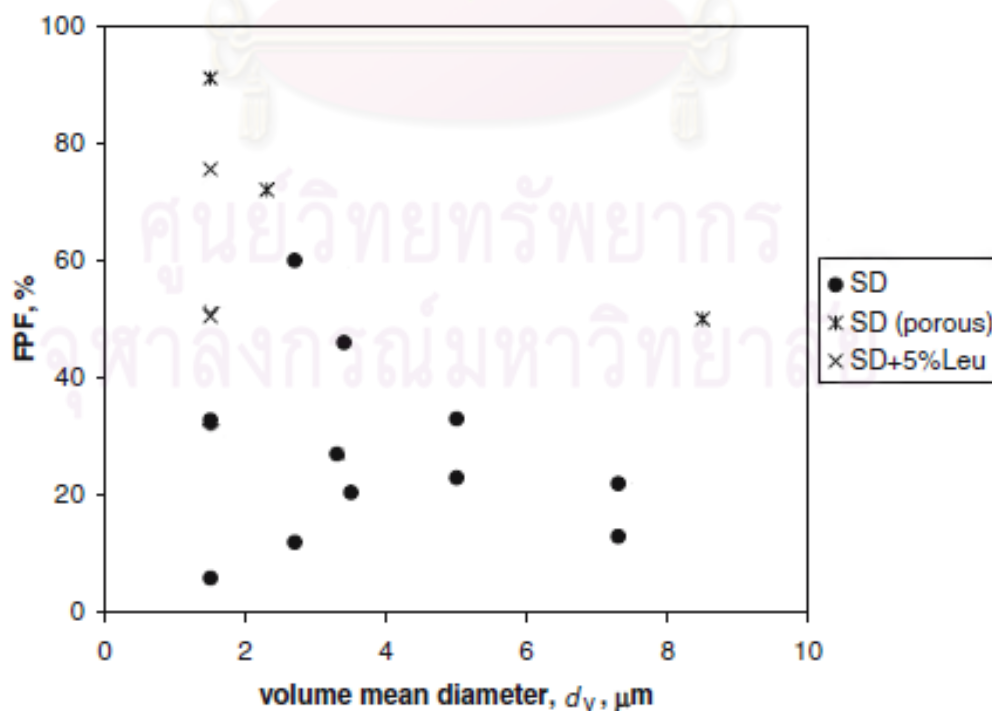


Figure 2 Effect of leucine on fine particle fraction (FPF)(Chow et al., 2007)

Other common approach for sustained release inhalation is dispersion of nano- and microparticles of hydrophilic ionized drugs within the hydrophobic matrix of microspheres. Such formulation can use a multi-step process to suspend those particles in a polymer solution and then spray drying. For example, the drug is first emulsified into an organic phase with up to 10% surfactant, and the resulting w/o emulsion is frozen with liquid nitrogen, followed by freeze drying. The nanoparticles produced are then dispersed into a non-solvent of the drug containing hydrophobic excipients, such as glyceryl behenante, tripalmitin and hydrogenated palm oil. Finally, dispersion containing nanoparticles and hydrophobic excipients was sprayed to dry powders (Cook et al., 2005). Silmiliary, PLGA polymer was used in the spray drying process to coat particles of a model protein (β -glucuronidase, previously co-spray dried with mannitol or lactose) to develop a tuberculosis vaccine formulation (Chow et al., 2007).

Other common approach for sustained release inhalation is dispersion of nano- and microparticles of hydrophilic ionized drugs within the hydrophobic matrix of microspheres. Such formulation can use a multi-step process to suspend those particles in a polymer solution and then spray drying. For example, the drug is first emulsified into an organic phase with up to 10% surfactant, and the resulting w/o emulsion is frozen with liquid nitrogen, followed by freeze drying. The nanoparticles produced are then dispersed into a non-solvent of the drug containing hydrophobic excipients, such as glyceryl behenante, tripalmitin and hydrogenated palm oil. Finally, dispersion containing nanoparticles and hydrophobic excipients was sprayed to dry powders (Cook et al., 2005). Silmiliary, PLGA polymer was used in the spray drying process to coat particles of a model protein (β -glucuronidase, previously co-spray dried with mannitol or lactose) to develop a tuberculosis vaccine formulation (Chow et al., 2007).

Other approach to preparation of composite particles or sustained release utilizes liposomal formulations (Chow et al., 2007). The drug-loaded liposomes are prepared using a thin film technique followed by high-pressure homogenization and co-spray drying with an excipient (such as lactose, sucrose, or mannitol) and anti-adherent (e.g. glycine).

Evaluation of spray dried powder

The aerodynamic behavior of spray dried powder consists of particle size and morphology, particle density and porosity, aerodynamic diameter (or mass median aerodynamic diameter; MMAD), fine particle fraction (FPF), and emitted dose (ED). In addition, geometric diameter such as mass median diameter (MMD) or volume median diameter (VMD), polymorphism, and moisture content of resultant powder may be considered (Table 3). To obtain optimal aerosol properties, the evaluation of the spray dried powder must be concerned.



Table 3 The measurement of aerodynamic properties

Aerodynamic properties	Measurement	Reference
Particle shape and morphology	Scanning electron microscopy (SEM)	Bosquillon et al., 2001, Chan et al., 1997, Cook et al., 2005, Learoyd et al., 2008, Lucas et al., 1999, Rabbani and Se, 2005,
	Confocal laser scanning microscopy	Vanbever et al., 1999 Cook et al., 2005, Shama et al., 2004
Particle density	Tapped density meter	Bezerraa et al., 2008, Vanbever et al., 1999
	Jolting volumeter	Lucas et al., 1999
	Tamping volumeter	Learoyd et al., 2008
Particle size (geometric diameter)	Coulter multisizer	Bosquillon et al., 2001
	Laser diffraction	Chan et al., 1997, Cook et al., 2005, Learoyd et al., 2008, Lundstedt et al., 1998, Rabbani and Se, 2005
	Photon correlation spectroscopy	Shama et al., 2004
Particle size	Andersan Cascade impactor	Bosquillon et al., 2001, Shama et al., 2004, Vanbever et al., 1999
Aerodynamic diameter	Twin stage impactor	Rabbani and Se, 2005
Fine particle fraction (FPF)	Multiple stage liquid impinger	Chan et al., 1997, Learoyd et al., 2008
Emitted dose (ED)	Glass twin stage impinge	Lucas et al., 1999
Polymorphism	X-ray powder diffraction	Chan et al., 1997
	Differential scanning calorimetry (DSC)	Cook et al., 2005, Learoyd et al., 2008
	Thermogravimetric analysis (TGA)	Learoyd et al., 2008
Moisture content	Thermogravimetric analysis (TGA)	Chan et al., 1997

Experimental design and Response surface methodology

Experimental design and optimization are useful tools to determine the problems that happen during development and production state. It seems that if experiments are performed randomly the result obtained will also be random. Thus, the planning will be obtained. The traditional experimental planning needed many an effort and time. The most efficient way for increasing the value of the research and decreasing process development time is experimental designs.

Experimental design

Experimental design can be defined as the strategy for setting up experiments in such a manner that the information required is obtained as efficiently and precisely as possible (Lewis et al., 1999). The main purpose of experimentation is to study the relationship between parameters on the response or the properties of the product. This information is used to achieve or develop the required product in the future.

Before using the statistical approach in designing and analyzing an experiment, it is necessary to clearly understand the procedure of experimental design. Montgomery suggested the guidelines for designing an experiment as show on figure 3 (Montgomery, 2009). If the pre-experimental planning is done, the next step is choosing an appropriate experimental design. Choice of design involves consideration of sample size (number of replicates), selection of a suitable run order for the experimental trials and determination of whether or not blocking or other randomization restrictions are involved (Montgomery, 2009). It is important to keep the experimental objectives in mind while design selection. Each design have recommended to use in different purpose, for example, if the objective is to screening parameters, the suitable design may be fractional factorial design or Plackette-Burman design instead of using full factorial design. To set up the appropriate experiments, all designs required the minimum and maximum values for each factor that defines the investigated experimental domain.

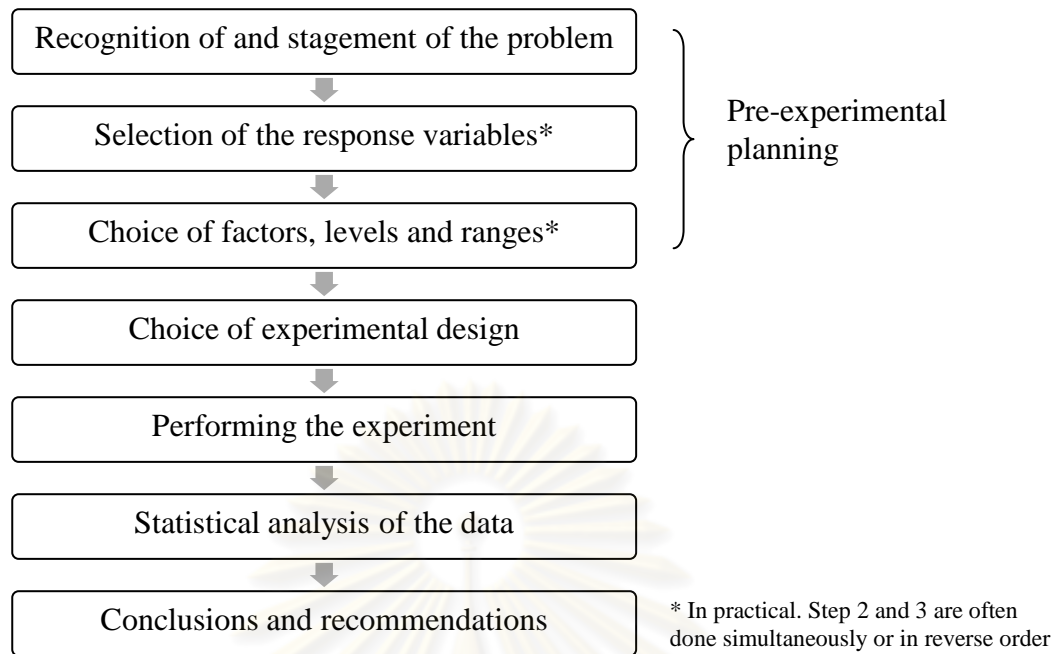


Figure 3 The guidelines for designing an experiment

Response surface methodology

Response surface methodology, or RSM, is a collection of mathematical and statistical techniques useful for the modeling and analysis of problems in which a response is influenced by several variables (Montgomery, 2009). The purpose of this method is to obtain a model for predict the values of the interested responses. Thus, the first step in RSM is to find an appropriate function that shows the relationship between response (y) and the set of independent variables (x_n). The second step is mapping the response over the experimental domain to form a surface. This map is performed by describing the responses in term of a function of variables which are normally quantitative and continuous (Lewis et al., 1999). This function can be visualized using contour plots and surface plots.

There are two considerations imply certain conditions for using response surface modeling (Lewis et al., 1999)

- The strategy is often sequential. The simplest model is initially performed. If that model was found inadequate for describing the response, the higher order model would need.

- The number of factors studied is usually between 2 and 5 and in any case should not exceed 7.

In most response surface methodology problem, a low-order polynomial is firstly employed. If the response is well modeled by a linear function, then the approximating function is the first-order model. But if there is curvature in the system, a polynomial of high degree must be used, such as the second-order model (Montgomery, 2009).

The method of least squares is used to estimate the coefficient of the parameters in the predicting model. After perform the suitable model, the response surface analysis is performed using the fitted surface. If the fitted surface is an adequate approximation of the true response function, then analysis of the fitted surface will be approximately equivalent to analysis of the actual system (Montgomery, 2009).

Response surface design

The experimental designs for fitting response surfaces are called response surface designs. The suitable experimental designs facilitate fitting and analyzing response surfaces. So the important point is choosing experimental design. When selecting a response, some of the features of a desirable design are as follow (Montgomery, 2009):

- Provides a reasonable distribution of data points (and hence information) throughout the region of interest
- Allows model adequacy, including lack of fit, to be investigated
- Allows experiments to be performed in blocks
- Allows designs of higher order to be built up sequentially
- Provides an internal estimate of error
- Provides precise estimates of the model coefficients
- Provides a good profile of the prediction variance throughout the experimental design
- Provides reasonable robustness against outliers or missing values
- Does not require a large number of run

- Does not require too many levels of the independent variables
- Ensures simplicity of calculation of the model parameters

These features are sometimes conflicting, so judgement must often be applied in design selection.

The most commonly used designs are the full factorial fractional designs and the more complex central composite design. Although the factorial designs can be used to determine response surface but only linear response surface show in all factors. Thus, factorial designs are normally used to determine which investigated factors are significant or insignificant on interested responses.

Designs of fitting the first-order model

In a first-order design the influences of all factors and their interaction on the interested responses are investigated. The statistical model of a two-level factorial design is linear (as shown below).

$$y = \beta_0 + \sum_{i=1}^k \beta_i X_i + \sum \sum_{i < j} \beta_{ij} X_i X_j + \epsilon \quad (2)$$

where y is the response, β_0 is the constant, β_i is the parameter estimate, X is the independent parameter and ϵ is the residual error. This first-order designs includes the 2^k factorial and fractions of the 2^k series in which main effects are not aliased with each other (Montgomery, 2009). The low and high levels of the k factors are usually coded to -1 and +1 level, respectively. If the factors are investigated at two levels, a factorial design will consist of 2^2 experiments. In table 4 the full factorial designs for 2, 3 and 4 experimental factors are shown.

The 2^k design dose not effort as estimate of the experimental error unless some runs are replicated (Montgomery, 2009). To estimate the experimental error and allow for checking the adequacy of the first-order model, replication at the center is performed. These consist of n_c replicates run at the point $X_i = 0$ ($i = 1, 2, \dots, k$)

After fitting data to first-order model by least square, the adequacy of the model should be investigated (Montgomery, 2009). The 2^k design with center points allows the experimenter to

- Obtain an estimate of error ($\hat{\sigma}^2$) that calculate through the equation below

$$\hat{\sigma}^2 = \frac{\sum y_n^2 - \frac{(\sum y_n)^2}{n}}{n-1} \quad (3)$$

where n is number of center points and y_n is value of the response

- Check for interaction (cross-product terms) inter model

Interaction between the variables would be represented by the coefficient of the cross-product terms.

- Check for quadratic effects (curvature)

When \bar{y}_F is the average of the runs at the factorial points and \bar{y}_C is the average of n_C runs at the center point, the difference between \bar{y}_F and \bar{y}_C define a curvature of the model. If $\bar{y}_F - \bar{y}_C$ is small, there is no quadratic curvature. On the other hand, if $\bar{y}_F - \bar{y}_C$ is large, then quadratic curvature is present. The single-degree-of-freedom sum of square associated with the null hypothesis, $H_0: \beta_{11} + \beta_{22} = 0$, is

$$SS_{Pure\ quadratic} = \frac{n_F n_C (\bar{y}_F - \bar{y}_C)^2}{n_F + n_C} \quad (4)$$

where n_F and n_C are the number of points in the factorial portion and the number of center points, respectively.

The first-order models represent surfaces or hyper surfaces more or less warped owing to the maxima or minima and are called first order model. If the interaction term is negligible the response surface is planar. The more important the interaction term, the greater is the degree of twisting the planar response surface experiences. If the linear model is not sufficient to represent the experimental data, more experiments can be performed in addition (Ferreira et al., 2007).

Another first-order design is the simplex design. This design is a regularly sided figure with $k + 1$ vertices in k dimensions. Thus, the simplex design for $k = 2$ is an equilateral triangle, and it is a regular tetrahedron for $k = 3$ (Montgomery, 2009).

Table 4 Full factorial designs of two, three and four factors (The levels of the factors are gives by – (minus) for low level and + (plus) for high level)(Lundstedt et al., 1998)

Experimental Number	Two factors		Three factors			Four factors			
	X_1	X_2	X_1	X_2	X_3	X_1	X_2	X_3	X_4
1	-	-	-	-	-	-	-	-	-
2	+	-	+	-	-	+	-	-	-
3	-	+	-	+	-	-	+	-	-
4	+	+	+	+	-	+	+	-	-
5			-	-	+	-	-	+	-
6			+	-	+	+	-	+	-
7			-	+	+	-	+	+	-
8			+	+	+	+	+	+	-
9						-	-	-	+
10						+	-	-	+
11						-	+	-	+
12						+	+	-	+
13						-	-	+	+
14						+	-	+	+
15						-	+	+	+
16						+	+	+	+

Designs for fitting the second-order model

The central composite design, or CCD, is the most popular designs used for fitting the second-order model. Usually, the CCD consists of a 2^k factorial (or fractional factorial of resolution V) with n_F factorial runs, $2k$ axial or star runs, and n_C center runs (Montgomery, 2009). In practical development, the CCD often performs through sequential experimentation. That is, a factorial design (2^k design) has been firstly performed but the first-order model show inadequacy. The axial runs

(also called star runs) are then added to allow the quadratic terms to be incorporated into the second-order model.

To perform the central composite design, there are two parameters that must be specified: the distance α of the axial runs from the design center and the number of center points, n_c (Montgomery, 2009). The value of α depends on the number of points in the factorial portion of the design. For k factors, the axial or star points were formed by $n_{ax} = 2k$ points with all their coordinates null except for one this is set equal to a certain value α (or $-\alpha$). The value of α usually range from 1 to \sqrt{k} . When $\alpha = \sqrt{k}$, the cubic and axial points are located on the (hyper)surface of a (hyper)sphere, are the design id called spherical. But if $\alpha = 1$, the axial points are located at the centers of the side of the square part of the two-level design and at the centers of the faces of the cubic part of the three-factor design. This design is suitable for square or cubic design space. The total number of two-level factors in a CCD is $2^k + 2k + C_0$ where C_0 is the number of center points (Ferreira et al., 2007).

CCD can be used to determine a quadratic response surface which has curvature and can be used to predict factor levels that produces required response values. To evaluate curvature of response surfaces, a second-order model must be used.

$$y = \beta_0 + \sum_{i=1}^k \beta_i X_i + \sum_{i=1}^k \beta_{ii} X_i^2 + \sum \sum_{i < j} \beta_{ij} X_i X_j + \epsilon \quad (5)$$

where y is the response, β_0 is the constant, β_i is the parameter estimate, X is the independent parameter and ϵ is the residual error.

Evaluation of the fitted model

The more reliable way to evaluate the quality of the model fitted is using the analysis of variance (ANOVA). The ANOVA table for model validation is presented in table 5 (Ferreira et al., 2007).

The data on analysis of variance table is divided into two contributions, the sum of squares explained by the regression, SS_R , and the residual sum of squares, SS_r . Large SS_R and small SS_r values tend to occur for accurate model. The $\frac{SS_R}{SS_r}$ ratio

represents the fraction of explained variation and is commonly represented as R^2 , the coefficient of determination that varies between 0 and 1. If pure error exists it is impossible for R^2 to actually attain 1 (Ferreira et al., 2007).

Regression lack of fit is determined performing an F - test by comparing the $\frac{SS_{lof}}{SS_{pe}}$ ratio with the table F value for $m - p$ and $n - m$ degree of freedom at the desired confidence level, normally 95% (Ferreira et al., 2007). If the calculated F value is greater than the accepted value from F value that mean the model show lack of fit and this model should be reject.

Table 5 Analysis of variance table for the least squares fit of a model that is in its parameters^a

Source of variation	Sum of squares	Degree of freedom	Mean square
Regression	$SS_R = \sum_i^m \sum_j^{n_i} (\hat{y}_i - \bar{y})^2$	$p - 1$	$MS_R = \frac{SS_R}{p - 1}$
Residual	$SS_r = \sum_i^m \sum_j^{n_i} (y_{ij} - \hat{y}_i)^2$	$n - p$	$MS_r = \frac{SS_r}{n - p}$
Lack of fit	$SS_{lof} = \sum_i^m \sum_j^{n_i} (\hat{y}_i - \bar{y}_i)^2$	$m - p$	$MS_{lof} = \frac{SS_{lof}}{m - p}$
Pure error	$SS_{pe} = \sum_i^m \sum_j^{n_i} (y_{ij} - \bar{y}_i)^2$	$n - m$	$MS_{pe} = \frac{pe}{n - m}$
Total	$SS_T = \sum_i^m \sum_j^{n_i} (y_{ij} - \bar{y}_i)^2$	$n - 1$	
% explained variation: $\frac{SS_R}{SS_T}$			
Maximum % explainable variation: $\frac{SS_T - SS_{pe}}{SS_T}$			

^a n_i : number of replicates at the i^{th} level; m : number of distinct levels of the independent variables; $n = \sum n_i$ = total number of observations; p : number of parameters in the model.

The data on analysis of variance table is divided into two contributions, the sum of squares explained by the regression, SS_R , and the residual sum of squares, SS_r . Large SS_R and small SS_r values tend to occur for accurate model. The $\frac{SS_R}{SS_T}$ ratio

represents the fraction of explained variation and is commonly represented as R^2 , the coefficient of determination that varies between 0 and 1. If pure error exists it is impossible for R^2 to actually attain 1 (Ferreira et al., 2007).

Regression lack of fit is determined performing an F - test by comparing the $\frac{SS_{lof}}{SS_{pe}}$ ratio with the table F value for $m - p$ and $n - m$ degree of freedom at the desired confidence level, normally 95% (Ferreira et al., 2007). If the calculated F value is greater than the accepted value from F value that means the model shows lack of fit and this model should be rejected.

Moreover, the visual inspection of the residual graphs can also be used to evaluate the model suitability. If the model is well fitted, its residual graph shows a normal distribution (Bezerra et al., 2008).



คุรุศาสตร์วิทยาทรรพยากร
จุฬาลงกรณ์มหาวิทยาลัย

Design space

Design space is part of the US Food and Drug Administration (US FDA) which aims to move toward a new paradigm for pharmaceutical assessment as outlined in the International Conference on Harmonization (ICH). According to ICH Q8(R2), design space is defined as the multidimensional combination and interaction of process parameters that have been demonstrated to provide assurance of quality. It can be described as the relationship between the process input (material attributes and process parameters) and the critical quality attributes. Working within the design space is not considered as a change. Movement out of the design space is considered to be a change and would normally initiate a regulatory post approval change process. Design space is proposed by the applicant and is subject to regulatory assessment and approval ('ICH Pharmaceutical Development Q8(R2),' 2009)

Approaches for identifying the design space in the pharmaceutical industry usually rely on statistical design of experiments (DOE) (Sundaram et al., 2010). As shown in figure 4, the key steps in design space identification are: First, one or more acceptable critical quality attributes have been established, process parameters and their acceptable range should be identified. Second, studies were designed using DOE in order to use the resulting data to understand and define the design space. Third, the studies were executed and the results analyzed for decisions on the criticality of the parameters and establishing the design space.

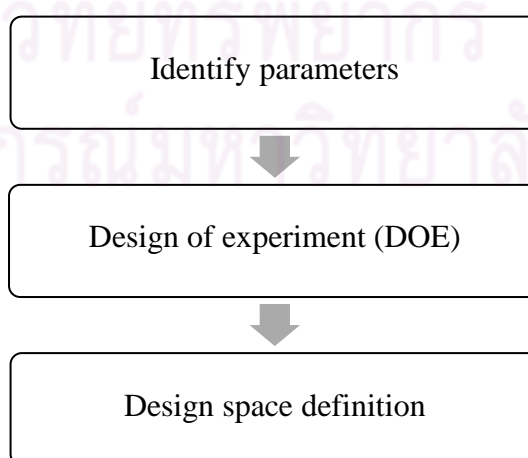
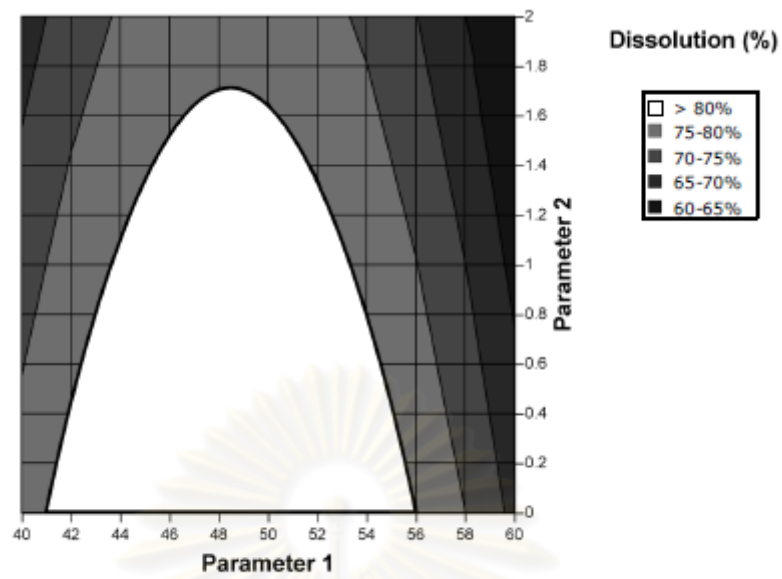


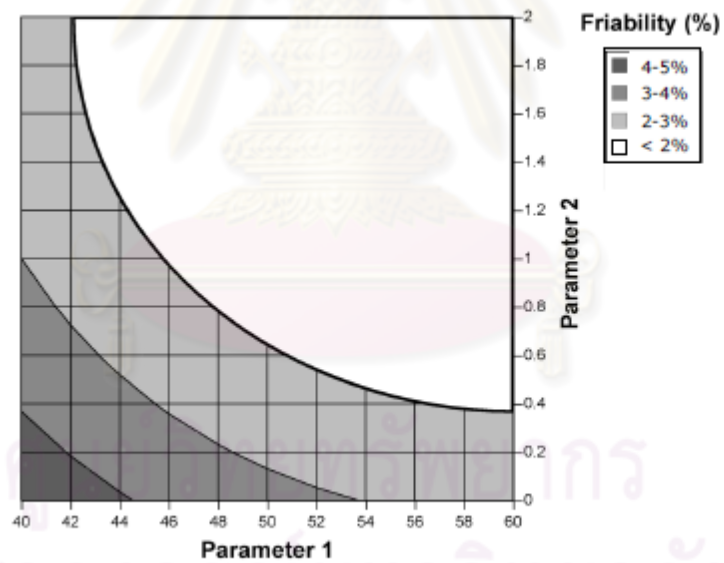
Figure 4 The key steps in design space identification

The design space can be built using a statistical model from the design of experiment. The final fitted model can be used to generate interaction profiles and contour plots to help visualize and understand the effect of the factors on the response. An interaction profile shows how the response changes as one factor changes at given levels of another factor. A contour plot is a two-dimensional graph of two factors and the fitted response. Vertical and horizontal axes of the contour plots represent factors from the design of experiment while the lines on the contour plot connect points in the factor plane that have the same response. When there are more than two factors in the experiment, contour plots can be made for several levels of the other factors (Altan et al., 2010). The design space thus can be presented for two parameters at different values (e.g., high, middle, low) within the range of the third parameter, the fourth parameter, and so on. Alternatively, the design space can be explained mathematically through equations describing relationships between parameters for successful operation ('ICH Pharmaceutical Development Q8(R2),' 2009).

If there are multiple response design, the simplest approach to built design space is overlaying contour plot of the fitted model for each response (Altan et al., 2010). Example of contour plot overlaying was shown in ICH Q8(R2) appendix 2. The contour plots of two process parameters of a granulation operation are shown in figure 5. The acceptant criteria of this experiment are percentage of dissolution more than 80% and percentage of granule friability less than 2%. The overlap of these regions and the maximum ranges of the proposed design space were shown in figure 6. The applicant can elect to use the entire region as the design space, or some subset thereof.



(a) Contour plot of dissolution as a function of parameters 1 and 2



(b) Contour plot of friability as a function of parameters 1 and 2

Figure 5 Contour plots of dissolution and friability for granulation process

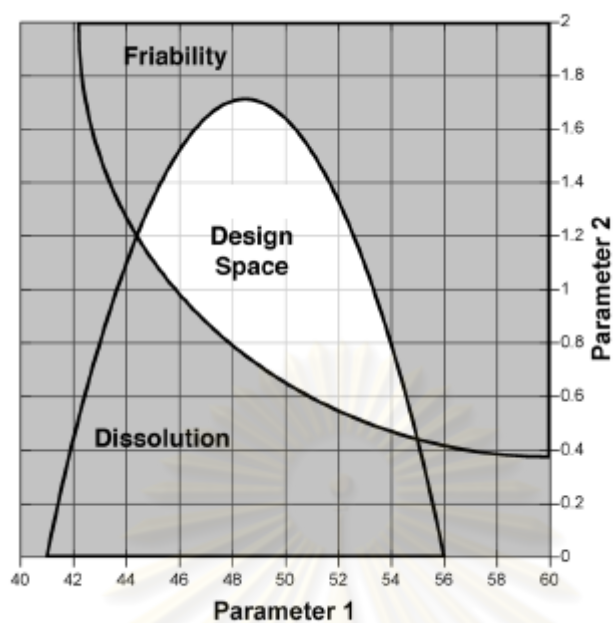


Figure 6 Proposed designs space which comprised of the overlap region of ranges for friability and or dissolution

ศูนย์วิทยทรัพยากร
จุฬาลงกรณ์มหาวิทยาลัย

CHAPTER III

EXPERIMENTAL

1. Materials

The following materials obtained from commercial sources were used.

1.1. Chemicals

- Rifampicin (obtained from Siam Pharmaceutical Co., Ltd., Bangkok, Thailand)
- Potassium chloride (Batch no. AF501338, Ajax Finechem, NSW, Australia)
- Poly(DL-lactide-co-glycolid) (PLGA, lactide:glycolide = 75:25, ester terminated nominal, inherent viscosity range 0.55-0.75 dL/g in chloroform)(Lot No. A08-030, Lactel International Absorbable Polymer, Pelham, AL, USA)
- Potassium phosphate, monobasic (Batch no. AF705005, Ajax Finechem, NSW, Australia)
- Sodium chloride (Batch no. 0811292, Ajax Finechem, NSW, Australia)
- di-Sodium hydrogen orthophosphate dodecahydrate (Batch no. 0903241, Ajax Finechem, NSW, Australia)
- Sodium hydroxide (Lot no. B131198 214, Merck KGaA, Damstadt, Germany)
- Tween 80 (Batch no. 809861, Srichand United Dispensary Co., Ltd, Thailand)

1.2. Reagents

- Acetonitrile HPLC grade (Batch no.10 04 0115, RCI Labscan Limited, Thailand)
- Chloroform HPLC grade (Batch no.08 07 0210, RCI Labscan Limited, Thailand)

- Dichloromethane Analytical grade (Batch no.J2EG1A, Honeywell Berdick & Jackson, Ulsan, Korea)
- Methanol HPLC grade (Batch no.K33G2H, Honeywell Berdick & Jackson, Ulsan, Korea)

1.3. Statistic program

- Design-Expert® Version 7.1.6 (Stat-Ease, Inc.)
Serial number: 3016-1675

2. Equipments

- Analytical Balance (Model PB3002, Mettler Toledo, Schwerzenbach, Switzerland and Model A200s, Sartorius Gbh, Goettingen, Germany)
- Büchi B-290 spray dryer (Büchi Labortechnik AG, Postfach, Switzerland)
- Scanning electron microscopy (SEM)(Model JSM-5800LV, Joel Ltd., Tokyo Japan)
- High performance liquid chromatograph (Shimadzu, Kyoto, Japan) assembled with
 - Liquid chromatograph pump (Model LC-20AB, Shimadzu, Japan)
 - Auto injector (Model SIL-20A, Shimadzu, Japan)
 - UV-VIS detector (Model SPD-20A UV, Shimadzu, Japan)
 - Inertsil ODS-3, 5 µm, C18, 4.6 mm x 250 mm i.d.(GL Sciences Inc., Japan)(C/N 5020-01732, S/N 7HT86018)
 - Alltima Guard column, 5 µm, C18 (Lot no. 50277378, Serial no. 609100731)
 - Liquid chromatograph pump (Model LC-10AB, Shimadzu, Japan)
- Laser diffraction particle sizer (Mastersizer 2000/Hydro 2000MU, Malvern instruments, Worcestershire, UK)
- pH meter (Model 210A+, Thermo orion, Germany)

3. Methods

3.1. Preparation of PLGA microspheres loaded with rifampicin

A spray-drying technique was used to produce PLGA microspheres loaded with rifampicin. A 0.08% (w/v) PLGA solution was prepared in dichloromethane. Rifampicin was added and dissolved to have clear solution. The solution was spray dried using a Büchi B-290 spray dryer with the 0.7 mm. orifice diameter of nozzle. Various conditions of inlet drying temperature, aspirator control, pump setting and nozzle gas flow setting (see Design of Experiment section). Spray dried particles were separated from the drying air with standard cyclone separator and were collected from the drying chamber and bottom part of the cyclone. The spray dried powders were stored in vials.

3.2. Characterization of rifampicin-PLGA microparticles

3.2.1. Process yield

The process yield (Y) was defined as the ratio between the amount of collected powder from collection jar and cyclone of spray dryer and the amount of rifampicin introduced in feeding solution. The unit was percent by weight.

$$\text{Process yield} = \frac{\text{the amount of collected powder}}{\text{the amount of introduced rifampicin}} \times 100 \quad (6)$$

3.2.2. Particle morphology

Microsphere shape and surface morphology were investigated by scanning electron microscopy (SEM). The powder was sprinkled on a SEM stub, covered with adhesive carbon tape and sputter coated with gold prior to scanning.

3.2.3. Particle size and size distribution

Dried rifampicin-PLGA microparticles were suspended in 0.02% Tween 80 and sonicated for 10 min to obtain a uniform suspension before measurements. The mass median diameter (MMD) and size distribution of microspheres were measured with laser diffraction particle sizer.

3.2.4. Drug entrapment efficiency

The rifampicin content in Rifampicin-PLGA microparticles was quantitatively determined by using reversed phase high performance liquid chromatography (RP-HPLC) method. The chromatographic condition was modified from Calleja et al., 2004. Drug entrapment efficiency of rifampicin in rifampicin-PLGA microparticles was determined in triplicate. The percentage of rifampicin entrapment was calculated as following equation:

$$\text{Drug Entrapment efficiency (DEE, \%)} = \frac{\text{AQ}}{\text{TQ}} \times 100 \quad (7)$$

where AQ = actual quantity of rifampicin entrapped in PLGA microparticles and TQ = theoretical quantity of rifampicin entrapped in PLGA microparticles.

HPLC analysis

HPLC chromatographic conditions:

Column	: Inertsil ODS-3, C18, 250 x 4.6 mm, 5 μ m
Mobile phase	: water (pH 2.27 adjusted with orthophosphoric acid): acetonitrile (1:1)
Flow rate	: 1.2 ml/min
Injection volume	: 10 μ l
Detector	: UV 333 nm
Retention times	: Rifampicin 3.0 – 3.8 min

Validation of the HPLC method

The typical analytical characteristics used in method validation which were specificity, accuracy, precision and linearity (*USP 33/NF 28*, 2010) are shown in Appendix A.

Preparation of standard solutions for validation:

Rifampicin was accurately weighed about 12.5 mg to 50 ml volumetric flask then diluted with chloroform:methanol (1:9). This solution was used as the standard stock solution and the final concentration was 250 µg/ml. Five dilutions were prepared as standard solution in the concentration range of 25 - 125 µg/ml. All standard were filtered through 0.45 µm membrane filter before analysis and injected on column in triplicate. The linear regression equation of means of area under curve of standard rifampicin peak in HPLC chromatogram versus actual standard concentrations was calculated.

Assay preparation:

An accurately weighed 5 mg of rifampicin-PLGA microparticles was placed into a 15 ml polyethylene tube. The solution for analysis was prepared by dissolving microparticles with chloroform:methanol (1:9) to 10 ml. The samples were prepared in triplicate and analyzed. All solutions were filtered through 0.45 µm membrane filter before analysis and injected on column in triplicate. Content of rifampicin in rifampicin-PLGA microparticles was calculated from the linear regression equation obtained calibration curve of standard solutions.

3.2.5. In vitro dissolution

The release of rifampicin from rifampicin-PLGA microparticles was studied using flow through cell method modified from Davies and Feddah, 2003. A flow through dissolution apparatus was use to determine the dissolution behavior of rifampicin-PLGA microparticles. A schematic diagram of this apparatus is shown in Figure 7.

This apparatus include the dissolution media reservoir equilibrated at 37 °C in a water bath, HPLC pump delivering the dissolution medium to the dissolution cell through a silicon tube (0.5 mm i.d). The dissolution medium pass through the microparticles which is immobilized onto the dissolution cell by the constant pressure applied through the HPLC pump. The dissolution medium is finally collected in a fraction collector. The dissolution cell consists of a 25 mm PALL® filter holder.

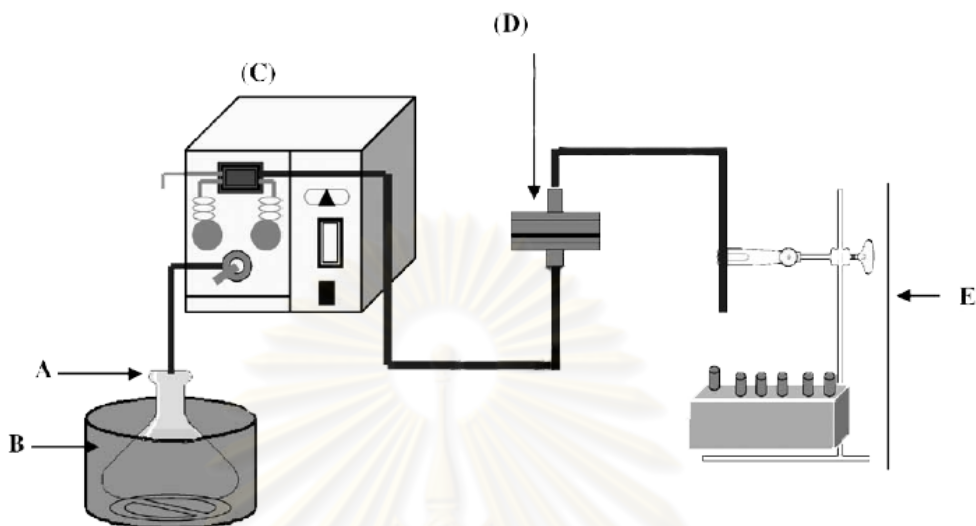


Figure 7 A schematic diagram of modified flow through dissolution apparatus (Davies and Feddah, 2003) consists of dissolution medium reservoir (A), water bath (B), HPLC pump (C), dissolution cell (D) and sample collector (E)

The dissolution medium was phosphate buffer saline pH 7.4. The 150 μl of 20% (w/v) of rifampicin-PLGA microparticles suspended in the buffer solution was inserted between two 0.45 μm nylon membrane filters. The sandwich-like filters containing the microparticles were placed into the dissolution cell. The dissolution medium which equilibrated to 37 $^{\circ}\text{C}$ was pumped upward through the dissolution cell with a constant flow of 0.7 ml/min. The dissolution fraction of the medium was collected separately at specified time intervals (5, 10, 20, 40, 60, 90 and 120 min).

The rifampicin content in dissolution solution was quantitatively determined by using reversed phase high performance liquid chromatography (RP-HPLC) method. The chromatographic condition was modified from Calleja et al., 2004.

HPLC analysis

HPLC chromatographic conditions:

Column	: Inertsil ODS-3, C18, 250 x 4.6 mm, 5 μ m
Mobile phase	: water (pH 2.27 adjusted with orthophosphoric acid): acetonitrile (1:1)
Flow rate	: 1.2 ml/min
Injection volume	: 100 μ l
Detector	: UV 333 nm
Retention times	: Rifampicin 3.0 – 3.8 min

Validation of the HPLC method

The typical analytical characteristics used in method validation which were specificity, accuracy, precision and linearity (*USP 33/NF 28*, 2010) are shown in Appendix B.

Preparation of standard solutions for validation:

Rifampicin was accurately weighed about 10 mg to 10 ml volumetric flask then diluted with methanol. This solution was used as the standard stock solution and dilute with phosphate buffer saline pH 7.4 to the final concentration (10 μ g/ml). Five solutions were prepared as standard solution in the concentration range of 0.04 - 8 μ g/ml. All standard were filtered through 0.45 μ m membrane filter before analysis and injected on column in triplicate. The linear regression equation of means of area under curve of standard rifampicin peak in HPLC chromatogram versus actual standard concentrations was calculated.

Assay preparation:

The sampling solutions at selected time interval were filtrated through 0.45 μ m membrane filter before analysis by HPLC method. Content of rifampicin was calculated from the linear regression equation obtained calibration curve of standard solutions.

3.3. Design of experiment (DOE)

3.3.1. Full factorial design

A full factorial design was created to investigate the influence of spray drying process parameters - the inlet drying temperature (T_{in}), aspirator control (A), pump setting (P) and nozzle gas flow setting (N) as called factors on the interested responds as called responses. To understand the process parameters setting, the description of spray drying parameters were shown in Appendix C. Furthermore, this design was chosen to create a linear model and to evaluate the relationship between factors and responses. In this study, the design consisted of 16 experiments representing a two-level full factorial design (2^4 design). The levels of the different process parameters were chosen based on preliminary investigation and on literature. Inlet drying temperature was selected based on dichloromethane and PLGA properties. The ranges of other parameters were chosen as broad as possible. The independent variables were process yield (Y_1), mass median diameter (Y_2), drug entrapment efficiency (Y_3) and dissolution after 20 minute (Y_4). The two levels of each variable and experimental domain were shown in table 6 and table 7.

Table 6 Experimental factors and their level in full factorial design

Factor significance	Level (-1)	Level (+1)
Inlet drying temperature (T_{in})(°C)	55	75
Aspirator control (A) (%)	55	100
Pump setting (P) (%)	10	30
Nozzle gas flow setting (N) (mm)	30	60

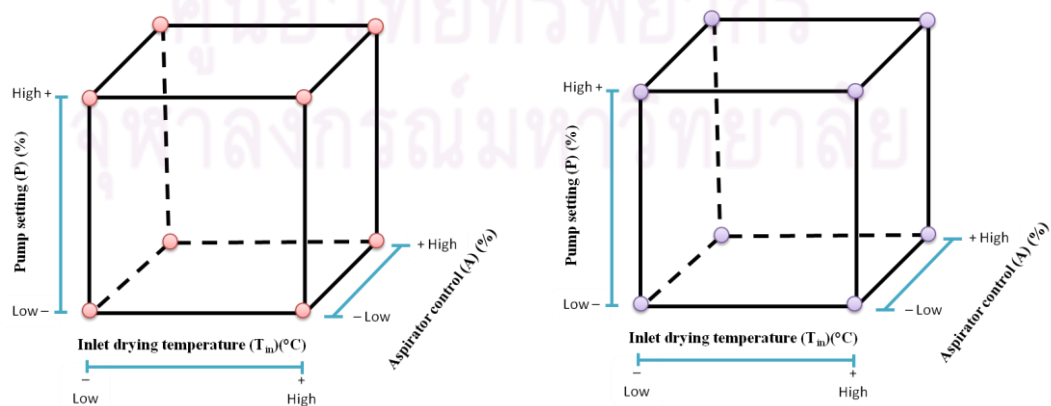
Table 7 Experiment design of two-level full factorial design

Experimental No.	T _{in}	A	P	N
1	55	55	10	30
2	75	55	10	30
3	55	100	10	30
4	75	100	10	30
5	55	55	30	30
6	75	55	30	30
7	55	100	30	30
8	75	100	30	30
9	55	55	10	60
10	75	55	10	60
11	55	100	10	60
12	75	100	10	60
13	55	55	30	60
14	75	55	30	60
15	55	100	30	60
16	75	100	30	60

There are three different notations that are widely used for represent the run in the 2^k design. The first is using “ + and – ” notation to represent the high and low levels of the factors, often called the geometric notation. Second is using the lowercase letter label as (1), a, b, ... to indentify. Finally, the last notation is using +1 and -1 to denote high and low factor levels, respectively, instead of + and – as called coded notation. The different notations of 2^4 design was shown in table 8. According to four factors each at two levels are interested, the 16 experiments can be displayed geometrically as a cube as show in figure 8.

Tablet 8 The three different notations of 2^4 design

Experimental No.	Geometric notation				Latter labels	Coded notation			
	T_{in}	A	P	N		T_{in}	A	P	N
1	-	-	-	-	(1)	-1	-1	-1	-1
2	+	-	-	-	a	+1	-1	-1	-1
3	-	+	-	-	b	-1	+1	-1	-1
4	+	+	-	-	ab	+1	+1	-1	-1
5	-	-	+	-	c	-1	-1	+1	-1
6	+	-	+	-	ac	+1	-1	+1	-1
7	-	+	+	-	bc	-1	+1	+1	-1
8	+	+	+	-	abc	+1	+1	+1	-1
9	-	-	-	+	d	-1	-1	-1	+1
10	+	-	-	+	ad	+1	-1	-1	+1
11	-	+	-	+	bd	-1	+1	-1	+1
12	+	+	-	+	abd	+1	+1	-1	+1
13	-	-	+	+	cd	-1	-1	+1	+1
14	+	-	+	+	acd	+1	-1	+1	+1
15	-	+	+	+	bcd	-1	+1	+1	+1
16	+	+	+	+	abcd	+1	+1	+1	+1



(a) High nozzle gas flow setting (N)

(b) Low nozzle gas flow setting (N)

Figure 8 The geometric present of 2^4 design

3.3.2. Central composite face centered design

A central composite face centered design (CCF) was constructed to investigate influence of spray dried process parameter on properties of rifampicin-PLGA microparticles. This design was chosen to create a full quadratic model and it is feasible for limitation of spray drying instrument.

In this study, the design consisted of 27 experiments. Sixteen experiments represented a two-level full factorial design (2^4 designs) from 3.3.1. Eight experiments were axial points with a high and low level of each parameter and three experiments were center points. The levels of the different process parameters were chosen the same way as full factorial design and center point of each parameter define as the average value of high value and low value. The three levels of each variable and experimental domain were shown in table 9 and the experimental design was given in table 10.

This CCF design which is $\alpha = 1$ located the axial points on the centers of the face of the cube as show in figure 9 and the coded notation of this design was using “+, – and 0” notation to represent the high, low and medium (or center) levels of the factors was shown in table 11.

The independent variables were interested properties that show relation with process parameters from first-model in section 3.3.1.

Table 9 Experimental factors and their level in central composite face centered design

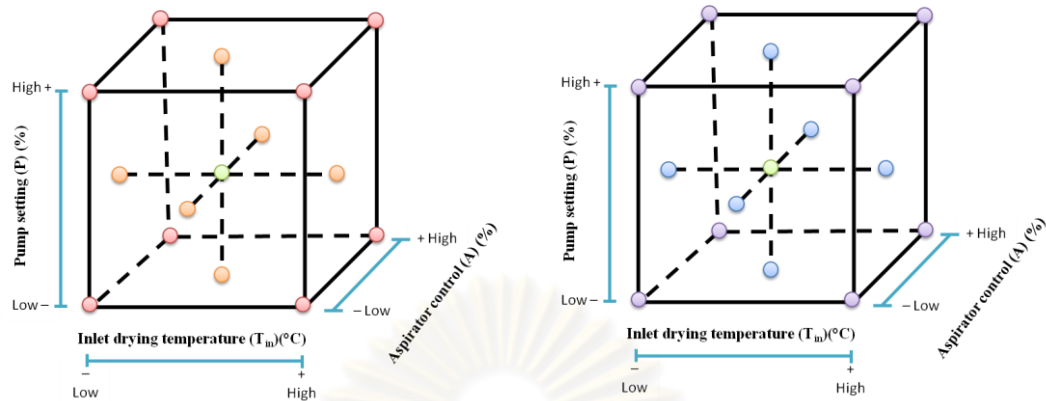
Factor significance	Level (-1)	Level (0)	Level (+1)
Inlet drying temperature (Tin)(°C)	55	65	75
Aspirator control (A) (%)	55	78	100
Pump setting (P) (%)	10	20	30
Nozzle gas flow setting (N) (mm)	30	45	60

Table 10 Experiment design of central composite face centered design

Experimental No.	T _{in}	A	P	N
1	55	55	10	30
2	75	55	10	30
3	55	100	10	30
4	75	100	10	30
5	55	55	30	30
6	75	55	30	30
7	55	100	30	30
8	75	100	30	30
9	55	55	10	60
10	75	55	10	60
11	55	100	10	60
12	75	100	10	60
13	55	55	30	60
14	75	55	30	60
15	55	100	30	60
16	75	100	30	60
17	55	78	20	45
18	75	78	20	45
19	65	55	20	45
20	65	100	20	45
21	65	78	10	45
22	65	78	30	45
23	65	78	20	30
24	65	78	20	60
25	65	78	20	45
26	65	78	20	45
27	65	78	20	45

Table 11 Coded notation of central composite face centered design

Experimental No.	T_{in}	A	P	N
1	-1	-1	-1	-1
2	+1	-1	-1	-1
3	-1	+1	-1	-1
4	+1	+1	-1	-1
5	-1	-1	+1	-1
6	+1	-1	+1	-1
7	-1	+1	+1	-1
8	+1	+1	+1	-1
9	-1	-1	-1	+1
10	+1	-1	-1	+1
11	-1	+1	-1	+1
12	+1	+1	-1	+1
13	-1	-1	+1	+1
14	+1	-1	+1	+1
15	-1	+1	+1	+1
16	+1	+1	+1	+1
17	-1	0	0	0
18	+1	0	0	0
19	0	-1	0	0
20	0	+1	0	0
21	0	0	-1	0
22	0	0	+1	0
23	0	0	0	-1
24	0	0	0	+1
25	0	0	0	0
26	0	0	0	0
27	0	0	0	0



(a) High nozzle gas flow setting (N)

(b) Low nozzle gas flow setting (N)

Figure 9 The geometric present of 2⁴ design

3.4. Statistical analysis

3.4.1. Full factorial design

The response data from 16 experiments and 3 center point experiment were evaluate using the Design-Expert® version 7.1.6 to evaluate prediction models and determine which parameters were statistically significant in the independent variables. The linear equation of the model is as follows:

$$y = \beta_0 + \sum_{i=1}^k \beta_i X_i + \sum \sum_{i < j} \beta_{ij} X_i X_j + \epsilon \quad (8)$$

where y is the response, β_0 is the constant, β_i is the parameter estimate, X is the independent parameter and ϵ is the residual error.

In order to evaluate the importance of each parameter, the regression coefficients were calculated individually for evaluate the effect of each variables and their factor interactions. A backward elimination was used to produce the fitted linear model. The prediction equations of each variable were estimated using the least squares method. Factors and two factor interactions which were found significant at a 95% confidence level were include and the main factors which were present in the significant two factor interactions were also include, even if they were not significant to themselves. Models were accepted when there was no lack of fit ($p > 0.05$),

regression test ($p < 0.05$), high goodness of fit (R^2), no correlation in the residual plots and the residuals were normally distributed.

The response data of three center points were included to estimate the experimental error and lack-of-fit and to evaluate possible response curvature. The curvature is the difference between the average of the center points and the average of the factorial points. In case, if the quadratic curvature shown statistically significant at $p < 0.05$, the relationship between parameters and response was non-linear regression and the quadratic model would be used

The fitted equations are to be interpreted as follows: a positive sign in front of the parameters means that increasing parameters value causes the increasing of response value. In contrast, when the sign is negative, an increase in the parameter value results in a decrease of the response value.

3.4.2. Central composite face centered design

The central composite face centered design was performed to evaluate the response surface and to perform the quadratic equation model to optimize the suitable process parameters. The quadratic equation of the model is as follows:

$$y = \beta_0 + \sum_{i=1}^k \beta_i X_i + \sum_{i=1}^k \beta_{ii} X_i^2 + \sum \sum_{i < j} \beta_{ij} X_i X_j + \epsilon \quad (9)$$

where y is the response, β_0 is the constant, β_i is the parameter estimate, X is the independent parameter and ϵ is the residual error.

The Design-Expert® version 7.1.6 was used to determine which parameters were statistically significant in determining the independent variables. The regression coefficients were calculated individually for evaluate the effect of each variables and their two factor interactions. The prediction equations of each variable were estimated using the least squares method. A backward elimination procedure was adopted to fit the data to the second-order model. In the final prediction model, the parameters which were significant at a 95% confidence level were included. Factors and two factor interactions which were found significant at a 95% confidence level were include and the main factors which were present in the significant two factor

interactions were also include, even if they were not significant to themselves. In order to evaluate the importance of each parameter, p-values were used. The final models were accepted when there was no lack of fit ($p < 0.05$), regression model test ($p < 0.05$) and high goodness of fit (R^2), no correlation in the residual plots and the residuals were normally distributed. The non-significant terms were excluded from the equation for better models. The fitted equations are interpreted as follows: positive value in front of the response represents a direct effect and negative value indicates an inverse relationship between response and a factor.

Moreover, interaction term indicates that the effect of a variable produced by changing one parameter level depends on the level of the other parameter in the interaction term and quadratic terms implying that a minimum or approach to a minimum if the term is positive or a maximum or approach to maximum if the term is negative.

The contour plot and response surface plot were performed to show the effect of parameters on responses.

3.5. Optimization

The optimum spray dried conditions was performed using Design-Expert®. The criterion for selection of optimum was high process yield, particle size 3-5 μm which is appropriate to deliver into the alveolar of lung, high drug entrapment efficiency and high dissolution at the first 20 min. The highest desirability function condition was chosen. The spray dried condition corresponding to this optimum was performed in triplicate and the obtained rifampicin-PLGA microparticles were evaluated for various response properties. The observed response values of those microparticles were quantitatively compared with predicted values.

3.6. Design space

Design space represents the multidimensional combination of factors that have been demonstrated to provide the required quality (Florea and Leucuta, 2008). To present an optimum domain in which the process spray drying condition parameters give the inhalable particle, design space has been evaluated.

From the quadratic model, the contour plots between the significant interaction parameters were performed. The contour of the acceptance response in the (x_1, x_2) space represents the design space in the inhalable rifampicin-PLGA microparticles.

In pulmonary drug delivery, particle size of the microparticles is very important requirement. The inhalable particle size must between 3 – 5 μm with narrow particle size distribution and low aerodynamic dispersion force. Thus, the desired particle size of rifampicin-PLGA microparticles for inhalation is between 3 – 5 μm . Moreover, other properties (process yield, drug entrapment efficiency and dissolution at first 20 min) should be concluded. In the design space, the optimum values of desired rifampicin-PLGA microparticles have been set by the following restriction: process yield not less than 30%, mass median diameter between 3 – 5 μm , drug entrapment efficiency not less than 80% and dissolution at 20 min not less than 40%.



ศูนย์วิทยทรัพยากร
จุฬาลงกรณ์มหาวิทยาลัย

CHAPTER IV

RESULTS AND DISCUSSION

All spray drying experiments produced red micron size powders. There are varying amount of powder deposited on the walls in the drying chamber and the cyclone.

1. Morphology of the rifampicin-PLGA loaded microparticle

Scanning electron microphotographs of rifampicin-PLGA microspheres are presented in figure 10 showing “raisin-like” or shriveled shape particle the same as previously described in other report (O’Hara and Hickey, 2000). This could be explained by the temperature that above the solvent boiling point and also above the glass transition temperature of the polymer making it less rigid during drying.

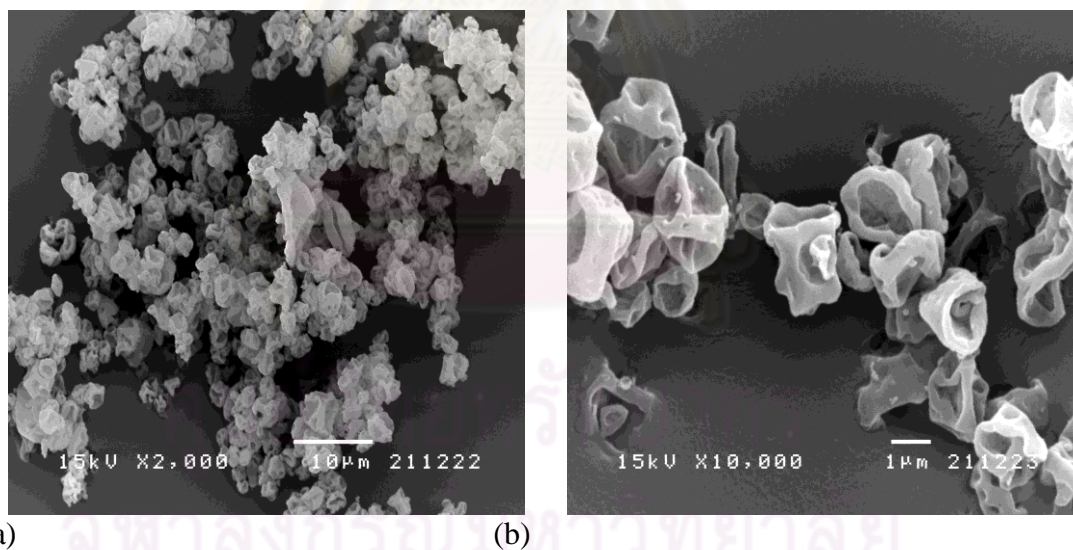


Figure 10 Scanning electron microphotographs of rifampicin-PLGA microspheres

- (a) an overview of the particles, at the lower magnification of 2,000x
- (b) “raisin-like” particles, at the higher magnification of 10,000x

2. Full factorial design

The full factorial with center points design was used to determine influence of main factors and interaction factors on interested responses. The linear model was

evaluated in the term of statistical significant using analysis of variance (ANOVA) and only two interaction factors were studied.

Results of the process yield (Y_1), mass median diameter (Y_2), drug entrapment efficiency (Y_3) and dissolution after 20 minute (Y_4) from full factorial and center point design were shown in table 12.

Table 12 The data of interested responses from full factorial with center points design

Experiment	Process parameter				Reponses			
	T_{in}	A	P	N	Y_1	Y_2	Y_3	Y_4
1	55	55	10	30	21.0312	3.416	97.9209	22.8780
2	75	55	10	30	41.7376	3.639	88.8713	40.6376
3	55	100	10	30	41.2390	3.665	86.7113	45.3930
4	75	100	10	30	40.7707	3.511	90.2285	30.6197
5	55	55	30	30	39.8516	4.644	89.1526	28.8401
6	75	55	30	30	34.2986	4.059	90.4178	50.3404
7	55	100	30	30	43.1993	4.525	86.9171	17.1463
8	75	100	30	30	40.7471	5.458	91.5779	43.5751
9	55	55	10	60	20.0511	3.714	90.8359	32.4058
10	75	55	10	60	39.8501	3.668	88.9423	24.8831
11	55	100	10	60	40.1247	3.687	88.8866	42.9460
12	75	100	10	60	15.9714	2.460	93.5574	23.4343
13	55	55	30	60	7.2384	4.219	90.5824	29.7633
14	75	55	30	60	12.8814	2.962	85.8246	32.4996
15	55	100	30	60	18.1279	3.281	89.0269	22.5980
16	75	100	30	60	18.0894	2.787	92.5223	38.1796
17	65	78	20	45	25.2223	3.357	90.2160	21.9619
18	65	78	20	45	23.1839	2.759	89.3473	48.3985
19	65	78	20	45	34.3012	3.322	92.0782	24.7819

2.1 Process yield

From the response data obtained from full factorial and center point experiments, process yield varied from 7.2384% to 43.1993%. The factor effect estimate of process yield and ANOVA table for process yield in the full factorial design were shown on table 13 and table 14, respectively.

Table 13 The factor effect estimate of linear model for process yield

Term	Effect	% Contribution
T _{in} -Inlet drying temperature	1.6854	0.4482
A-Aspirator control	5.1662	4.2111
P-Pump setting	-5.7928	5.2945
N-Nozzle gas flow setting	-16.3176	42.0116
T _{in} A	-8.4635	11.3019
T _{in} P	-2.2855	0.8242
T _{in} N	-1.3728	0.2974
AP	1.3072	0.2696
AN	-2.0931	0.6912
PN	-9.1223	13.1299

ศูนย์วิทยทรัพยากร
จุฬาลงกรณ์มหาวิทยาลัย

Table 11 ANOVA table for the linear model for process yield

Source of Variation	Sum of Squares	df	Mean Square	F Value	p-value
Model	1936.7835	6	322.7973	6.0502	0.0052*
T _{in} -Inlet drying temperature	11.3620	1	11.3620	0.2130	0.6535
A-Aspirator control	106.7574	1	106.7574	2.0009	0.1849
P-Pump setting	134.2243	1	134.2243	2.5158	0.1410
N-Nozzle gas flow setting	1065.0561	1	1065.0561	19.9623	0.0010*
T_{in}A	286.5208	1	286.5208	5.3702	0.0408**
PN	332.8630	1	332.8630	6.2388	0.0296**
Curvature	11.4772	1	11.4772	0.2151	0.6518
Residual	586.8873	11	53.3534		
Lack of Fit	516.8284	9	57.4254	1.6393	0.4356
Pure Error	70.0588	2	35.0294		
Cor Total	2535.1480	18			

* Significant at p-value < 0.01

** Significant at p-value < 0.05

The linear model explaining process parameters on process yield (Y_1) is

$$Y_1 = -76.5156 + 1.5419(T_{in}) + 1.3373(A) + 1.0787(P) + 0.0642(N) - 0.0188(T_{in})(A) - 0.0030(P)(N) \quad (10)$$

The analysis of process yield data showed the significant effects were the nozzle gas flow setting (N), the inlet drying temperature-aspirator control interaction and pump setting-nozzle gas flow setting interaction. The main effect of nozzle gas flow setting was plotted in figure 11 that showed negative effect means the process yield increased when nozzle gas flow setting was decreased. Decreased nozzle gas flow setting decreases the atomization energy and producing enlarged droplets. These droplets were dried to be large particles which are more easily captured through the

centrifugal force in the cyclone. This result was a confirmation of a report by Stahl et al., 2002.

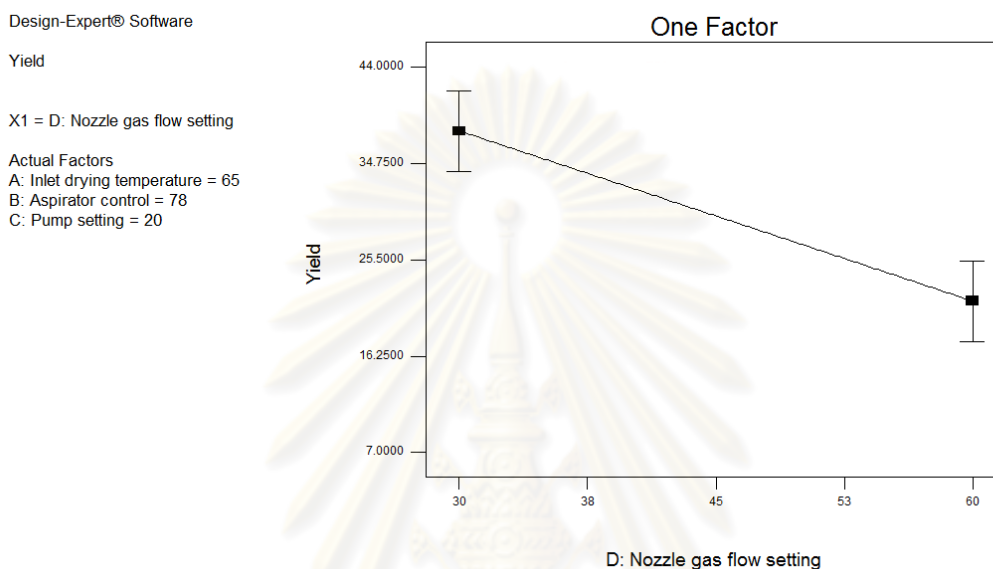


Figure 11 Main effect plot of nozzle gas flow setting for process yield on the linear model

However, the main effects do not have much meaning when they are involved in significant interactions (Montgomery, 2009) so the interactions between inlet drying temperature and aspirator control and the interaction between pump setting and nozzle gas flow setting were the key to explain the model. From the inlet drying temperature-aspirator control interaction plot (Figure 12), the aspirator control effect is small when the inlet drying temperature is at the high level and large when the inlet drying temperature is at the low level. Moreover, the inlet drying temperature effect is positive at the low level of aspirator control but show negative effect when aspirator control is at the high level. Decreasing inlet drying temperature increased drying time period of rifampicin-PLGA solutions (Tomoda et al., 2008). The obtained microparticles will be large. The large microparticles were also easily captured into the spray dryer cyclone. When aspirator control was increased, the separation rate in

cyclone was also increased. At the condition with high inlet drying temperature, particle size was increased, the large particles were then separated and only small particles were collected in cyclone. Finally, the process yield decreased. In contrast, at low aspirator control, the separation rate was decreased so the larger particles can be collected. Thus, the process yield from the spray drying condition with low aspirator control increased. The highest process yield thus obtained with low inlet drying temperature and high aspirator control.

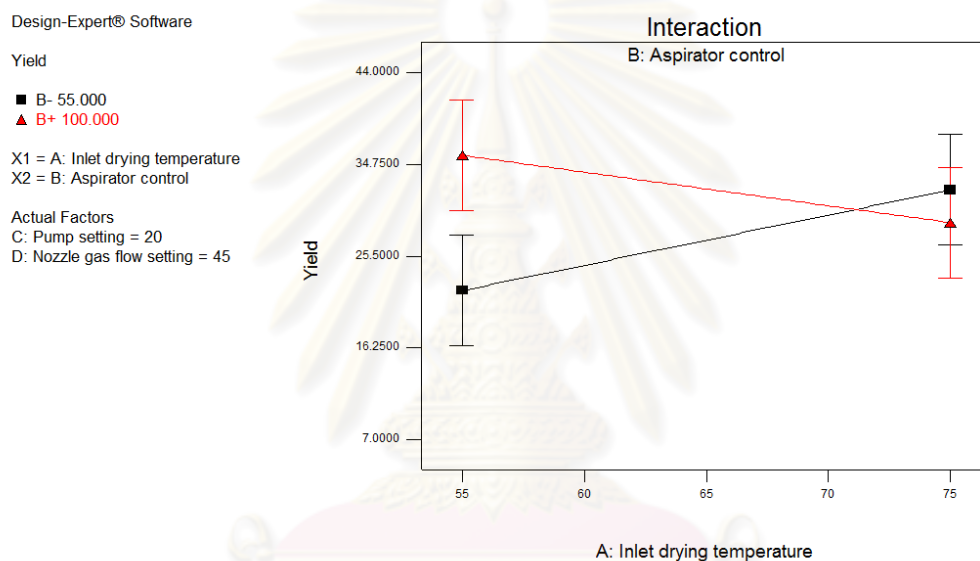


Figure 12 Interaction plot between inlet drying temperature and aspirator control of linear model for process yield (high level shown as red line and low level shown as black line)

The interaction between pump setting and nozzle gas flow setting can also be explained that nozzle gas flow effect is small when pump setting is at the low level and large when pump setting is at the high level. The pump setting effect is positive at the low level of nozzle gas flow setting but negative at the high level of nozzle gas flow setting. When pump setting was increased, the solution droplets also increased. But high nozzle gas flow setting caused the small particle (as describe above). Condition with high nozzle gas flow setting and pump setting produced small particles which were less captured into the spray dryer cyclone. The process yield thus

decreased. In contrast, low nozzle gas flow setting condition provided large particle. The process yield so that increased when pump setting was increased. The highest process yield obtained with high pump setting and low nozzle gas flow (Figure 13).

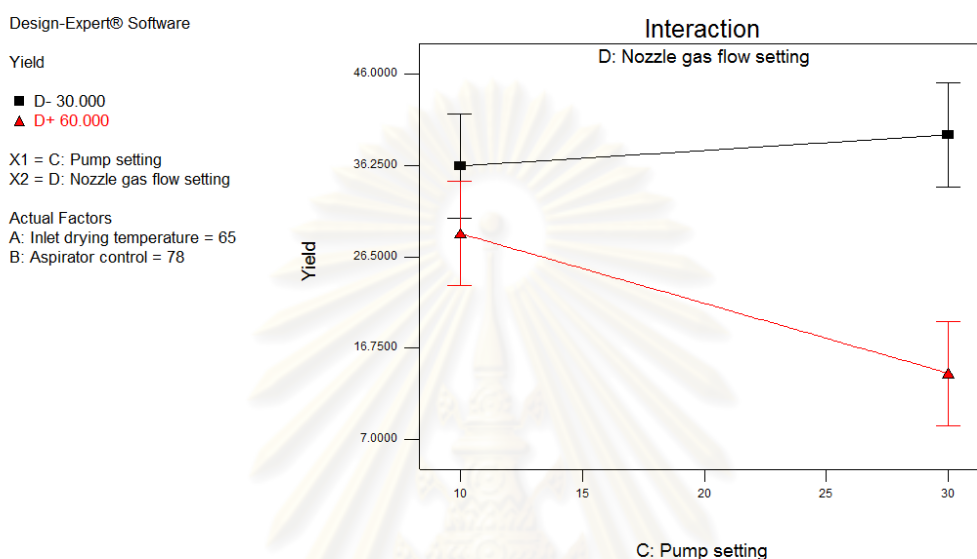
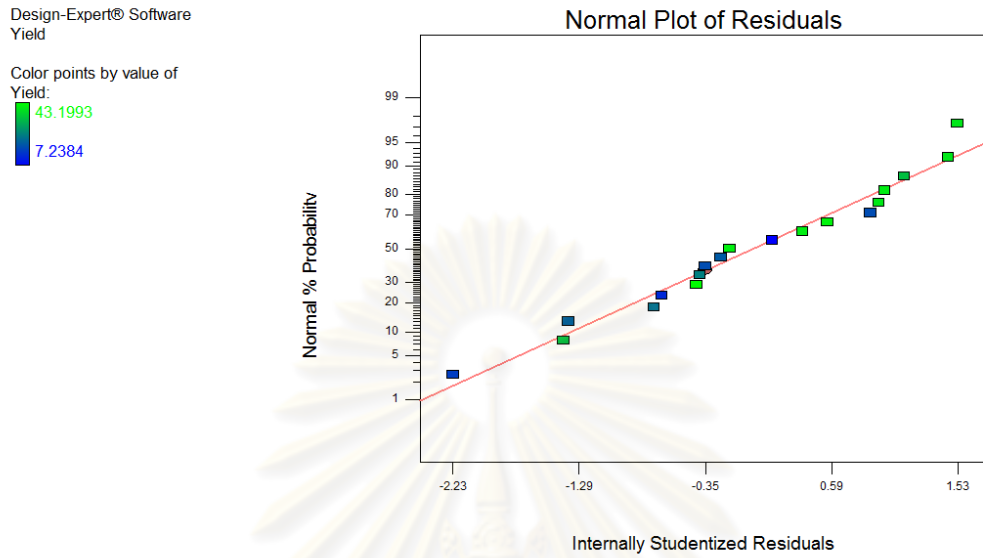


Figure 13 Interaction plot between pump setting and nozzle gas flow setting of linear model for process yield (high level shown as red line and low level shown as black line)

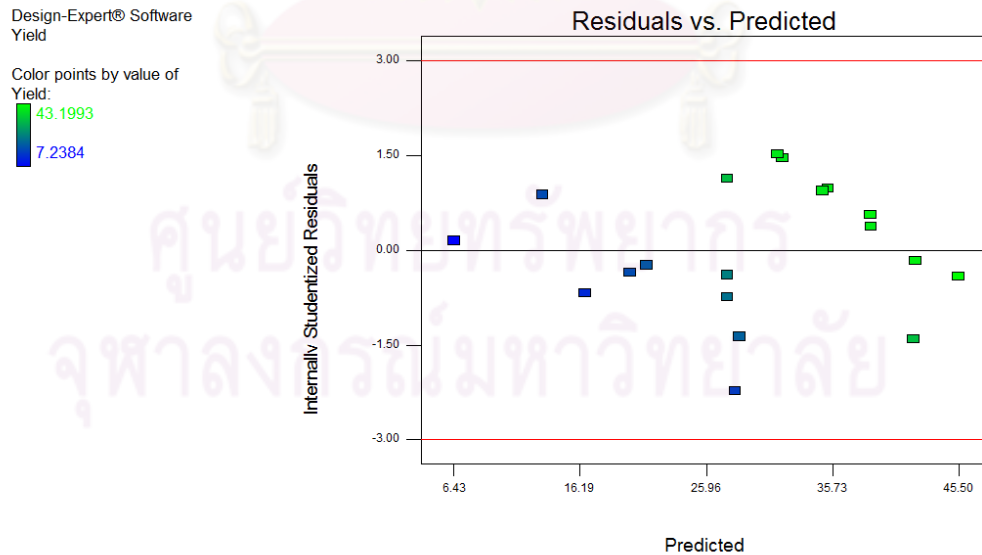
In summary, the spray drying condition with low inlet drying temperature, high aspirator control, high pump setting and low nozzle gas flow setting produce the highest process yield of rifampicin-PLGA microparticles.

The R^2 value of this fitted equation was 0.7674 (show a reasonably good fit). This linear model show no lack of fit ($p = 0.4356$), no correlation in the residual plots and the residuals distribution was normal (as shown on figure 14).

Although the curvature of the linear model for process yield showed non-significant ($p = 0.6518$) but the contour plot and response surface plot of the interaction effects showed non-linear correlation (Figure 15 and 16). The quadratic response surface methodology would be used in further section to indicate the response model and optimization.

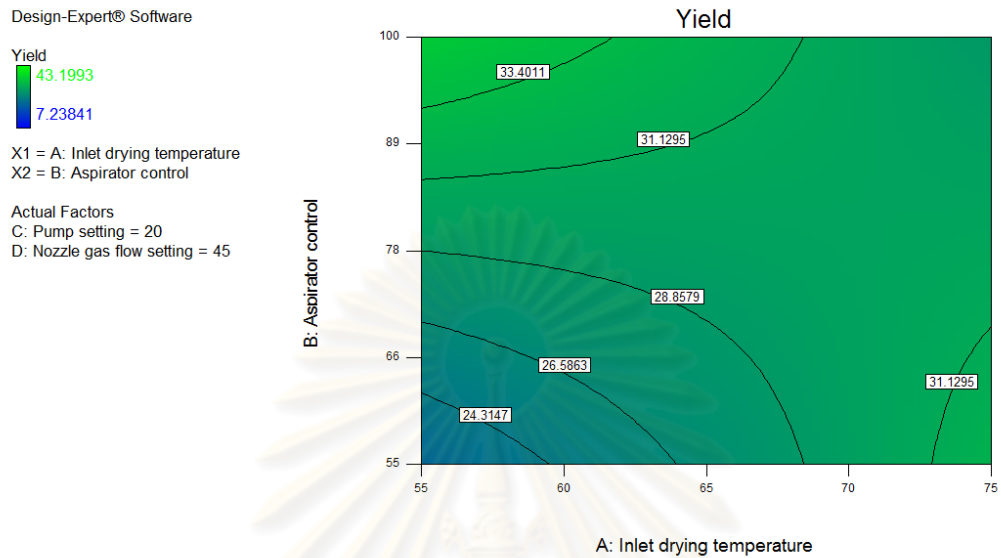


(a) Normal probability plot of residuals revealed no serious violation

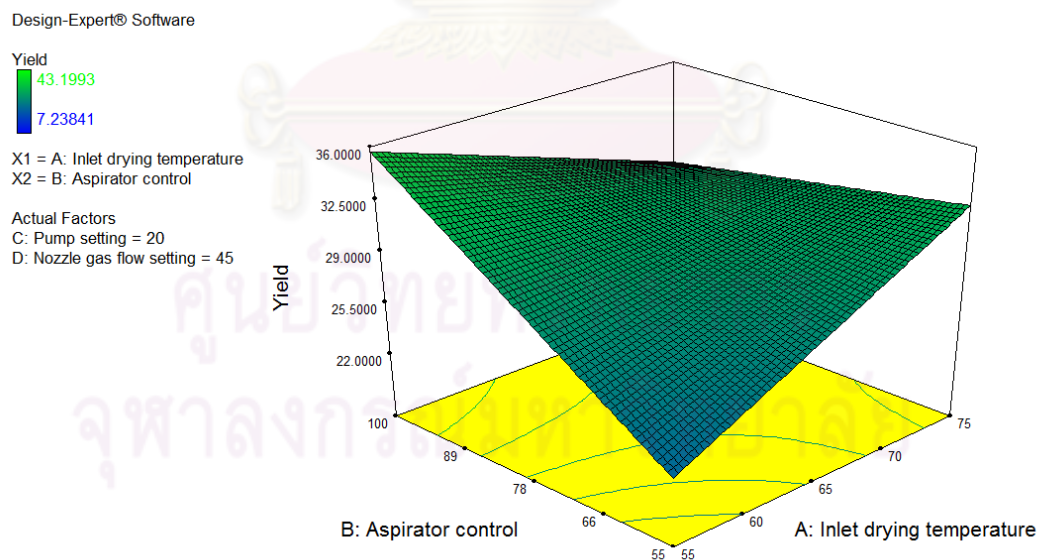


(b) Residuals versus predicted values did not revealed any obvious pattern

Figure 14 Residual analysis of the linear model for process yield

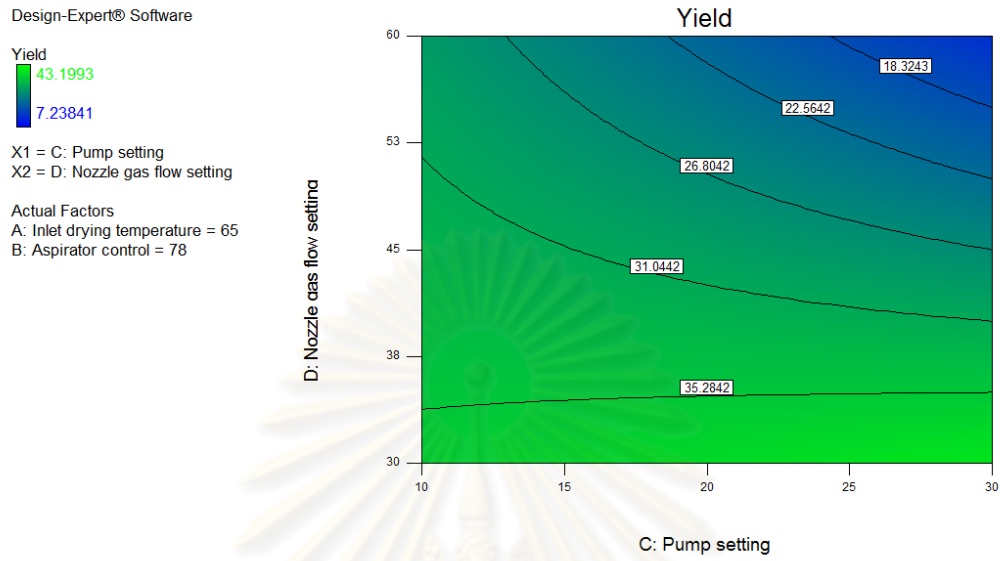


(a) Contour plot between inlet drying temperature and aspirator control

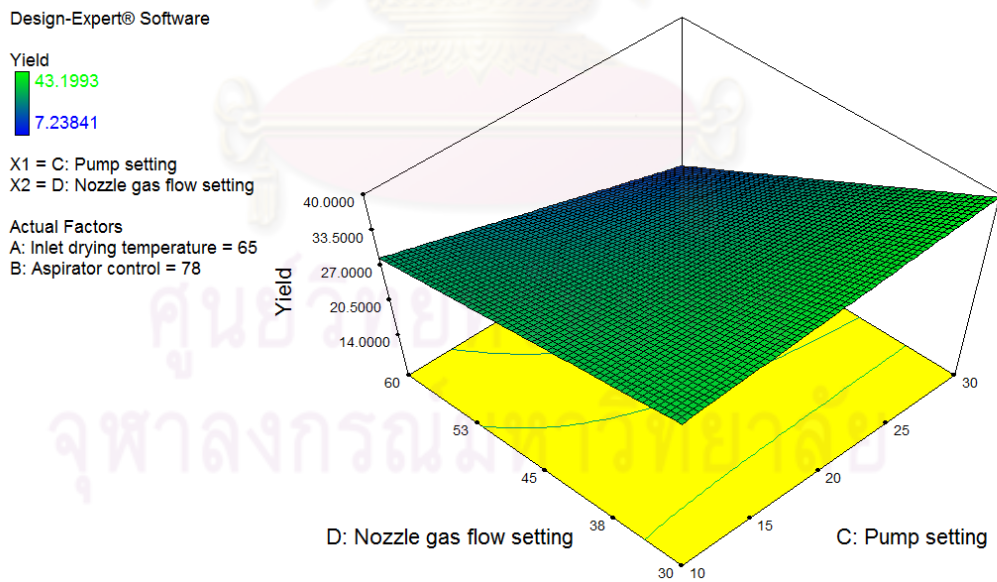


(b) Surface plot between inlet drying temperature and aspirator control

Figure 15 Contour plot and surface plot between inlet drying temperature and aspirator control of linear model for process yield



(a) Contour plot between pump setting and nozzle gas flow setting



(b) Surface plot between pump setting and nozzle gas flow setting

Figure 16 Contour plot and surface plot between pump setting and nozzle gas flow setting of linear model for process yield

2.2 Mass median diameter (MMD)

From the response data obtained from full factorial design and center point design, the mass median diameter of spray dried microparticles ranged from 2.460 to 5.454 μm depending on the variable level selected during spray drying operations. The factor effect estimate of MMD was shown in table 14 and ANOVA table for MMD in the full factorial design was shown in table 15.

Table 14 The factor effect estimate of mass median diameter

Term	Effect	% Contribution
T _{in} -Inlet drying temperature	-0.3259	4.5436
A-Aspirator control	-0.1184	0.5995
P-Pump setting	0.5219	11.6527
N-Nozzle gas flow setting	-0.7674	25.1948
T _{in} A	0.0904	0.3495
T _{in} P	-0.0249	0.0265
T _{in} N	-0.4301	7.9156
AP	0.1601	1.0970
AN	-0.4686	9.3961
PN	-0.5919	14.9884

ศูนย์วิทยทรัพยากร
จุฬาลงกรณ์มหาวิทยาลัย

Table 15 ANOVA table for the linear model for mass median diameter

Source of Variation	Sum of Squares	df	Mean Square	F Value	p-value
Model	6.9454	7	0.9922	6.4463	0.0046*
T _{in} -Inlet drying temperature	0.4248	1	0.4248	2.7598	0.1276
A-Aspirator control	0.0561	1	0.0561	0.3642	0.5596
P-Pump setting	1.0894	1	1.0894	7.0779	0.0239**
N-Nozzle gas flow setting	2.3555	1	2.3555	15.3034	0.0029*
T _{in} N	0.7400	1	0.7400	4.8080	0.0531
AN	0.8784	1	0.8784	5.7072	0.0380**
PN	1.4013	1	1.4013	9.1040	0.0130**
Curvature	0.8644	1	0.8644	5.6159	0.0393**
Residual	1.5392	10	0.1539		
Lack of Fit	1.3139	8	0.1642	1.4582	0.4690
Pure Error	0.2253	2	0.1126		
Cor Total	9.3490	18			

* Significant at p-value < 0.01

** Significant at p-value < 0.05

From ANOVA table, the linear model explaining process parameters on MMD (Y₂) is

$$\begin{aligned}
 Y_2 = & -2.77675 + 0.0482(T_{in}) + 0.0286(A) + 0.1149(P) \\
 & + 0.1609(N) - 0.0014(T_{in})(N) - 0.0007(A)(N) \\
 & - 0.0020(P)(N)
 \end{aligned}
 \tag{11}$$

Statistic analysis revealed the main factors affecting on MMD (Y₂) were pump setting (P) (p = 0.0239) and nozzle gas flow setting (N) (p = 0.0029). The main effect of pump setting and nozzle gas flow setting were plotted in figure 17 that showed positive and negative effect, respectively.

Design-Expert® Software

MMD

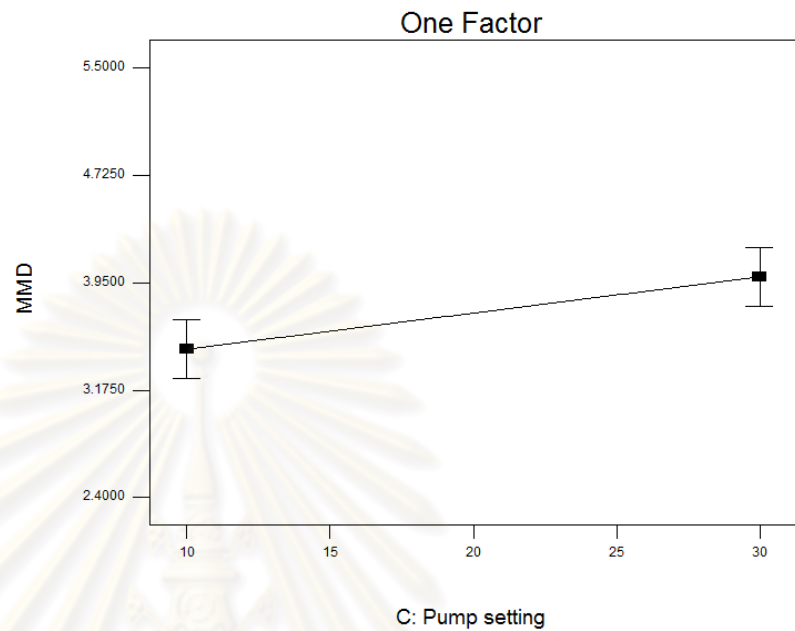
X1 = C: Pump setting

Actual Factors

A: Inlet drying temperature = 65

B: Aspirator control = 78

D: Nozzle gas flow setting = 45



(a) Pump setting (positive effect)

Design-Expert® Software

MMD

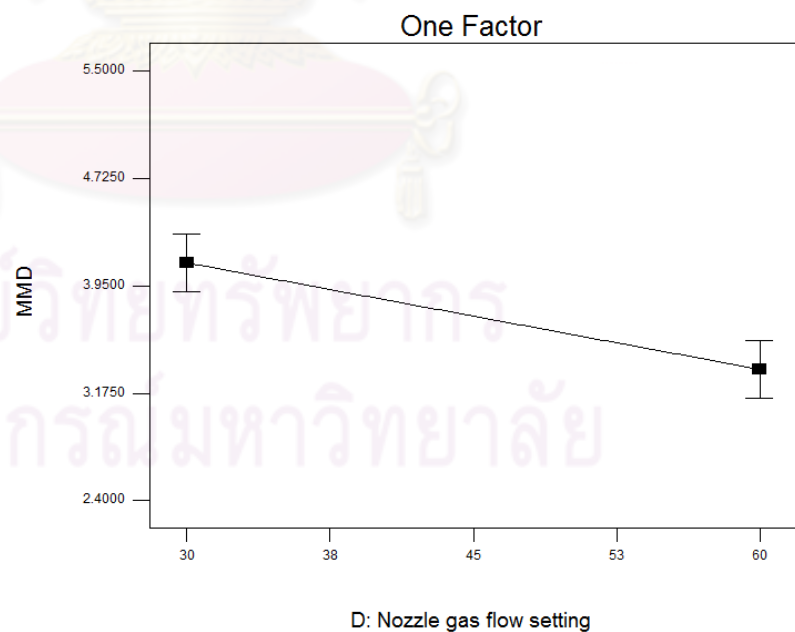
X1 = D: Nozzle gas flow setting

Actual Factors

A: Inlet drying temperature = 65

B: Aspirator control = 78

C: Pump setting = 20



(b) Nozzle gas flow setting (negative effect)

Figure 17 Main effect plots of linear model for mass median diameter

The main effect of pump setting can be explained that decreasing pump setting caused particle size decreased. Because the solution droplets were smaller when pump setting was decrease. The negative effect of nozzle gas flow setting can be explained that particle size decrease when nozzle gas flow setting was increase. Higher air spray and lower liquid flow setting which flow through the nozzle increased the shear force between the air and the liquid. This higher atomizing energy led to smaller droplets and consequently to smaller solid particles. In conclusion, decrease in microparticles size was observed with decreasing pump setting and increasing nozzle gas flow setting.

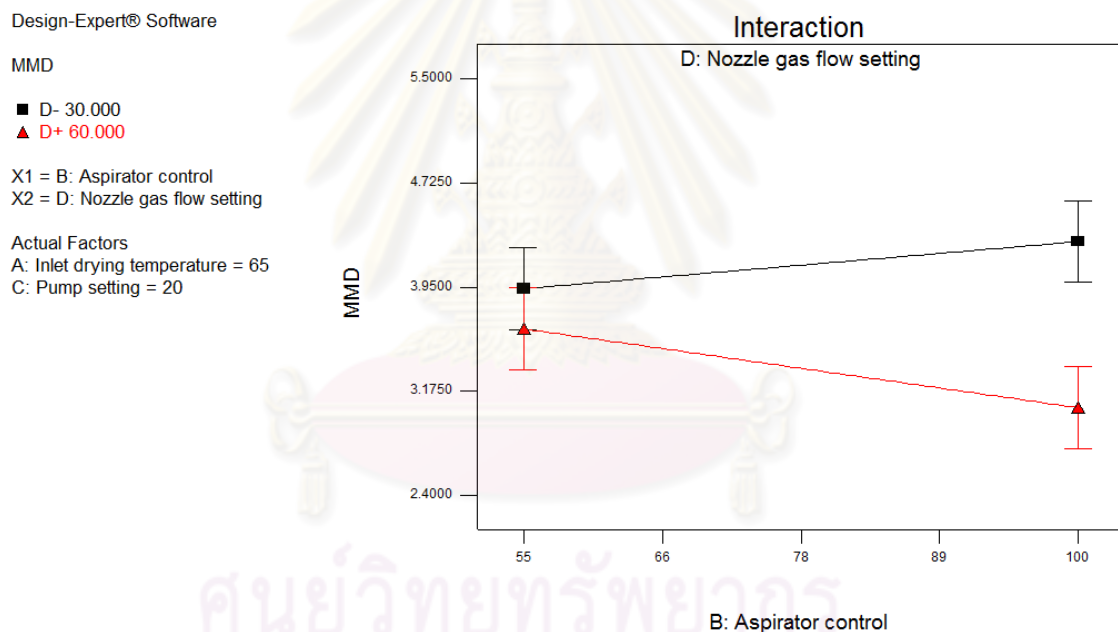


Figure 18 Interaction plot between aspirator control and nozzle gas flow setting of linear model for mass median diameter (high level shown as red line and low level shown as black line)

Moreover, there were statistically significant on the interaction between aspirator control and nozzle gas flow setting and the interaction between pump setting and nozzle gas flow setting. The interaction between aspirator control and nozzle gas flow setting (Figure 18) can be explained that nozzle gas flow setting effect is small

when aspirator control is at low level and large when the aspirator control is at the high level. Aspirator control showed positive effect when nozzle gas flow setting is at high level but showed negative effect on mass median diameter when nozzle gas flow setting is at low level. When nozzle gas flow setting was higher, the atomization force was increased that caused the obtained particle size was smaller. And the separation rate was increase when the aspirator control was at high level. Thus, spray drying condition with high nozzle gas flow setting and aspirator control produced small particles which were collected into the cyclone. The smallest mass median diameter obtained with high aspirator control and high nozzle gas flow setting condition.

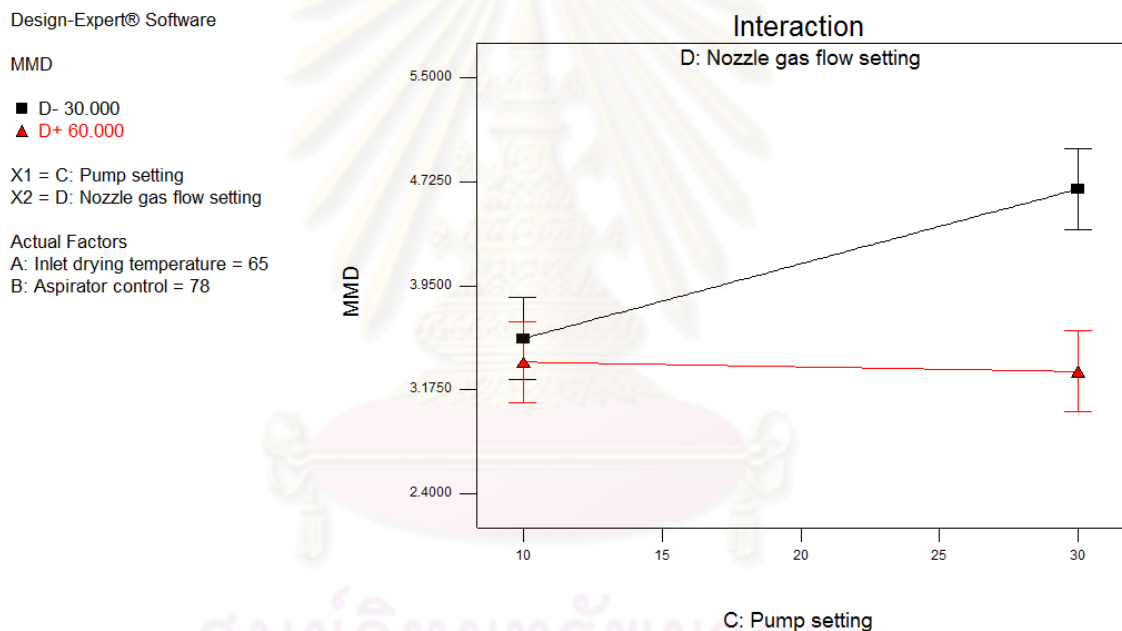


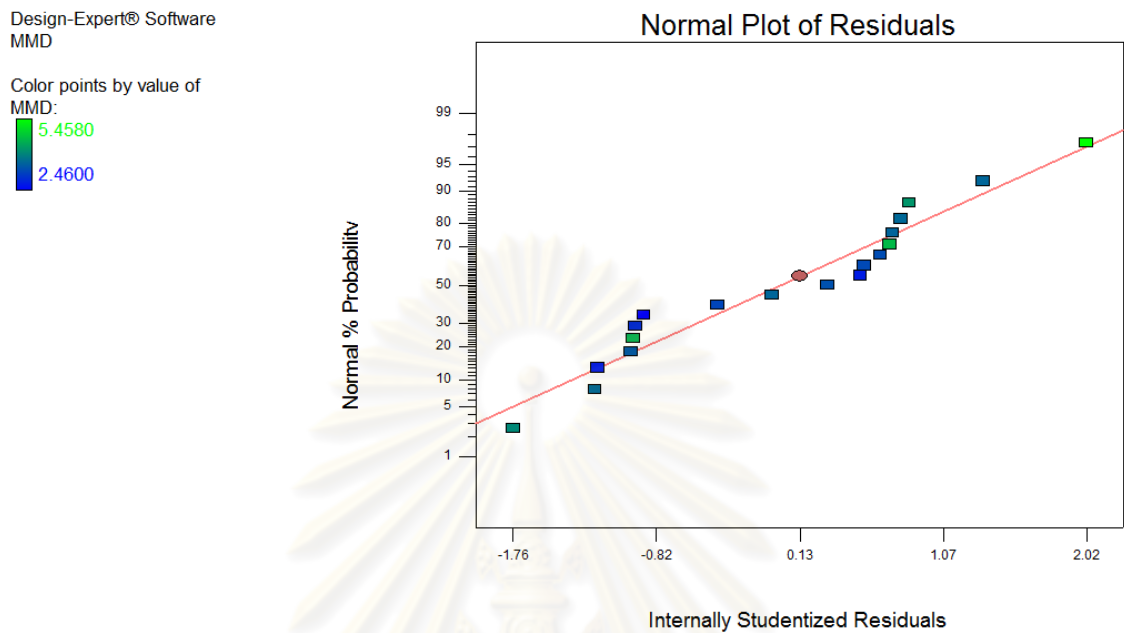
Figure 19 Interaction plot between pump setting and nozzle gas flow setting of linear model for mass median diameter (high level shown as red line and low level shown as black line)

In the same way, the interaction between pump setting and nozzle gas flow setting (Figure 19) can be explained that nozzle gas flow setting effect is small when the pump setting is at the low level and large when the pump setting is at the high level. Like aspirator control-nozzle gas flow setting interaction, the pump setting effect positively when nozzle gas flow setting is at low level and effect negatively

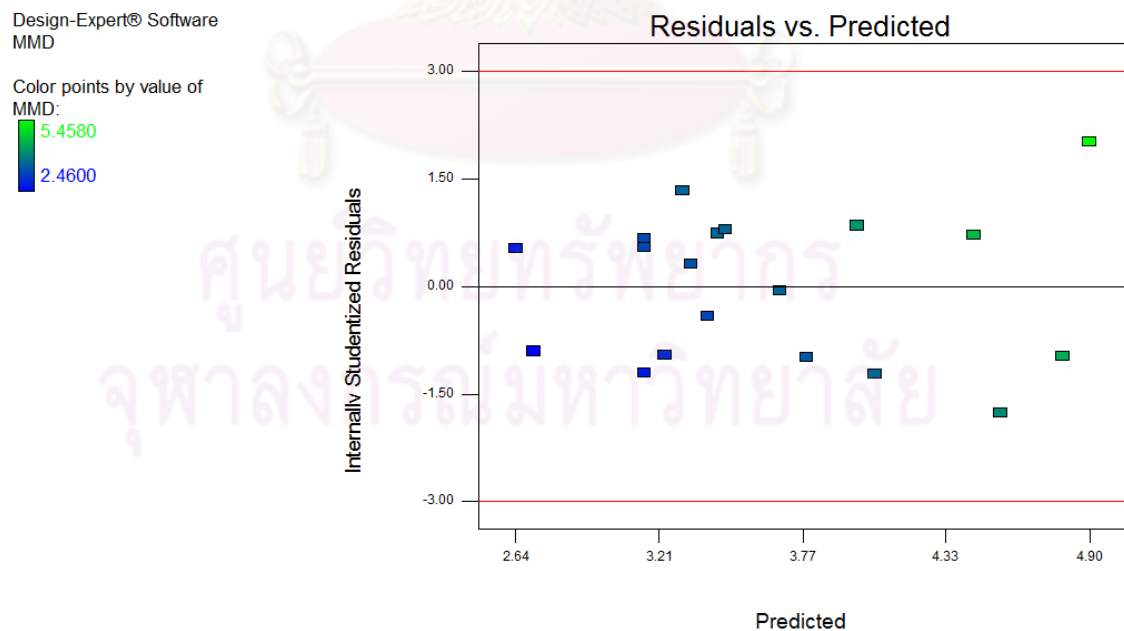
when nozzle gas flow setting is at high level. The solution droplets were enlarged when pump setting was increased. At low level of nozzle gas flow setting, the mass median diameters of the microparticles were larger when pump setting was increased. But when nozzle gas flow setting was increased, atomization force also increased so that the small particles were performed. The smallest particles obtained from low pump setting and high nozzle gas flow setting. In conclusion, the spray dried condition with high aspirator control, high pump setting and high nozzle gas flow setting could produce the smallest particle.

The R^2 value of this fitted equation was 0.8186, indicating a reasonably good fit. This linear model showed no lack of fit ($p = 0.4690$), no correlation in the residual plots and the residuals distribution was normal (as shown on figure 20).

The curvature of linear model (from table 15) showed significant ($p = 0.0393$) and the contour plot and response surface plot of both interaction effects showed non-linear correlation (Figure 21 and 22). The second-model would be used for further optimization of the spray drying parameters.

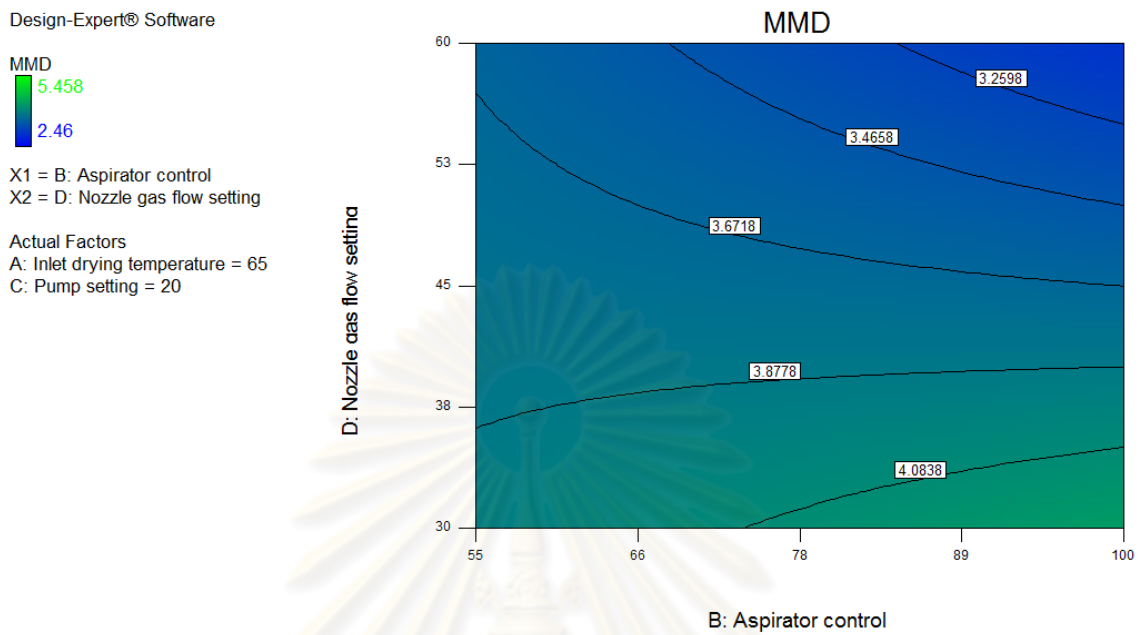


(a) Normal probability plot of residuals reveals no serious violation

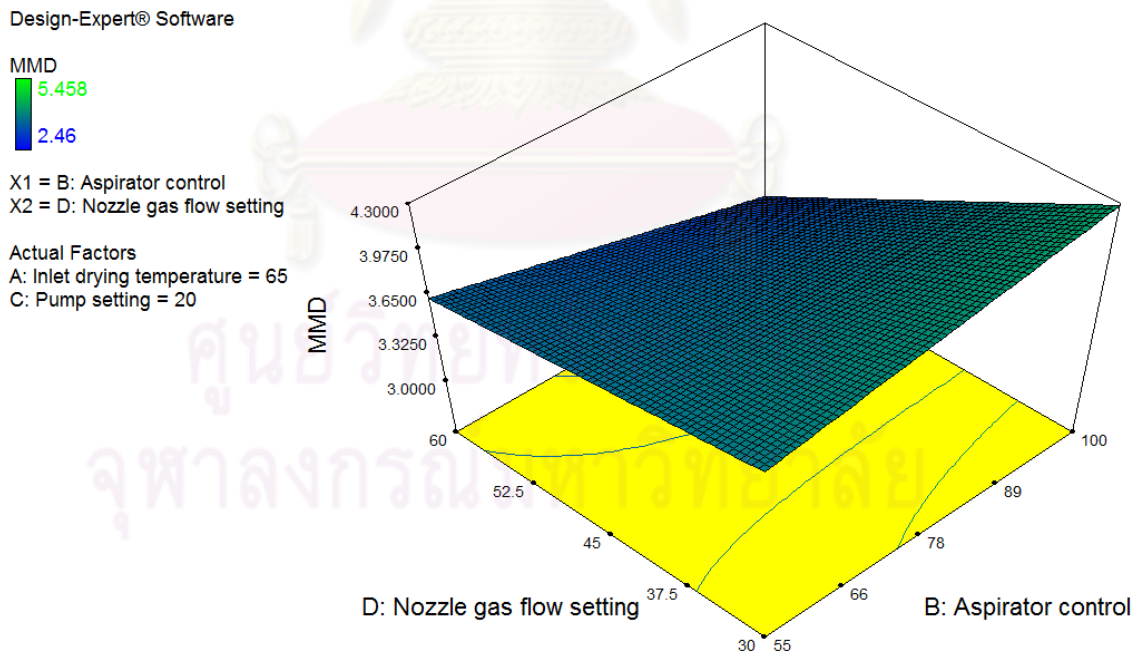


(b) Residuals versus predicted values did not reveals and obvious pattern

Figure 20 Residual analysis of linear model for mass median diameter

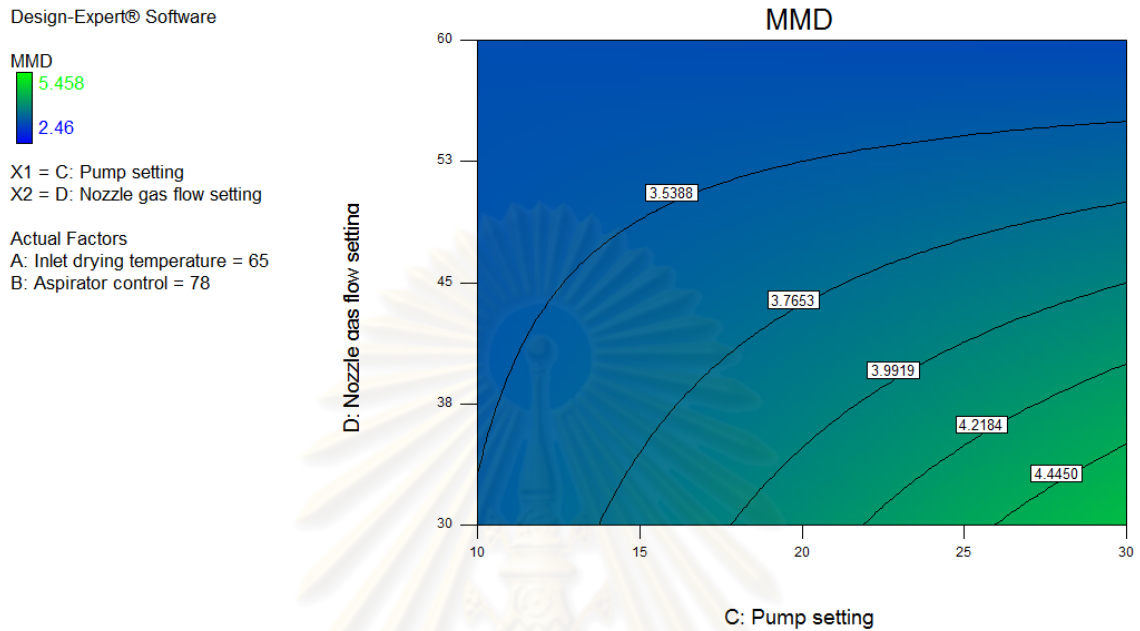


(a) Contour plot between aspirator control and nozzle gas flow setting

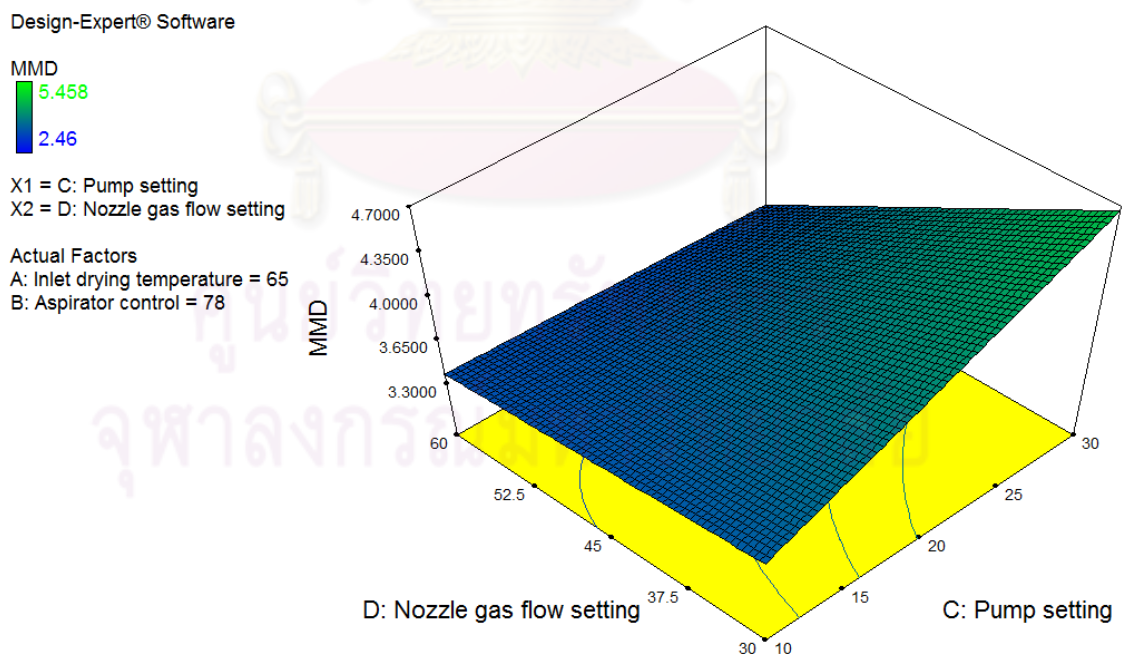


(b) Surface plot between aspirator control and nozzle gas flow setting

Figure 21 Contour plot and surface plot between aspirator control and nozzle gas flow setting of linear model for mass median diameter



(a) Contour plot between pump setting and nozzle gas flow setting



(b) Surface plot between pump setting and nozzle gas flow setting

Figure 22 Contour plots and surface plot between pump setting and nozzle gas flow setting of linear model for mass median diameter

2.3 Entrapment efficiency

From the response data obtained from full factorial and center points experiments. The entrapment efficiency of rifampicin-PLGA loaded microparticles lay from 85.5246% to 93.5574%. The factor effect estimate of entrapment efficiency in the 2^4 full factorial design was shown in table 16.

Table 16 The factor effect estimate of entrapment efficiency from a 2^4 factorial design

Term	Effect	% Contribution
T_{in} -Inlet drying temperature	1.4511	11.2024
A-Aspirator control	0.8975	4.2859
P-Pump setting	-0.0291	0.0045
N-Nozzle gas flow setting	1.0101	5.4287
$T_{in}A$	2.6350	36.9410
$T_{in}P$	-0.3601	0.6901
$T_{in}N$	-1.1474	7.0039
AP	0.1942	0.2006
AN	1.1295	6.7874
PN	-1.1124	6.5840

In general, if we have a single replicate of a 2^k design, and if h ($h < k$) factors are negligible and can be dropped, then the original data correspond to a full two-level factorial in the remaining $k - h$ factors with 2^h replicates (Montgomery, 2009). Pump setting show extremely less percentage of contribution than other factors. So, this factor and its interactions were negligible.

After pump setting was discarded, the design becomes a 2^3 factorial design in inlet drying temperature, aspirator control and nozzle gas flow setting with two replicates. The high order interactions were concluded. Table 17 and 18 show the factor effect estimate and the ANOVA table of entrapment efficiency from a 2^3 factorial design, respectively.

Table 17 The factor effect estimate of entrapment efficiency from a 2³ factorial design

Term	Effect	% Contribution
T _{in} -Inlet drying temperature	1.4510	8.4222
A-Aspirator control	0.8975	3.2222
N-Nozzle gas flow setting	1.0101	4.0814
T _{in} A	2.6350	27.7729
T _{in} N	-1.1473	5.2656
AN	1.1295	5.1029
T _{in} AN	1.1444	5.2386
Curvature	0.8483	2.8785
Lack Of Fit		0.0000
Pure Error		13.1974

Table 18 ANOVA table for the selected linear model of entrapment efficiency

Source of Variation	Sum of Squares	df	Mean Square	F Value	p-value
Model	39.4172	3	13.1391	5.5935	0.0098*
T_{in}-Inlet drying temperature	8.4222	1	8.4222	3.5854	0.0791**
A-Aspirator control	3.2222	1	3.2222	1.3717	0.2611
T_{in}A	27.7729	1	27.7729	11.8233	0.0040*
Curvature	2.8785	1	2.8785	1.2254	0.2870
Lack of Fit	19.6885	4	4.9221	3.7296	0.0416**
Pure Error	13.1974	10	1.3197		
Cor Total	75.1817	18			

* Significant at p-value < 0.01

** Significant at p-value < 0.05

The linear model explaining process parameters on entrapment efficiency (Y_3) is

$$Y_3 = 112.7154 - 0.3813(T_{in}) - 0.3607(A) + 0.0059(T_{in})(A) \quad (12)$$

Statistic analysis in table 18 revealed the significant main effect was inlet drying temperature. The main effect of inlet drying temperature plotted in figure 23 showed positive effect.

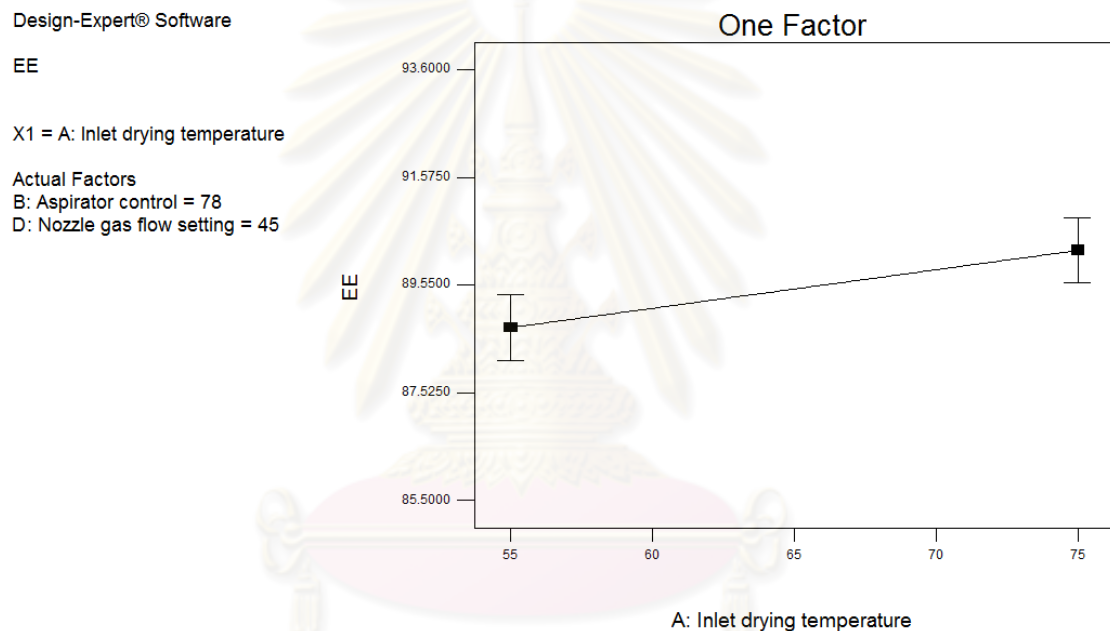


Figure 23 Main effect plots of first-model for entrapment efficiency

The interaction factors affecting on entrapment efficiency (Y_3) was the interaction between inlet drying temperature (T_{in}) and aspirator control (A) ($p = 0.0040$). The interaction between inlet drying temperature and aspirator control can be explained that aspirator control effect is small when the inlet drying temperature is at the low level and large when the inlet drying temperature is at the high level. At low level of aspirator control, inlet drying temperature showed negative effect but it showed positive effect at high level of aspirator control. The highest entrapment

efficiency obtained from high inlet drying temperature and high aspirator control (Figure 24).

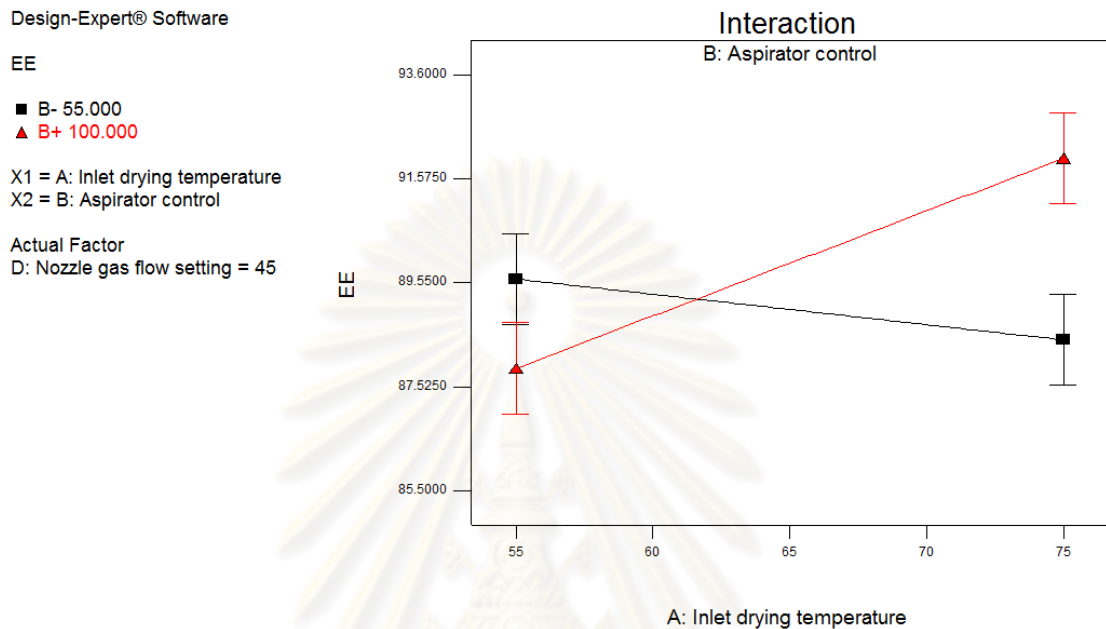


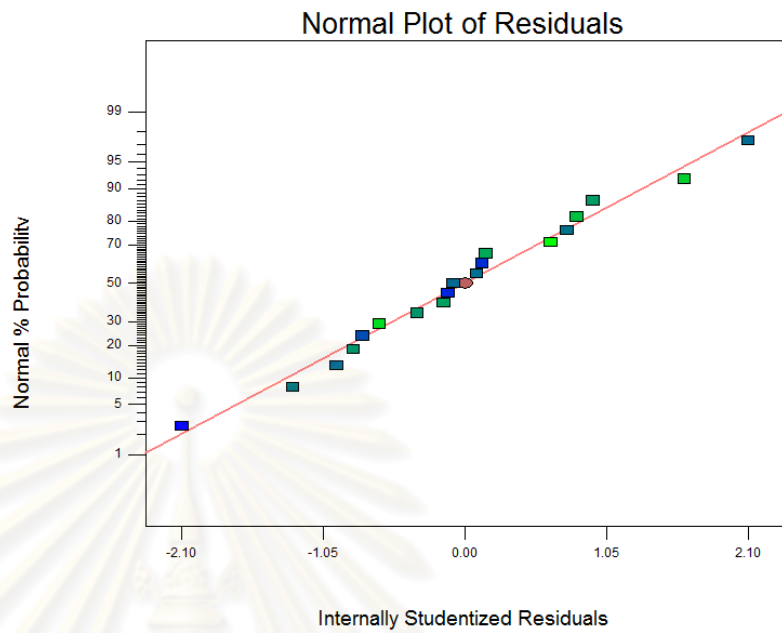
Figure 24 Interaction plot between inlet drying temperature and aspirator control of first-model for entrapment efficiency (high level shown as red line and low level shown as black line)

The correlation in the residual plots and the residuals distribution was shown on figure 25. The contour plot and response surface plot of both interaction effects showed non-linear correlation (Figure 26).

Although statistic analysis revealed the interaction factors affecting on entrapment efficiency but this linear model showed significantly lack of fit ($p = 0.0416$) and the R^2 value of this fitted equation was 0.5452 that also showed no goodness of fit. It indicated that entrapment efficiency was not affected all spray drying parameters (main effects). This may be due to the ratio between rifampicin and PLGA in the feeding solution was fixed. Therefore, the entrapment efficiency was not studied for the further optimization.

Design-Expert® Software
EE

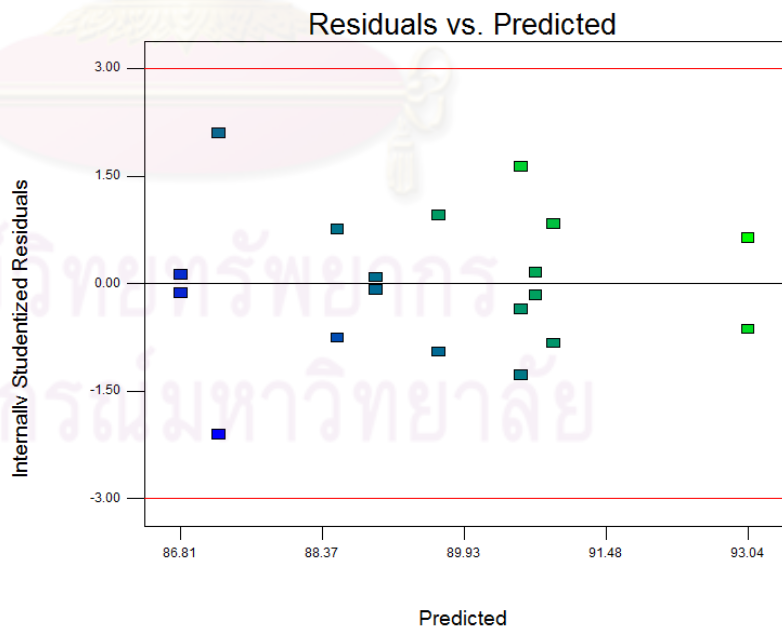
Color points by value of
EE:
93.5574
85.5246



(a) Normal probability plot of residuals reveals no serious violation

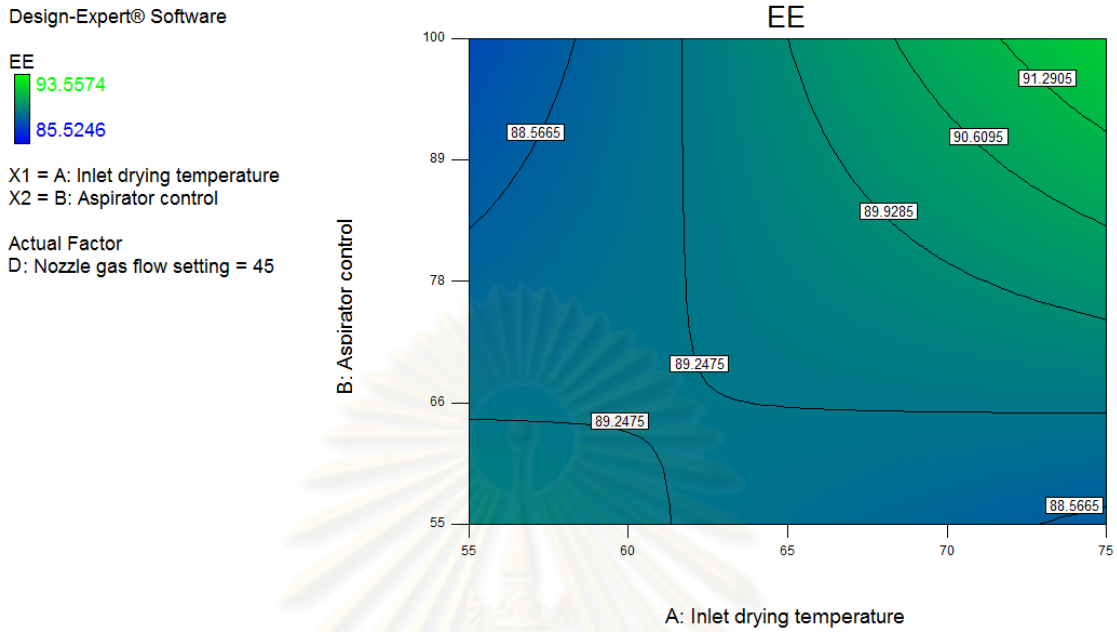
Design-Expert® Software
EE

Color points by value of
EE:
93.5574
85.5246

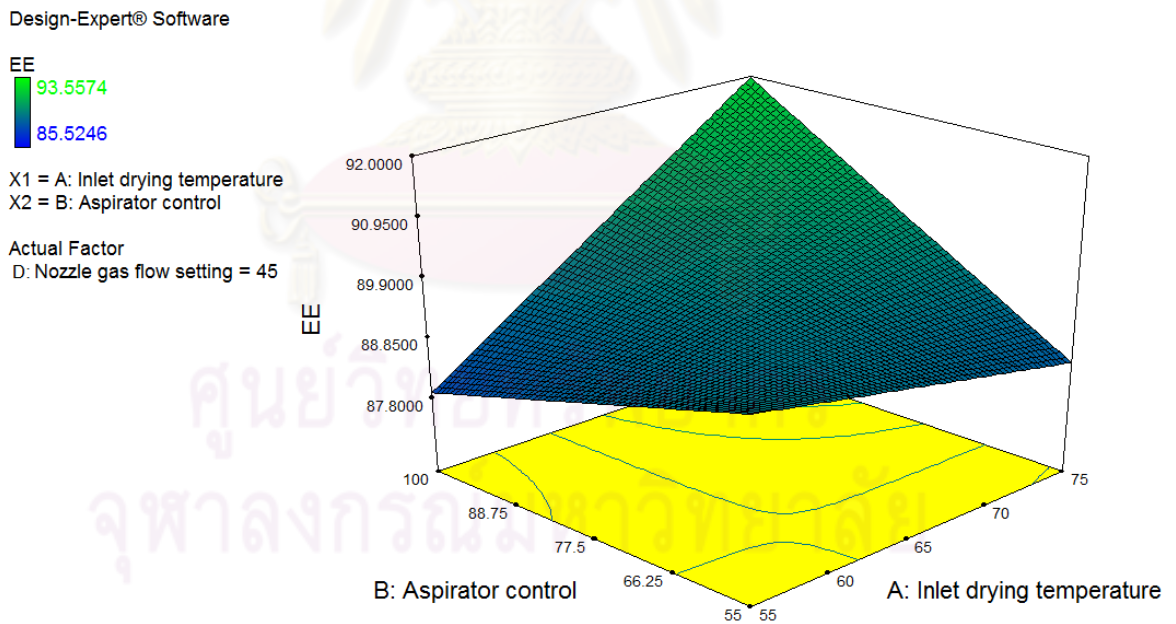


(b) Residuals versus predicted values reveals obvious pattern

Figure 25 Residual analysis of linear model for entrapment efficiency



(a) Contour plot between inlet drying temperature and aspirator control interaction



(b) Surface plot between inlet drying temperature and aspirator control interaction

Figure 26 Contour plot and surface plot between inlet drying temperature and aspirator control interaction of linear model for entrapment efficiency

2.4 Dissolution at 20 min

From the response data obtained from full factorial and center points design, dissolution at 20 min varied from 17.1463% to 50.3404%. The factor effect estimate of dissolution at 20 min was shown on table 19 and ANOVA table for dissolution at 20 min in the full factorial design was shown on table 20.

Table 19 The factor effect estimate of dissolution at 20 min

Term	Effect	% Contribution
T _{in} -Inlet drying temperature	5.2749	6.0871
A-Aspirator control	0.2055	0.0092
P-Pump setting	-0.0319	0.0002
N-Nozzle gas flow setting	-4.0901	3.6597
T _{in} A	-3.3435	2.4457
T _{in} P	11.2869	27.8701
T _{in} N	-7.4540	12.1553
AP	-5.1916	5.8965
AN	1.6960	0.6293
PN	-0.1253	0.0034

Table 18 ANOVA table for the selected factorial model of dissolution at 20 min

Source of Variation	Sum of Squares	df	Mean Square	F Value	p-value
Model	620.8761	3	206.9587	2.4064	0.1108
A-Inlet drying temperature	111.2967	1	111.2967	1.2941	0.2744
C-Pump setting	0.0041	1	0.0041	0.0000	0.9946
AC	509.5753	1	509.5753	5.9250	0.0289*
Curvature	3.4562	1	3.4562	0.0402	0.8440
Residual	1204.0637	14	86.0046		
Lack of Fit	782.5337	12	65.2111	0.3094	0.9246
Pure Error	421.5300	2	210.7650		
Cor Total	1828.3960	18			

* Significant at p-value < 0.05

The linear model explaining process parameters on dissolution at 20 min (Y_4) is

$$Y_4 = 89.1371 - 0.8649(T_{in}) - 3.6698(P) + 0.0564(T_{in})(P) \quad (13)$$

Statistic analysis revealed the interaction factors affecting on dissolution at 20 min (Y_4) was the interaction between inlet drying temperature (T_{in}) and pump setting (P) ($p = 0.0289$). This interaction can be explained that pump setting effect is small when the inlet drying temperature is at the high level and large when the inlet drying temperature is at the low level. The inlet drying temperature effect is positive at pump setting high level but it was negative effect at pump setting low level. The highest dissolution at 20 min obtained with high inlet drying temperature and high pump setting (Figure 27).

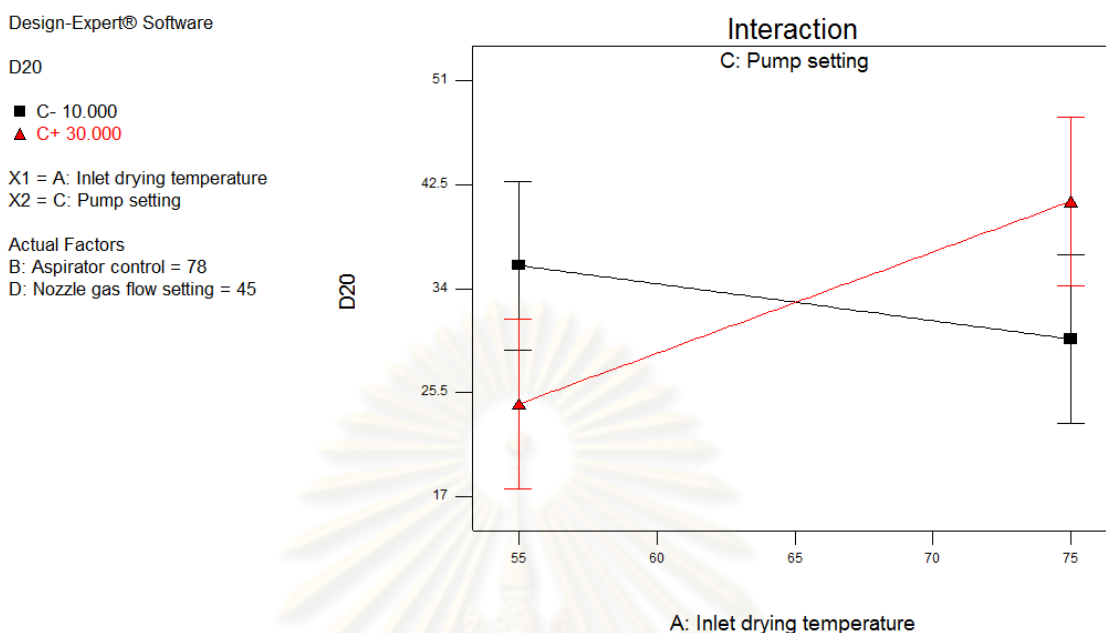
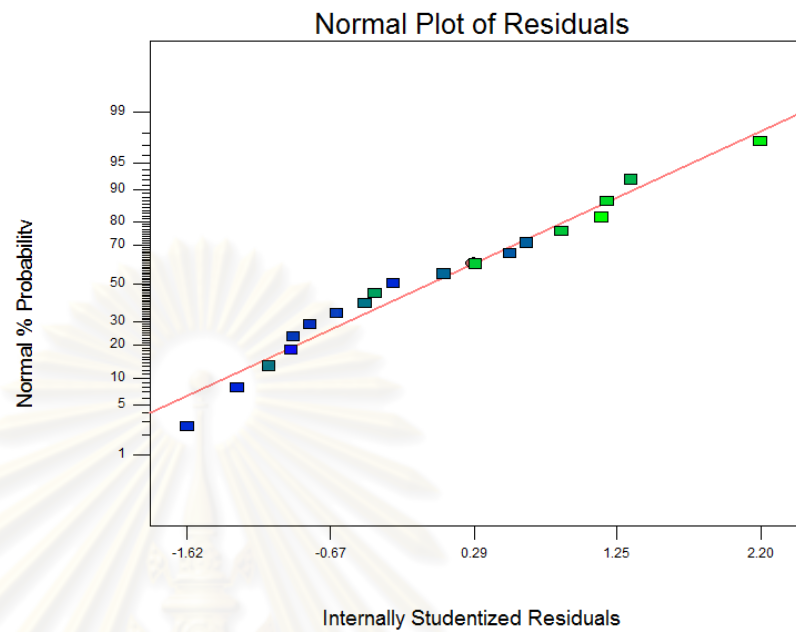
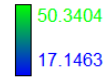


Figure 27 Interaction plot between inlet drying temperature and pump setting of linear model for dissolution at 20 min (high level shown as red line and low level shown as black line)

Although statistic analysis revealed the interaction factors affecting on dissolution at 20 min was the interaction between inlet drying temperature (T_{in}) and pump setting (P) and the linear model show no lack of fit ($p = 0.9246$). But the model statistic showed no significant ($p=0.1108$) and the R^2 value of this fitted equation was 0.3402 (low goodness of fit). The correlation in the residual plots and the residuals distribution was shown on figure 29. The contour plot and surface plot of interaction between inlet drying temperature and aspirator control was showed in figure28. Thus, like the entrapment efficiency, the main effects were not show the influence on dissolution at first 20 min. This may be due to the ratio between rifampicin and PLGA in the feeding solution was fixed. Therefore, the dissolution at 20 min response was not studied for the further optimization.

Design-Expert® Software
D20

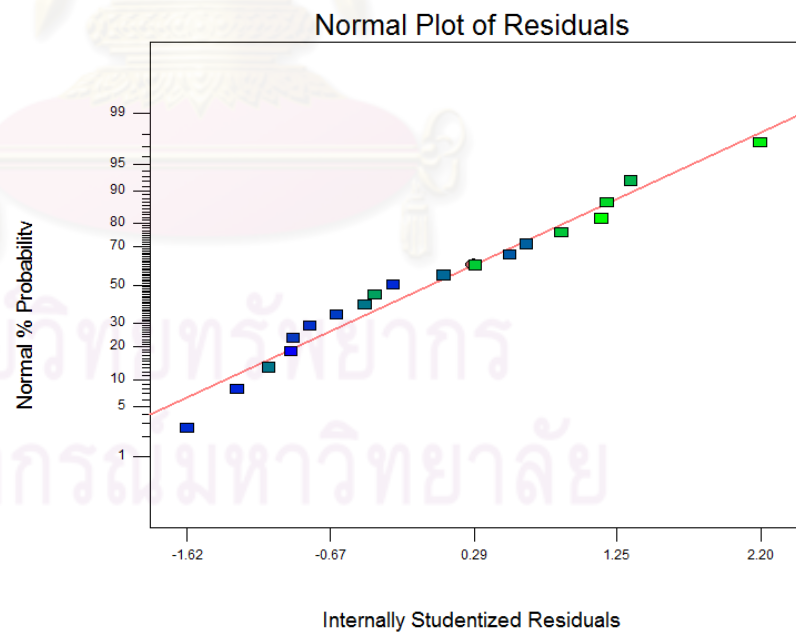
Color points by value of
D20:



(a) Normal probability plot of residuals reveals no serious violation

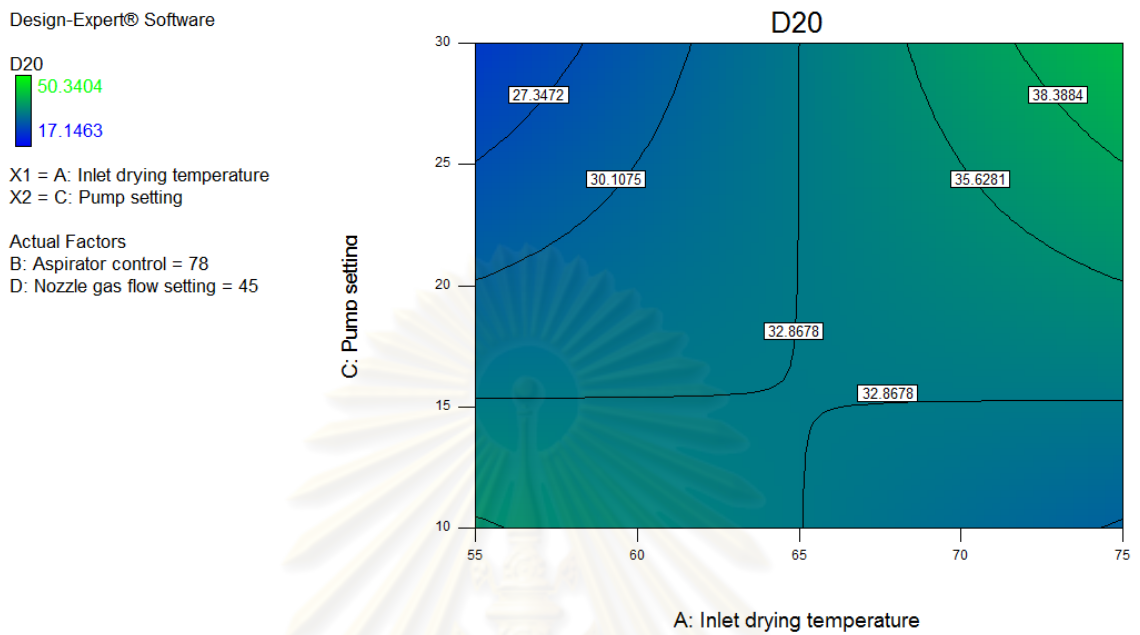
Design-Expert® Software
D20

Color points by value of
D20:

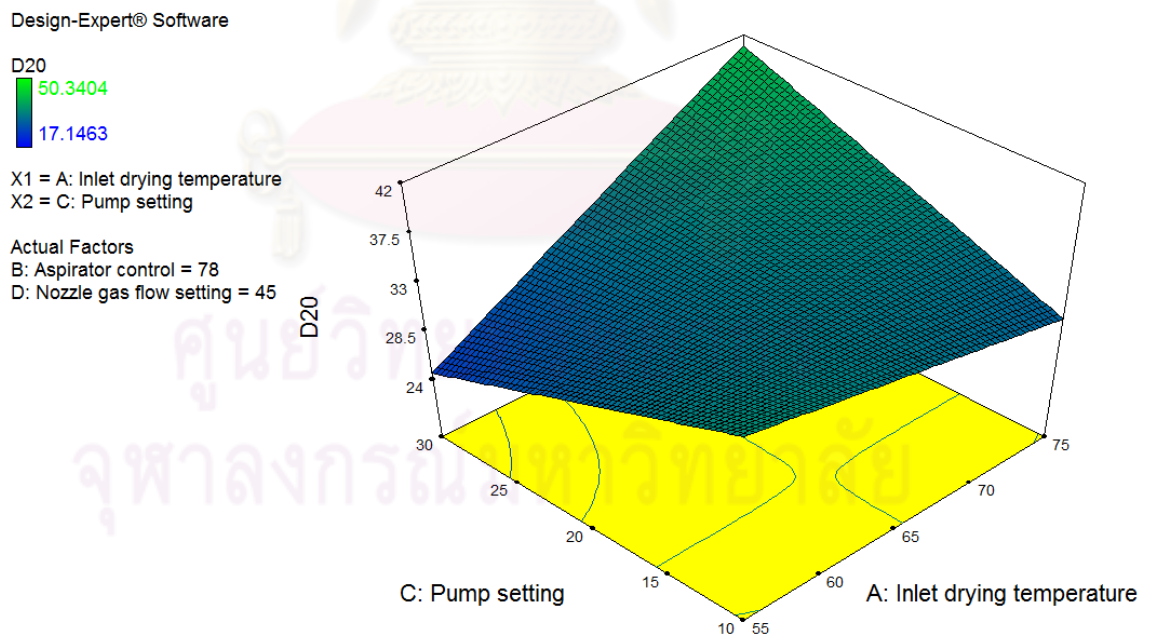


(b) Residuals versus predicted values reveal any pattern

Figure 28 Residual analysis of linear model for dissolution at 20 min



(a) Contour plot between inlet drying temperature and pump setting interaction



(b) Surface plot between inlet drying temperature and pump setting interaction

Figure 29 Contour plot and surface plot between inlet drying temperature and pump setting interaction of linear model for dissolution at 20 min

3. Central composite face centered (CCF) design

The main factors, interaction factors and quadratic terms in each equation were significant at the 95% confidence level. Selected model were accepted at no lack of fit ($p < 0.05$), regression model test ($p < 0.05$) and high goodness of fit (R^2). Only two interaction models were taken in to account. The non-significant terms were excluded from the equation for better models. The fitted equations are interpreted as follows: positive value in front of the response represents a direct effect and negative value indicates an inverse relationship between response and a factor.

Moreover, interaction term indicates that the effect of a variable produced by changing one parameter level depends on the level of the other parameter in the interaction term and quadratic terms implying that a minimum or approach to a minimum if the term is positive or a maximum or approach to maximum if the term is negative.

Results of the process yield (Y_1) and mass median diameter (Y_2) from central composite face centered design were shown in table 21.

Table 21 The data of interested responses from central composite face centered design

Experiment	Process parameter				Reponses	
	T _{in}	A	P	N	Y ₁	Y ₂
1	55	55	10	30	21.0312	3.416
2	75	55	10	30	41.7376	3.639
3	55	100	10	30	41.2390	3.665
4	75	100	10	30	40.7707	3.511
5	55	55	30	30	39.8516	4.644
6	75	55	30	30	34.2986	4.059
7	75	100	30	30	40.7471	5.458
8	55	55	10	60	20.0511	3.714
9	75	55	10	60	39.8501	3.668
10	55	100	10	60	40.1247	3.687
11	75	100	10	60	15.9714	2.460
12	55	55	30	60	7.2384	4.219
13	75	55	30	60	12.8814	2.962
14	55	100	30	60	43.1993	4.525
15	55	100	30	60	18.1279	3.281
16	75	100	30	60	18.0894	2.787
17	55	78	20	45	21.9201	2.939
18	75	78	20	45	22.7383	3.034
19	65	55	20	45	10.0403	3.353
20	65	100	20	45	12.7570	2.892
21	65	78	10	45	16.2414	3.099
22	65	78	30	45	17.8466	3.141
23	65	78	20	30	38.0235	3.777
24	65	78	20	60	10.5140	2.833
25	65	78	20	45	25.2223	3.357
26	65	78	20	45	23.1839	2.759
27	65	78	20	45	34.3012	3.322

3.1 Process yield

The obtained experiment data were used to fit the second-order equation. Process yield varied from 7.2384% to 43.1993%. The ANOVA table for process yield in the reduced quadratic design was shown on table 22.

The second-order model explaining the effects of process factors on process yield (Y_1) is

$$\begin{aligned}
 Y_1 = & -6.1332 + 1.5384(T_{in}) + 1.3320(A) \\
 & + 1.1198(P) - 3.4417(N) - 0.0188(T_{in})(A) \\
 & - 0.034(P)(N) - 0.0385(N)^2
 \end{aligned} \tag{14}$$

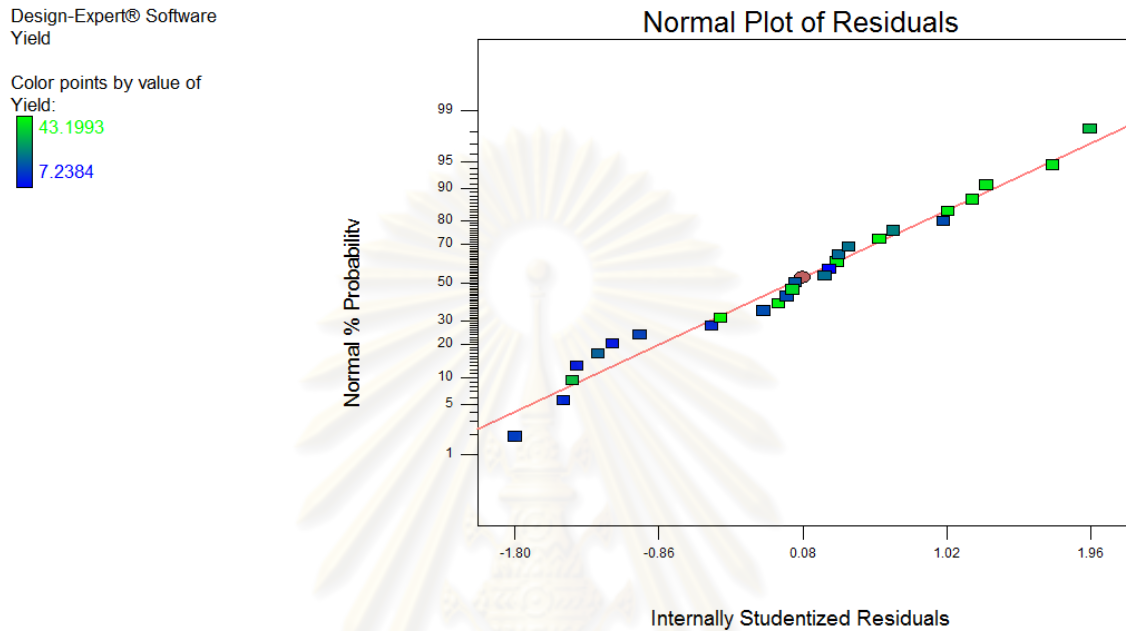
Table 22 ANOVA table for the reduced quadratic model of process yield

Source of Variation	Sum of Squares	df	Mean Square	F Value	p-value
Model	2684.8440	7	383.5491	6.8270	0.0004*
T_{in} -Inlet drying temperature	11.6634	1	11.6634	0.2076	0.6538
A-Aspirator control	108.6962	1	108.6962	1.9347	0.1803
P-Pump setting	111.1882	1	111.1882	1.9791	0.1756
N-Nozzle gas flow setting	1387.7715	1	1387.7715	24.7015	< 0.0001*
$T_{in}A$	286.6500	1	286.6500	5.1022	0.0358**
PN	332.8630	1	332.8630	5.9248	0.0250**
N^2	450.0552	1	450.0552	8.0107	0.0107**
Residual	1067.4507	19	56.1816		
Lack of Fit	997.3919	17	58.6701	1.6749	0.4384
Pure Error	70.0588	2	35.0294		
Cor Total	3752.2947	26			

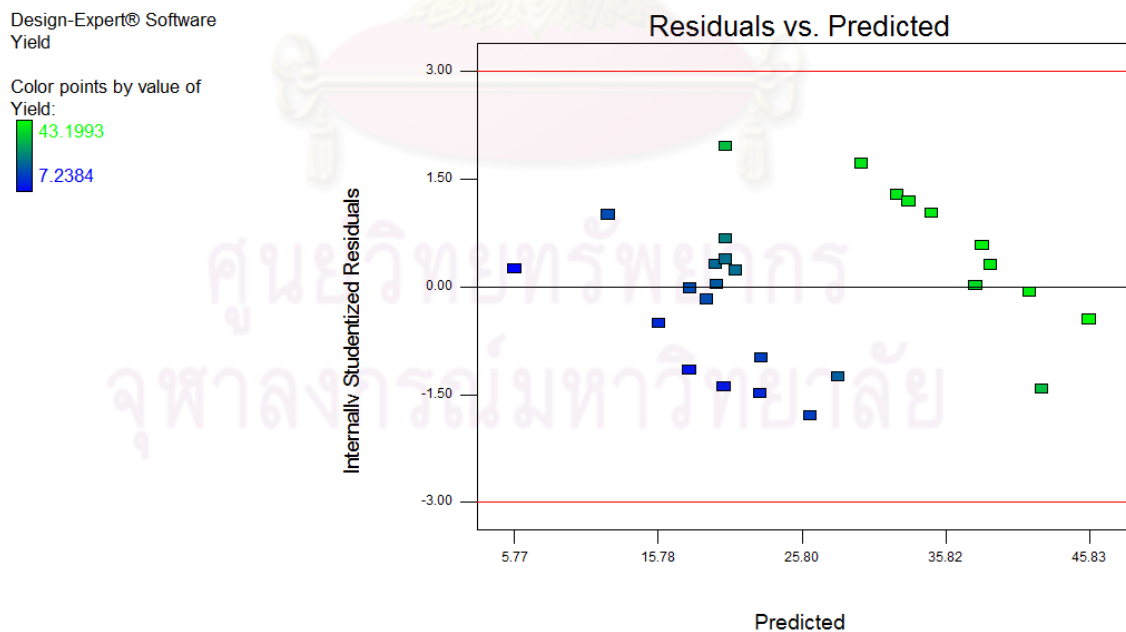
* Significant at p-value < 0.01

** Significant at p-value < 0.05

The normal probability plot of the residuals to check the violation of normality assumption and the plot of the residuals versus the predicted values for the process yield were shown in figure 30.



(a) Normal probability plot of residuals revealed no serious violation



(b) Residuals versus predicted values did not reveal any obvious pattern

Figure 30 Residual analysis of the quadratic model for process yield

Statistic analysis revealed the spray dried parameters affecting on process yield (Y_1) were the nozzle gas flow setting (at 99% confidence interval), the interaction between inlet drying temperature (T_{in}) and aspirator control (A) and the interaction between pump setting (P) and nozzle gas flow setting (N) (at 95% confidence interval). The effect of nozzle gas flow setting can be described that the process yield was increased when nozzle gas flow setting was decreased (Figure 31).

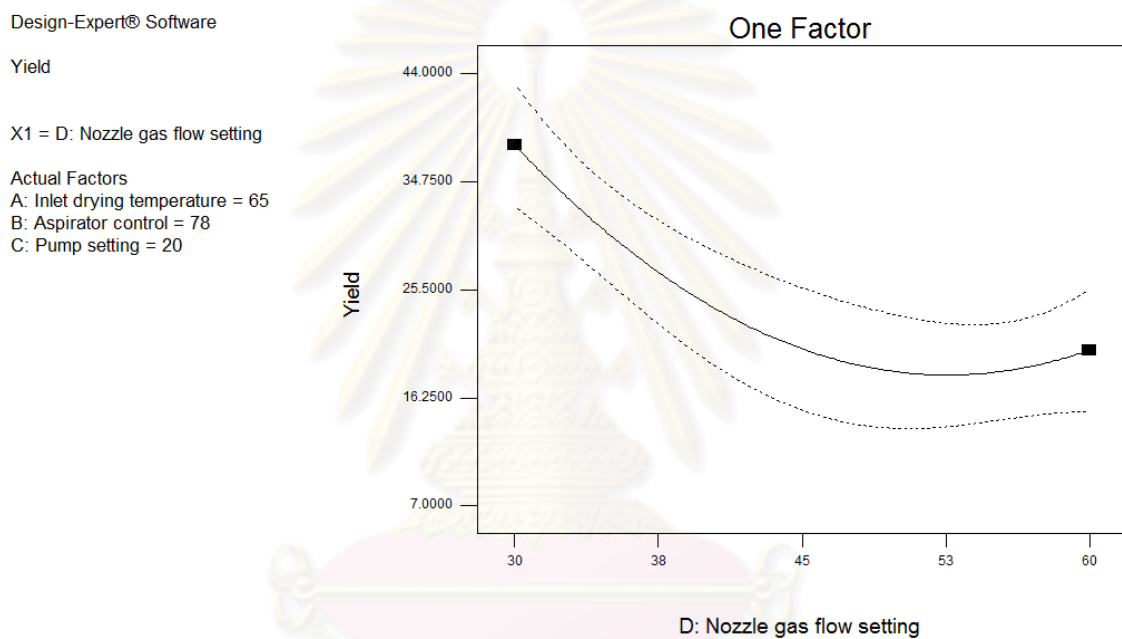


Figure 31 Main effect plot of nozzle gas flow setting for process yield on quadratic model

The interaction between inlet drying temperature and aspirator control can be explained that aspirator control effect is small when the inlet drying temperature is at the high level and large when the inlet drying temperature is at the low level. The inlet drying temperature effect is positive at the low level of aspirator control and negative at the high level. The highest process yield obtained with low inlet drying temperature and high aspirator control (Figure 32).

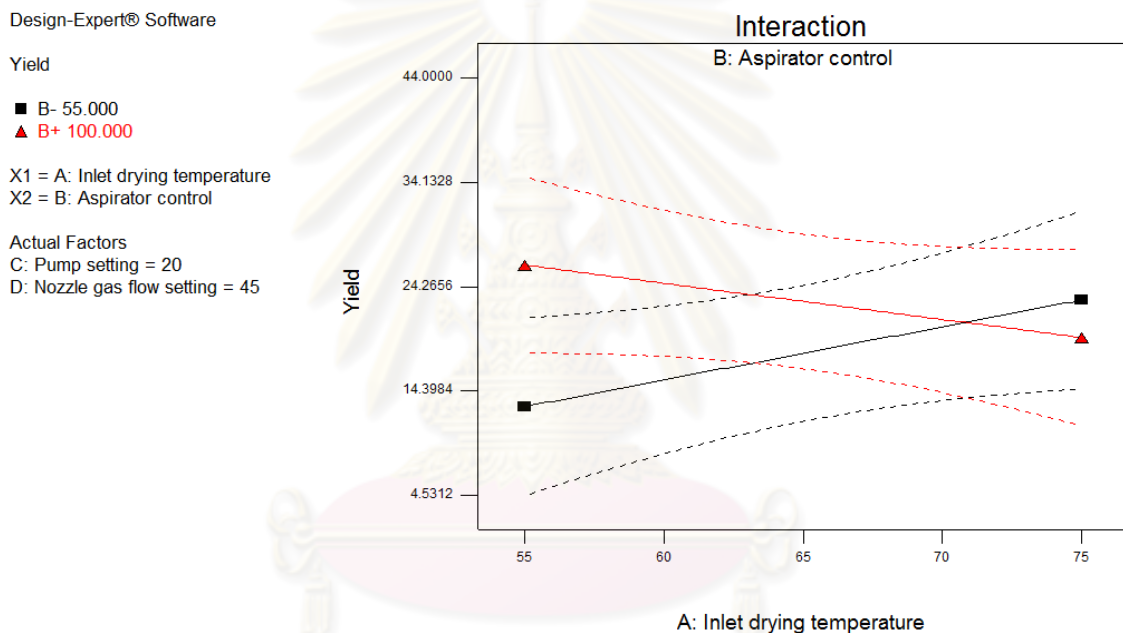


Figure 32 Interaction plot between inlet drying temperature and aspirator control of quadratic model for process yield (high level shown as red line and low level shown as black line)

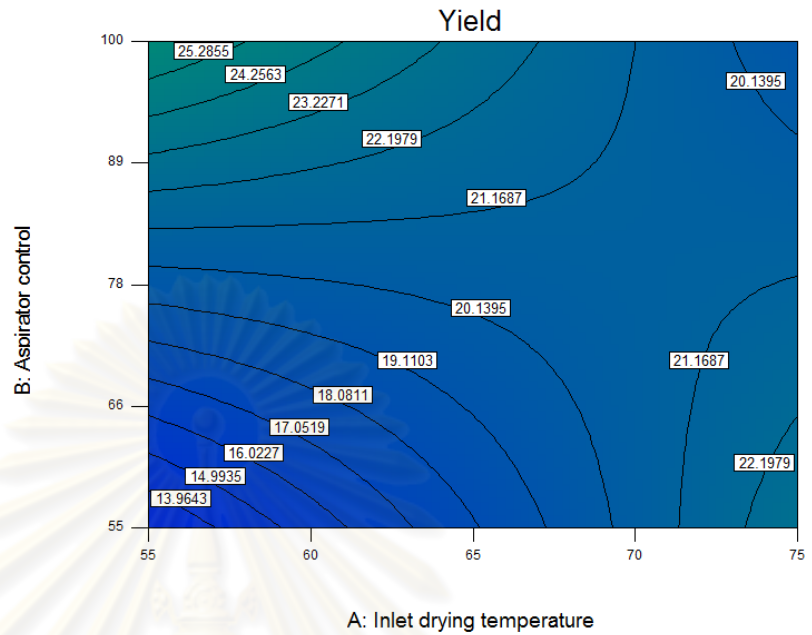
The contour plot and surface plot of interaction between inlet drying temperature and aspirator control of quadratic model was shown in figure 33.

Design-Expert® Software

Yield
 43.1993
 7.23841

X1 = A: Inlet drying temperature
 X2 = B: Aspirator control

Actual Factors
 C: Pump setting = 20
 D: Nozzle gas flow setting = 45



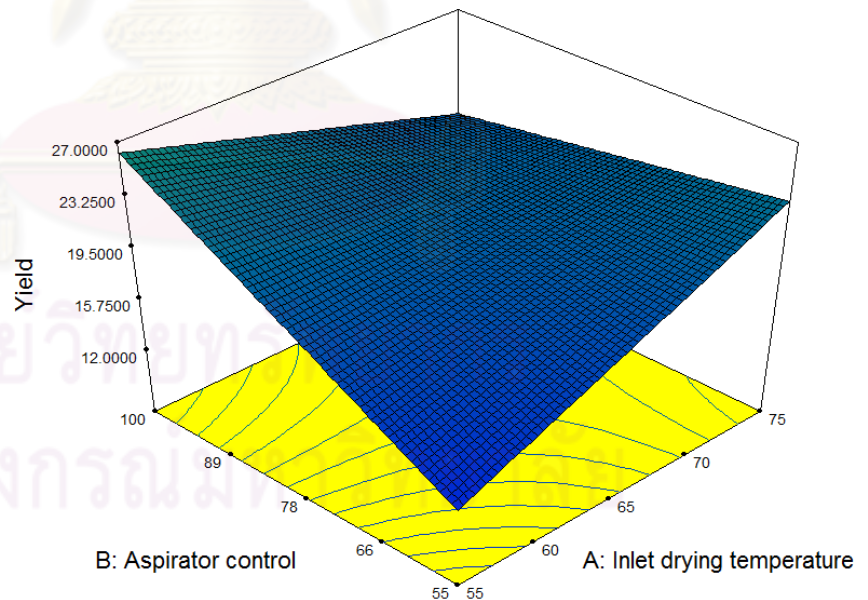
(a) Contour plot between inlet drying temperature and aspirator control

Design-Expert® Software

Yield
 43.1993
 7.23841

X1 = A: Inlet drying temperature
 X2 = B: Aspirator control

Actual Factors
 C: Pump setting = 20
 D: Nozzle gas flow setting = 45



(b) Surface plot between inlet drying temperature and aspirator control

Figure 33 Contour plot and surface plot between inlet drying temperature and aspirator control of quadratic model for the process yield

Moreover, the interaction between pump setting and nozzle gas flow setting can be explained that nozzle gas flow setting effect is small when the pump setting is at the low level and large when the pump setting is at the high level. The pump setting show positive effect at low level of nozzle gas flow setting and show negative effect when nozzle gas flow setting is at high level. The highest process yield obtained with high pump setting and low nozzle gas flow setting (Figure 34). The highest process yield thus obtain from low level of inlet drying temperature and nozzle gas flow setting while aspirator control and pump setting in high level. This result is same as the previous result obtaining from factorial design section.

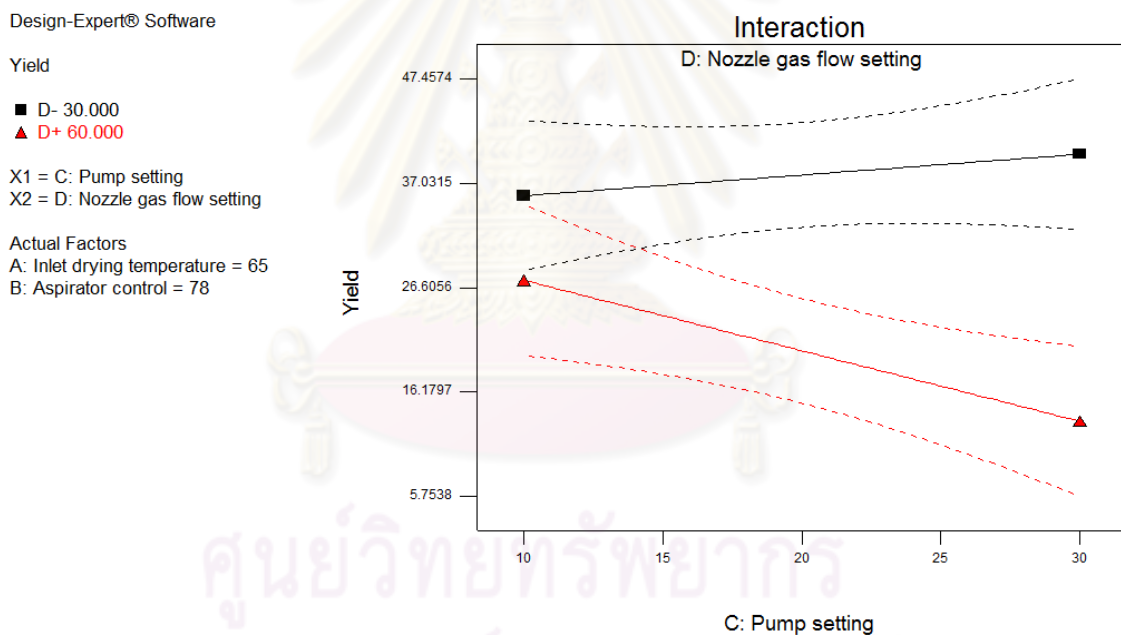
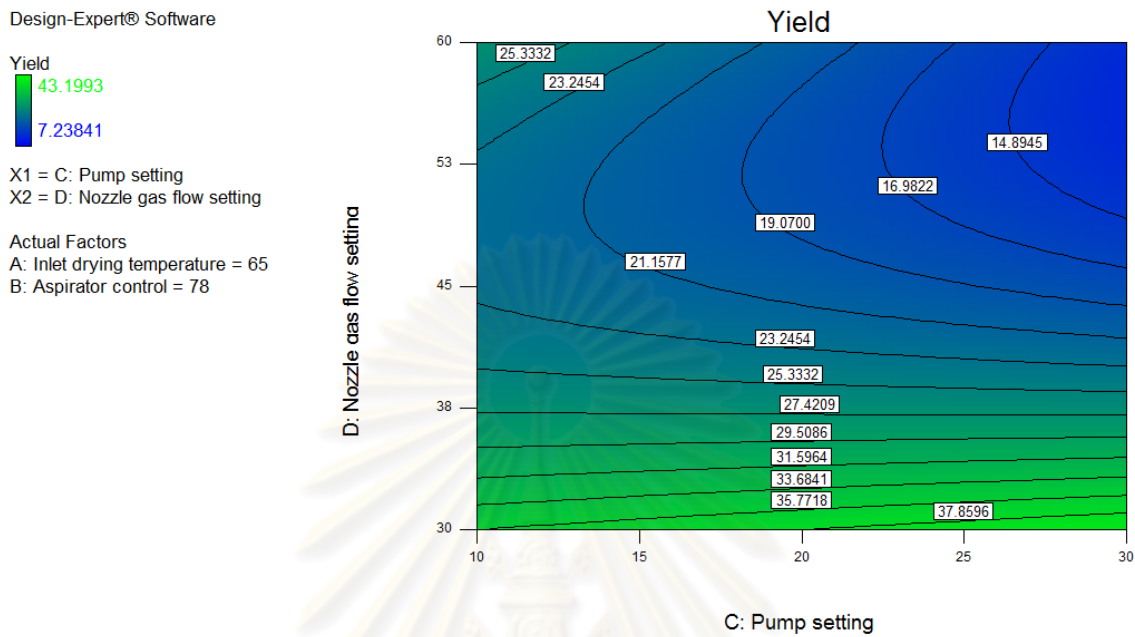
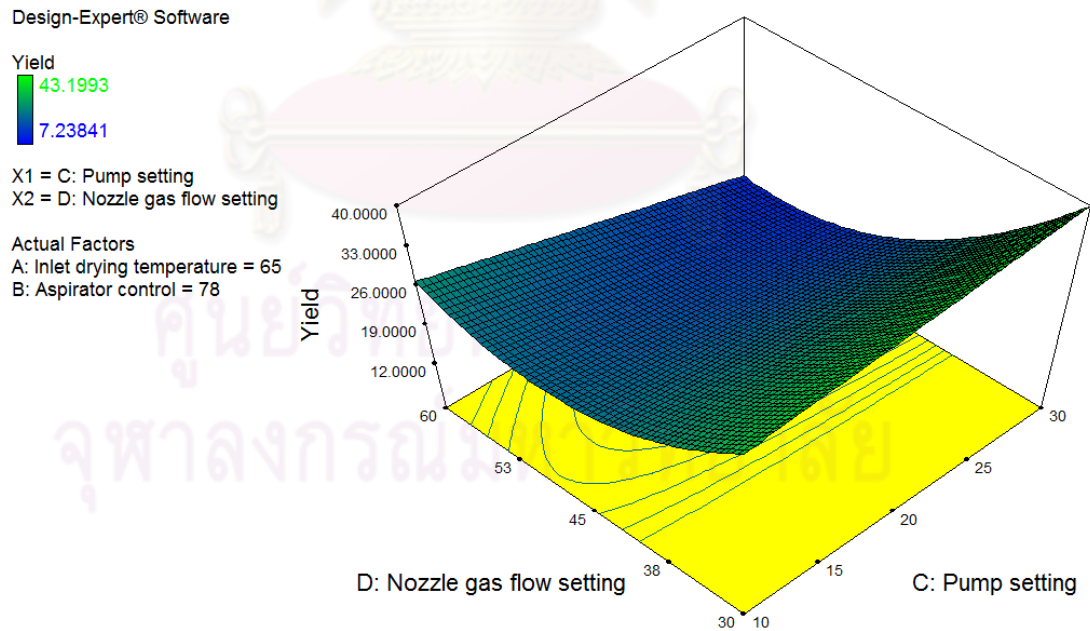


Figure 34 Interaction plot between pump setting and nozzle gas flow setting of quadratic model for process yield (high level shown as red line and low level shown as black line)

The contour plot and surface plot of interaction between pump setting and nozzle gas flow setting of quadratic model was shown in figure 35.



(a) Contour plot between pump setting and nozzle gas flow setting



(b) Surface plot between pump setting and nozzle gas flow setting

Figure 35 Contour plot and surface plot between pump setting and nozzle gas flow setting of quadratic model for the process yield

3.2 Mass median diameter (MMD)

The mass median diameter of spray dried microparticles ranged from 2.460 to 5.458 μm depending on the variable level selected during spray drying operations.

The quadratic model explaining the effects of process factors on mass median diameter (Y_2) is

$$\begin{aligned}
 Y_2 = & 1.8443 + 0.0506(T_{in}) + 0.0277(A) + 0.1122(P) \\
 & - 0.0728(N) - 0.0014(T_{in})(N) - 0.0007(A)(N) \\
 & - 0.0020(P)(N) + 0.00026(N)^2
 \end{aligned} \tag{15}$$

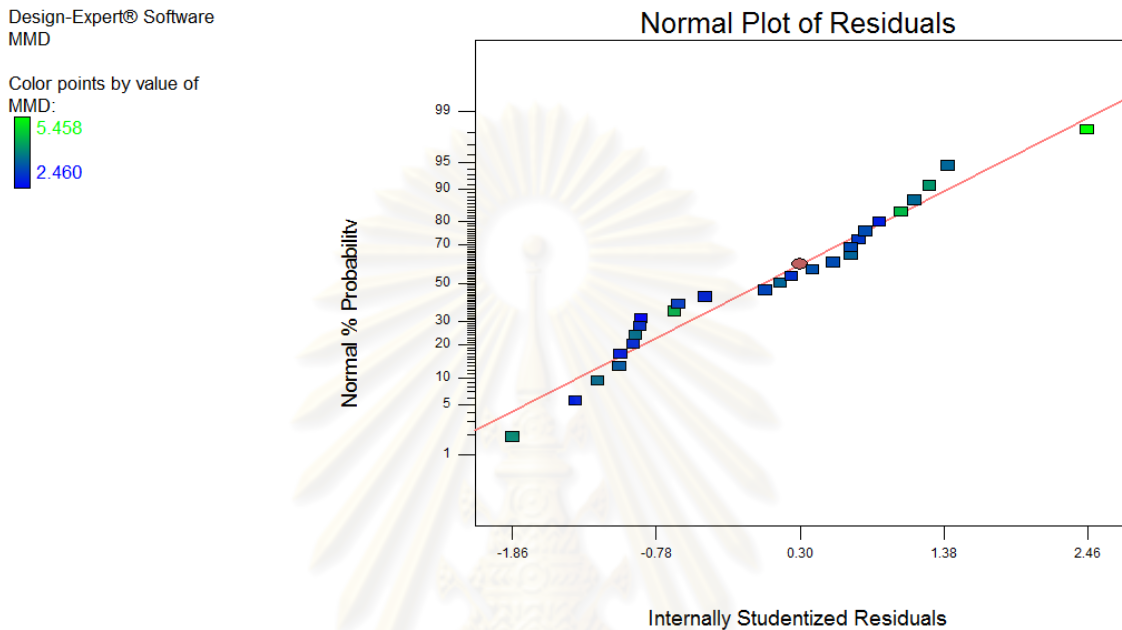
Table 23 ANOVA table for the reduced quadratic model of mass median diameter

Source of Variation	Sum of Squares	df	Mean Square	F Value	p-value
Model	9.3067	8	1.1633	9.7926	< 0.0001*
T_{in} -Inlet drying temperature	0.3506	1	0.3506	2.9509	0.1030
A-Aspirator control	0.1129	1	0.1129	0.9507	0.3425
C-Pump setting	0.9879	1	0.9879	8.3163	0.0099*
N-Nozzle gas flow setting	2.7789	1	2.7789	23.3923	0.0001*
$T_{in}N$	0.7400	1	0.7400	6.2294	0.0225**
AN	0.8800	1	0.8800	7.4078	0.0140**
CN	1.4013	1	1.4013	11.7954	0.0030*
N^2	2.0384	1	2.0384	17.1583	0.0006*
Residual	2.1384	18	0.1188		
Lack of Fit	1.9131	16	0.1196	1.0616	0.5896
Pure Error	0.2253	2	0.1126		
Cor Total	11.4450	26			

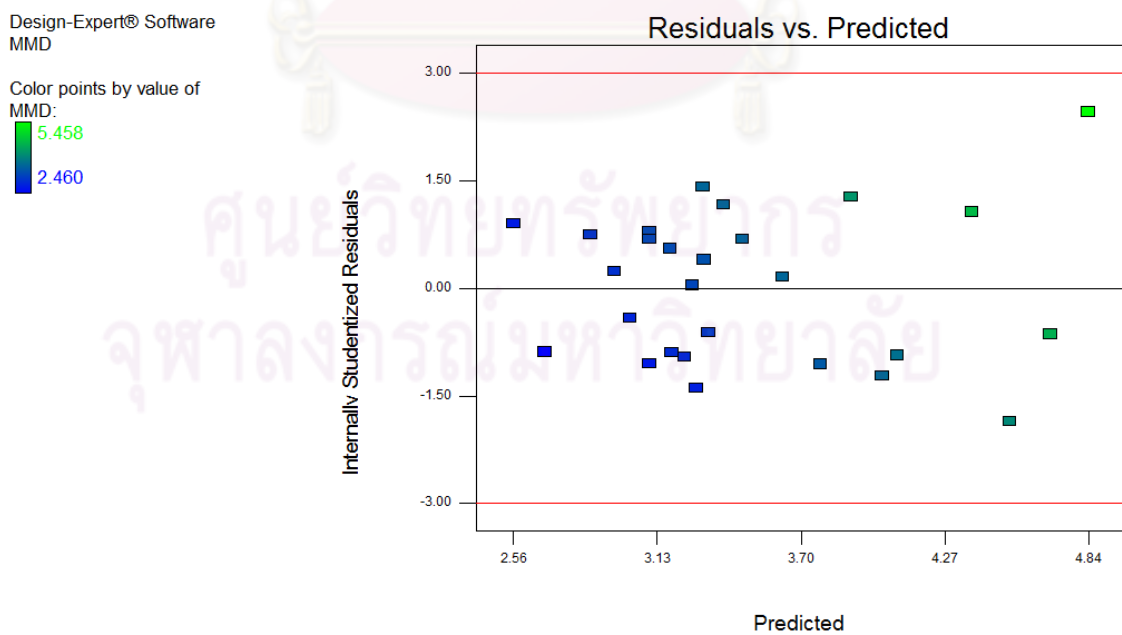
* Significant at p-value < 0.01

** Significant at p-value < 0.05

The normal probability plot of the residuals to check the violation of normality assumption and the plot of the residuals versus the predicted values for the process yield were shown in figure 36.



(a) Normal probability plot of residuals revealed no serious violation



(b) Residuals versus predicted values did not reveal any obvious pattern

Figure 36 Residual analysis of quadratic model for mass median diameter

Statistic analysis revealed the spray drying parameters affecting on mass median diameter (Y_2) were the pump setting and nozzle gas flow setting (at 99% confidence interval). The effect of pump setting can be explained that the mass median diameter was decreased when pump setting was decreased (Figure 37a). The effect of nozzle gas flow setting can be explained that the mass median diameter was decreased when nozzle gas flow setting was increased (Figure 37b).

Design-Expert® Software

MMD

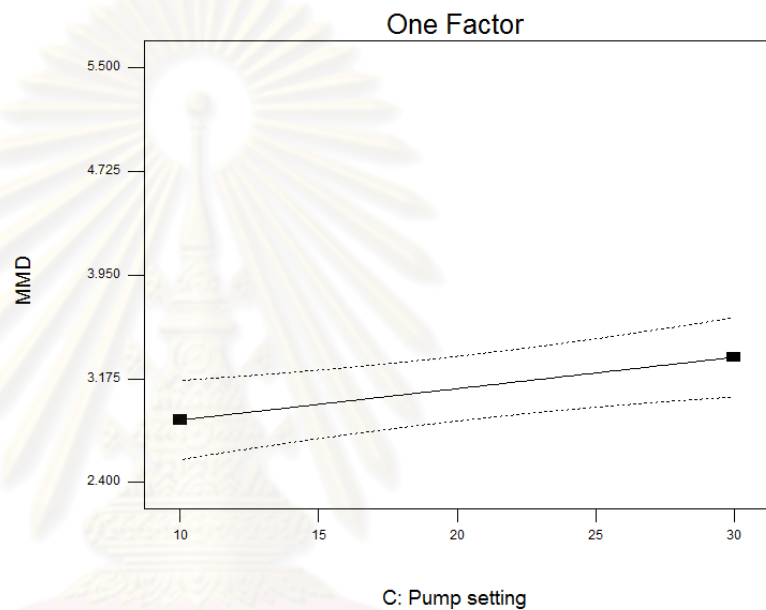
X1 = C: Pump setting

Actual Factors

A: Inlet drying temperature = 65

B: Aspirator control = 78

D: Nozzle gas flow setting = 45



(a) Pump setting (positive effect)

Design-Expert® Software

MMD

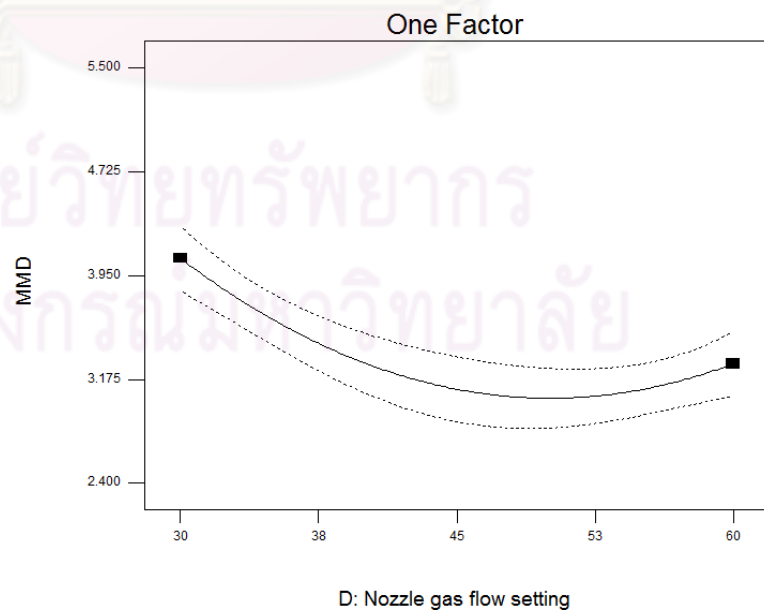
X1 = D: Nozzle gas flow setting

Actual Factors

A: Inlet drying temperature = 65

B: Aspirator control = 78

C: Pump setting = 20



(b) Nozzle gas flow setting (negative effect)

Figure 37 Main effect plots of quadratic model for mass median diameter

The interaction between inlet drying temperature and nozzle gas flow setting can be explained that nozzle gas flow setting effect is small when the inlet drying temperature is at the low level and large when the inlet drying temperature is at the high level. Inlet drying temperature effect is positive at low level of nozzle gas flow setting but negative at high level nozzle gas flow setting. The smallest particle obtained with high inlet drying temperature and high nozzle gas flow setting (Figure 38). The evaporation rate of solvent is increased by increasing inlet drying temperature. It causes the shrink of the microparticles and the obtained particles are smaller (Tomoda et al., 2008). High nozzle gas flow setting also caused particle size decreasing. So, the microparticles obtaining from high nozzle gas flow setting and high inlet drying temperature condition showed smaller mass median diameter that low nozzle gas flow setting and inlet drying temperature condition.

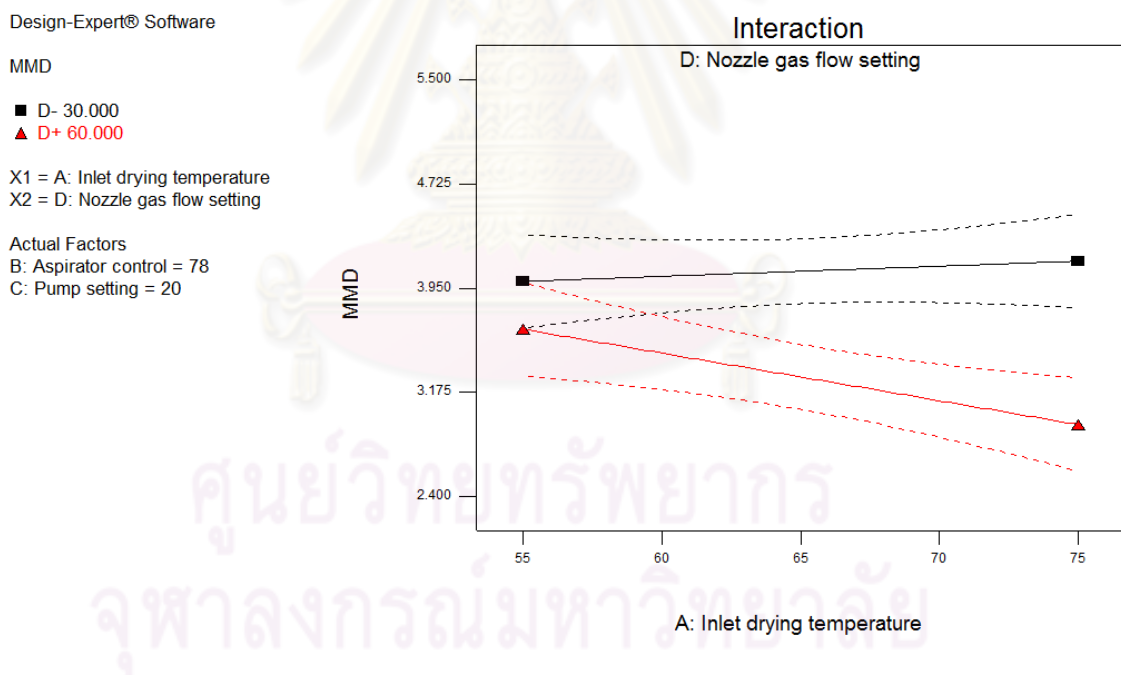
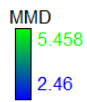


Figure 38 Interaction plot between inlet drying temperature and nozzle gas flow setting of quadratic model for mass median diameter (high level shown as red line and low level shown as black line)

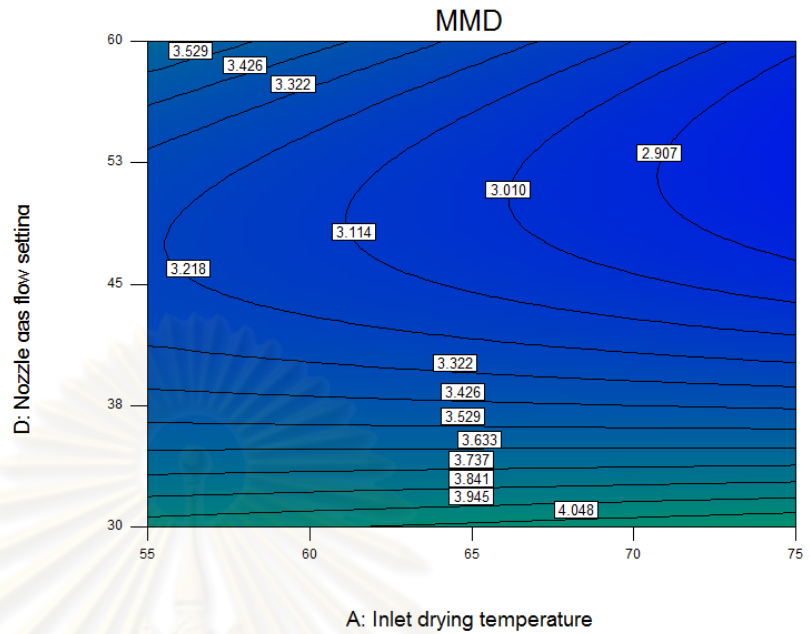
The contour plot and surface plot of interaction between inlet drying temperature and nozzle gas flow setting of quadratic model was shown in figure 39.

Design-Expert® Software



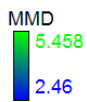
X1 = A: Inlet drying temperature
X2 = D: Nozzle gas flow setting

Actual Factors
B: Aspirator control = 78
C: Pump setting = 20



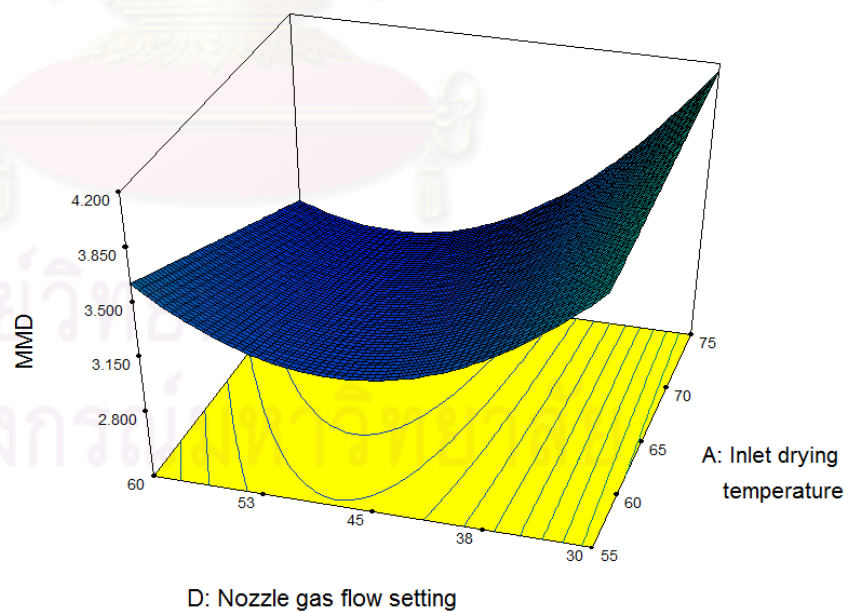
(a) Contour plot between inlet drying temperature and nozzle gas flow setting

Design-Expert® Software



X1 = A: Inlet drying temperature
X2 = D: Nozzle gas flow setting

Actual Factors
B: Aspirator control = 78
C: Pump setting = 20



(b) Surface plot between inlet drying temperature and nozzle gas flow setting

Figure 39 Contour plot and surface plot between inlet drying temperature and nozzle gas flow setting of quadratic model for mass median diameter

Like the result from a 2^4 factorial design, the interaction between aspirator control and nozzle gas flow setting can explain in the same way as interaction between inlet drying temperature and nozzle gas flow setting that nozzle gas flow setting effect is small when the aspirator control is at the low level and large when the aspirator control is at the high level. Aspirator control showed negative effect when nozzle gas flow setting was at high level but showed positive effect when nozzle gas flow setting was at low level. The smallest particle obtained with high aspirator control and high nozzle gas flow setting (Figure 40).

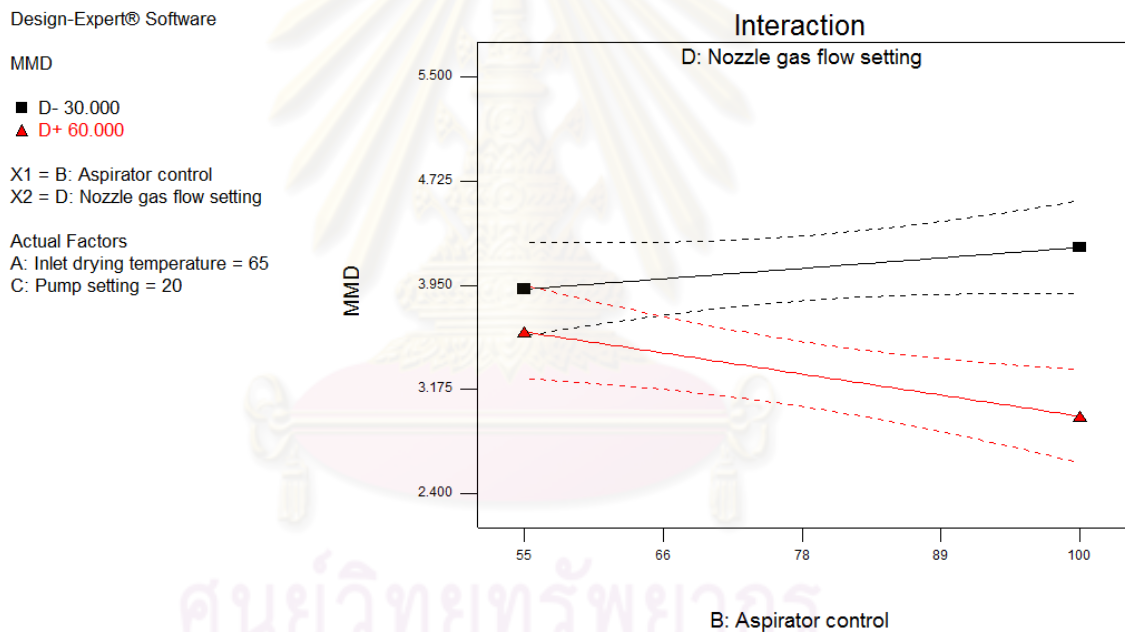
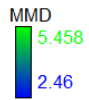


Figure 40 Interaction plot between aspirator control and nozzle gas flow setting of quadratic model for mass median diameter (high level shown as red line and low level shown as black line)

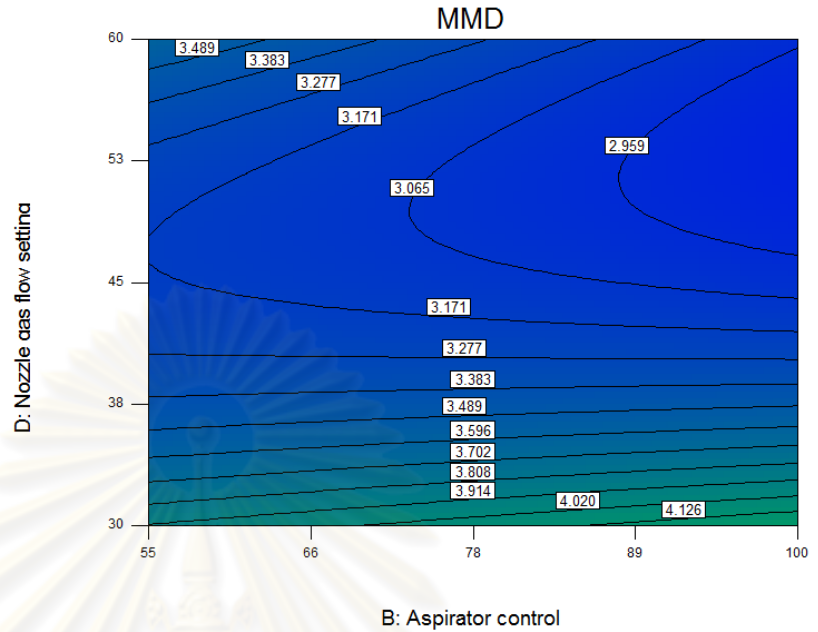
The contour plot and surface plot of interaction between aspirator control and nozzle gas flow setting of quadratic model was shown in figure 41.

Design-Expert® Software



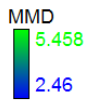
X1 = B: Aspirator control
X2 = D: Nozzle gas flow setting

Actual Factors
A: Inlet drying temperature = 65
C: Pump setting = 20



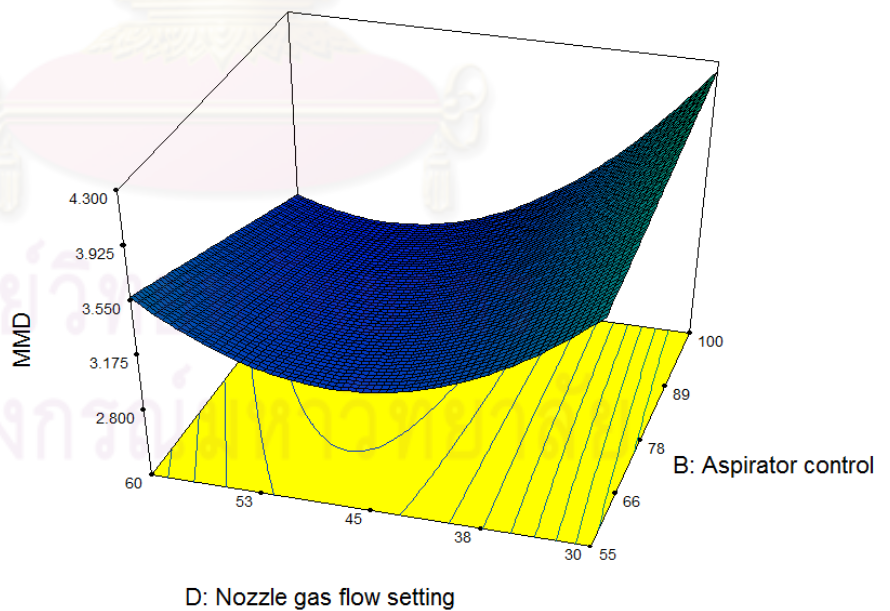
(a) Contour plot between aspirator control and nozzle gas flow setting

Design-Expert® Software



X1 = B: Aspirator control
X2 = D: Nozzle gas flow setting

Actual Factors
A: Inlet drying temperature = 65
C: Pump setting = 20



(b) Surface plot between aspirator control and nozzle gas flow setting

Figure 41 Contour plot and surface plot between aspirator control and nozzle gas flow setting of quadratic model for mass median diameter

Moreover, the interaction between pump setting and nozzle gas flow setting can be explained that nozzle gas flow setting effect is small when the pump setting is at the low level and large when the pump setting is at the high level. Aspirator control effect is positive at nozzle gas flow setting low level but negative at nozzle gas flow setting high level. The smallest particle obtained with high pump setting and high nozzle gas flow setting (Figure 42). In conclusion, the smallest particle size of rifampicin-PLGA microparticles obtained with the spray dried condition with high inlet drying temperature, high aspirator control, high pump setting and high nozzle gas flow setting.

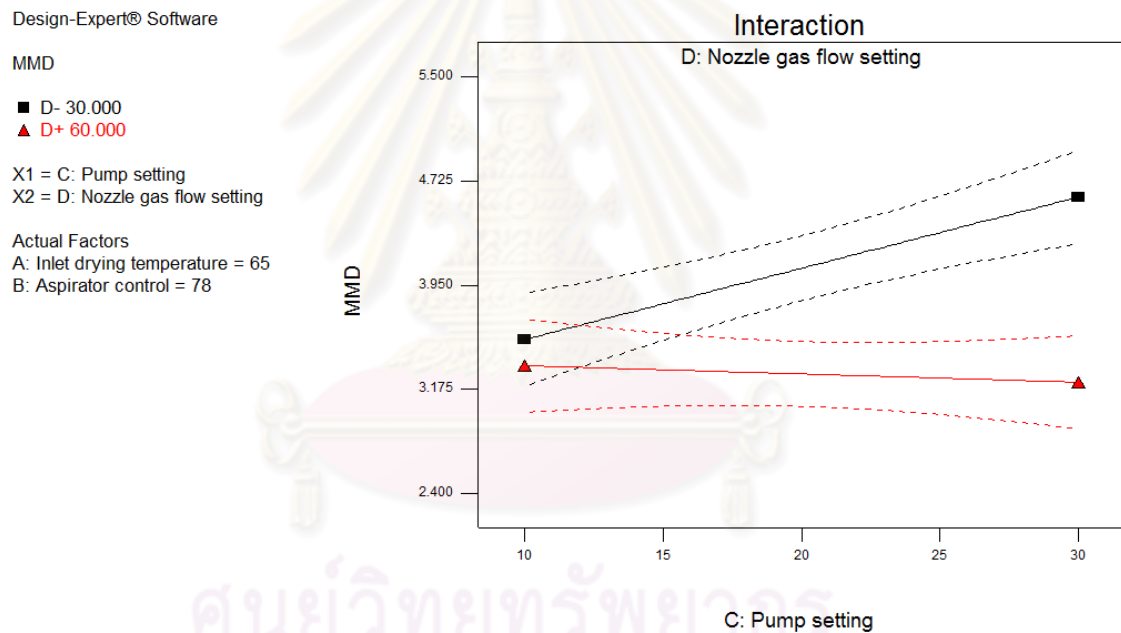
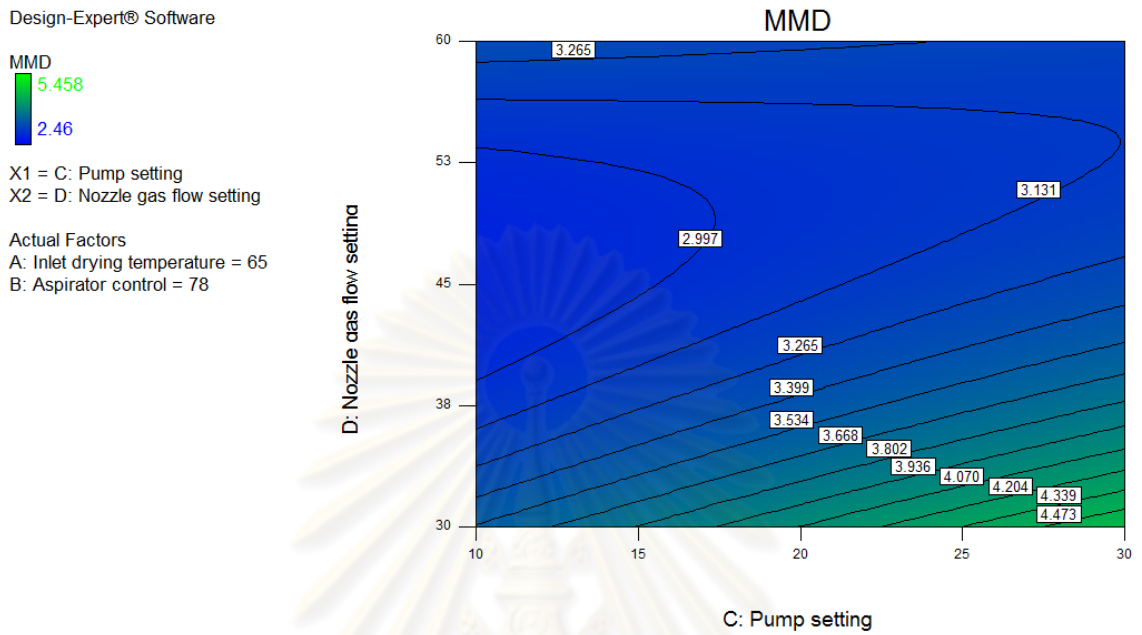
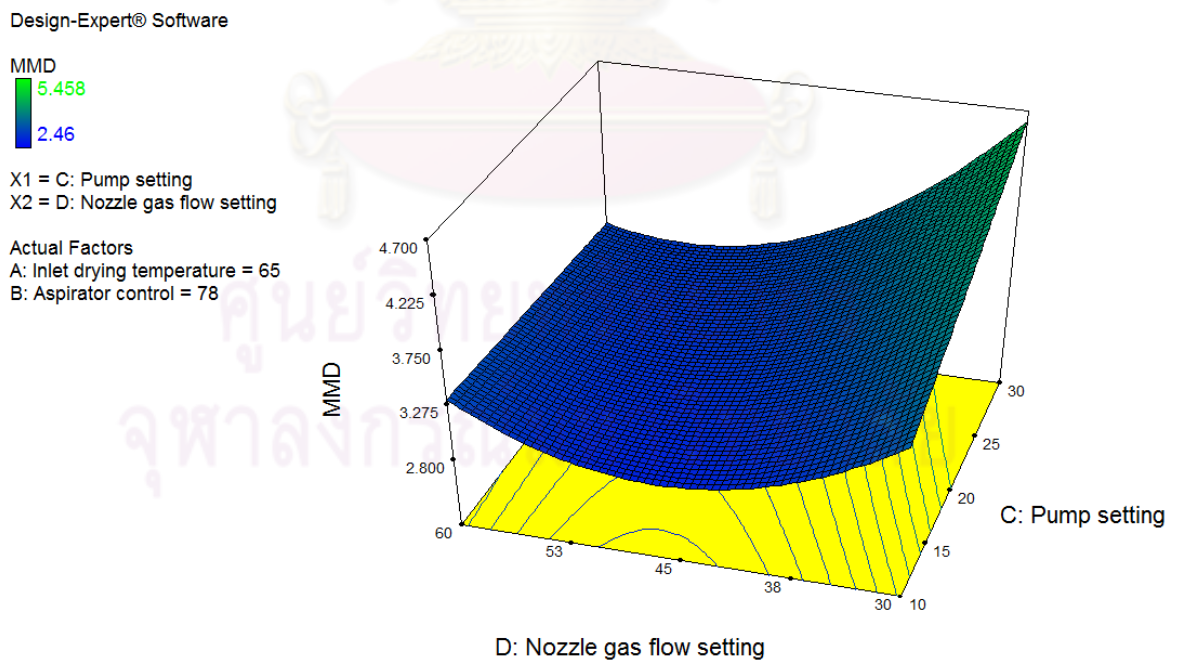


Figure 42 Interaction plot between pump setting and nozzle gas flow setting of quadratic model for mass median diameter (high level shown as red line and low level shown as black line)

The contour plot and surface plot of interaction between pump setting and nozzle gas flow setting of quadratic model was shown in figure 43.



(a) Contour plot between pump setting and nozzle gas flow setting



(b) Contour plot between pump setting and nozzle gas flow setting

Figure 43 Contour plot and surface plot between pump setting and nozzle gas flow setting of quadratic model for mass median diameter

4. Optimization of spray drying condition

From the quadratic model in section 3, the optimum spray drying process conditions were studied using the criteria as shown in table 24.

Table 24 Criteria for optimization of spray drying parameters

Parameters	Goal	Lower limit	Upper limit	Importance*
Inlet drying temperature (T_{in})	is in range	55	75	-
Aspirator control (A)	is in range	55	100	-
Pump setting (P)	is in range	10	30	-
Nozzle gas flow setting (N)	is in range	30	60	-
Process yield (Y_1)	maximize	7.2384	43.1993	4
Mass median diameter (Y_2)	is target = 3.000	2.460	5.458	5

* See detail in Appendix D

The optimum spray drying conditions with predicted responses and their desirability (see detail in Appendix D) determined from the response surface to obtain maximum process yield, minimum mass median diameter and maximum encapsulation efficiency were shown in table 25.

Table 25 Optimum spray drying parameters and their predicted response variables

Solutions No.	Spray drying parameter				Desirability
	Inlet drying temperature (°C)	Aspirator control (%)	Pump setting (%)	Nozzle gas flow setting (mm)	
1	55.00	100.00	10.00	33.31	0.8436
2	55.04	100.00	10.00	33.54	0.8436
3	55.00	100.00	10.00	34.74	0.8433

The spray drying condition with inlet drying temperature 55 °C, aspirator control 100%, pump setting 10% and nozzle gas flow setting 33 mm (solution number 1) was chosen as optimum condition because of the high desirability and the possibility of setting on spray dryer. The predicted values of this condition were shown in table 26.

From three batch of optimum condition, the observed values for process yield and mass median diameter response fall inside the 95% confidence interval as showed in table 26. The estimated biases of process yield and mass median diameter shown in table 27 were below 15%. All response showed good precision of the spray drying process from standard deviation from three batches.

Table 26 Predicted values and their 95% confidence interval of responses for the optimum condition

Responses	Predicted value	95% confidence interval
Process yield (%)	37.3468	28.2366 - 46.4569
Mass median diameter (μm)	3.3717	2.9428 - 3.8005

Table 27 Actual response value and their bias for optimum condition

Batch	Process yield		Mass median diameter	
	Actual (%)	Bias (%)	Actual (μm)	Bias (%)
1	33.8931	-9.2476	3.234	-4.0832
2	32.8390	-12.0700	3.195	-5.2399
3	33.6231	-9.9705	3.170	-5.9813
Average	33.4517	-10.4294	3.1997	-5.1015
SD	0.5475	1.4661	0.0323	0.9566

5. Design space

A design space is considered as a zone of robustness in the experimental domain because it allows to tolerate variability of materials and slight changes in the process (Lebrun et al., 2008).

In this study, design space has been evaluated considering combined and relative influences of all process condition parameters, by setting the flowing restriction: process yield not less than 30% and mass median diameter between 3 – 5 μm . The summary of design space of rifampicin-PLGA microparticles was show on table 28.

Table 28 Summary of design space for rifampicin-PLGA microparticles

Responses	Specification	Best fitted model
Process yield	Not less than 30%	$- 6.1332 + 1.5384(T_{in}) + 1.3320(A)$ $+ 1.1198(P) - 3.4417(N)$ $- 0.0188(T_{in})(A) - 0.034(P)(N)$ $- 0.0385(N)^2$
Mass median diameter (MMD)	3 - 5 μm	$1.8443 + 0.0506(T_{in}) + 0.027(A)$ $+ 0.1122(P) - 0.0728(N)$ $- 0.0014(T_{in})(N) - 0.0007(A)(N)$ $- 0.0020(P)(N) + 0.00026(N)^2$

From the quadratic model of process yield and mass median diameter, the design spaces of inhalable rifampicin-PLGA microparticles were performed. Figure 44 and 45 show the overlay plot of pump setting and nozzle gas flow setting when other factors varied. Each overlay plot, the undesirable area is gray and the yellow area represents required area that produce the inhalable rifampicin-PLGA microparticle with process yield more than 30%. All design spaces show that low nozzle gas flow setting spray drying condition produced the required microparticles and pump setting was not effect on their properties. Furthermore, at low level of inlet drying temperature, the design spaces were expanded when aspirator control was increased but they were contracted at high level of inlet drying temperature.

Design-Expert® Software

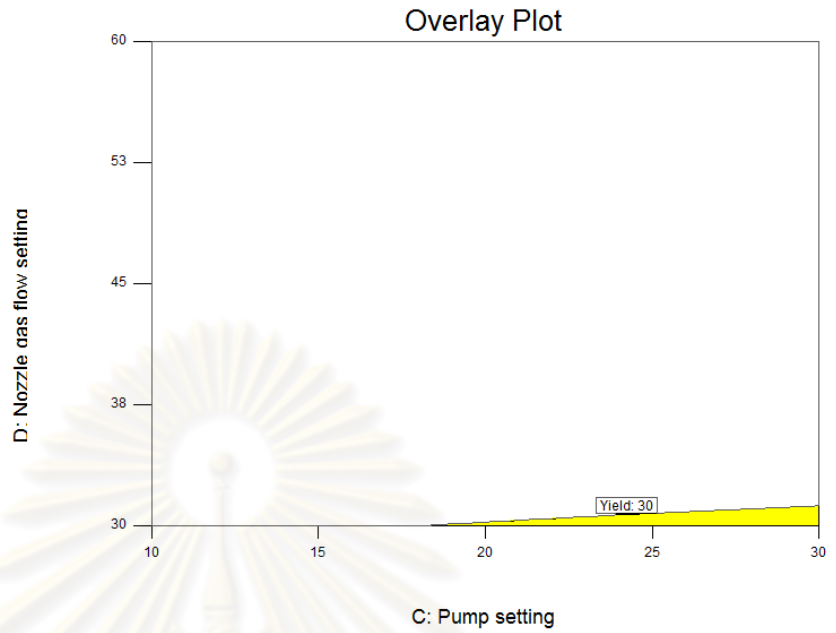
Overlay Plot

Yield
MMD

X1 = C: Pump setting
X2 = D: Nozzle gas flow setting

Actual Factors

A: Inlet drying temperature = 55
B: Aspirator control = 55



(a) Low level aspirator control

Design-Expert® Software

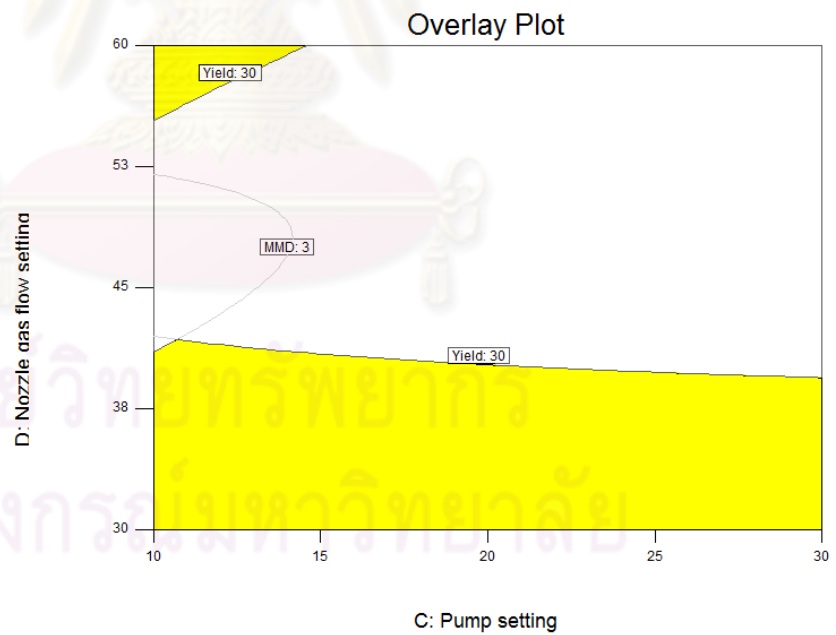
Overlay Plot

Yield
MMD

X1 = C: Pump setting
X2 = D: Nozzle gas flow setting

Actual Factors

A: Inlet drying temperature = 55
B: Aspirator control = 100



(b) High level aspirator control

Figure 44 Design spaces of inhalable rifampicin-PLGA microparticles when inlet drying temperature is at low level

Design-Expert® Software

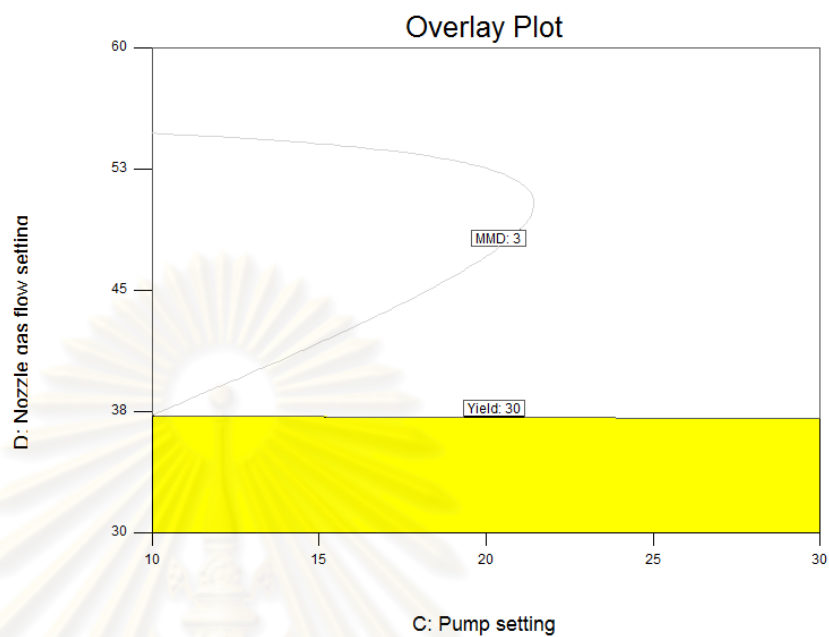
Overlay Plot

Yield
MMD

X1 = C: Pump setting
X2 = D: Nozzle gas flow setting

Actual Factors

A: Inlet drying temperature = 75
B: Aspirator control = 55



(a) Low level aspirator control

Design-Expert® Software

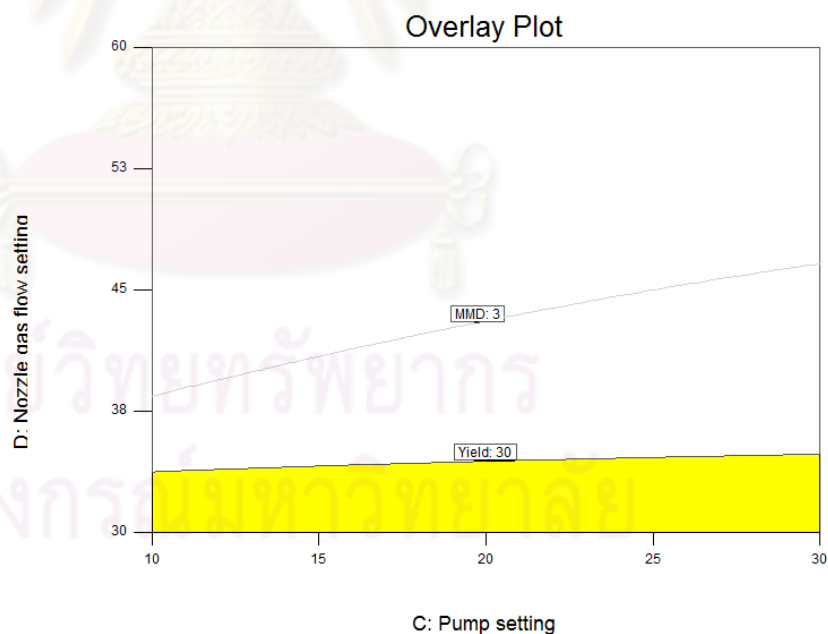
Overlay Plot

Yield
MMD

X1 = C: Pump setting
X2 = D: Nozzle gas flow setting

Actual Factors

A: Inlet drying temperature = 75
B: Aspirator control = 100



(b) High level aspirator control

Figure 45 Design spaces of inhalable rifampicin-PLGA microparticles when inlet drying temperature is at high level

In pharmaceutical industrial, one of the important issues that should be concerned is energy consuming. To save the energy, the operation setting of spray drying parameters should be lowest. According the safety while working with organic solvent, the spray drying process should be operate with low inlet drying temperature. In summary, to obtain the inhalable rifampicin-PLGA microparticles, the conditions with low inlet drying temperature and nozzle gas flow setting were recommended.



ศูนย์วิทยทรัพยากร
จุฬาลงกรณ์มหาวิทยาลัย

CHAPTER V

CONCLUSIONS

Two-level full factorial with center points design and central composite face centered (CCF) design were applied to investigate the influence of spray drying process parameters on the characteristics of inhalable rifampicin-PLGA microparticles. The investigated parameters were inlet drying temperature, aspirator control, pump setting and nozzle gas flow setting. Nozzle gas flow setting was found to be the most important process parameter for performing rifampicin-PLGA microparticles, follow by aspirator control, pump setting and inlet drying temperature.

Design of experiment (DOE) aided in understanding the effect of spray drying parameters on process yield, mass median diameter (MMD) of obtained microparticles, entrapment efficiency and dissolution at first 20 min. Process yield and mass median diameter were found to be affected by the spray drying parameters. In order to increase process yield, increasing aspirator control and pump setting while inlet drying temperature and nozzle gas flow setting were decrease. Meanwhile the mass median diameter of rifampicin-PLGA microparticles decreases when all process parameters were increased.

All process parameters were not shown directly to influence the entrapment efficiency and dissolution at 20 min. This may be due to the fix ratio between rifampicin and PLGA in feeding solution. There were also some reports shows the correlation between the formulation parameter (such as ratio between drug and polymer, concentration of the feeding solution) and the entrapment efficiency and dissolution of drug from microparticles.

The optimum spray drying condition that produce the inhalable rifampicin-PLGA microparticles with process yield more than 30% is condition with inlet drying temperature 55 °C, aspirator control 100%, pump setting 10% and nozzle gas flow setting 33 mm.

The result showed that spray drying method can be performed to produce rifampicin-PLGA microparticles in the inhalable size range. The process yield obtained in the investigation were relatively low, due to ineffective separation of the spray dried particles and air in the cyclone. For pharmaceutical industry, more effective separators such as filter systems, have to be required.

The design space with the process yield (more than 30%) and inhalable size criterion showed the nozzle gas flow setting should keep low level and pump speed was not effect on the required rifampicin-PLGA microparticle. Moreover, design space will increase when aspirator control was increased in low inlet drying temperature but decrease in high inlet drying temperature.

Designs of experiment and response surface methodology (RSM) proved to be useful tools for design space and were able to identify important parameters and variable correlations.

The future plans should be as follows:

1. Determination the influence of formulation parameters for preparation of PLGA microspheres loaded with rifampicin powder.
2. Evaluation the optimum values of spray drying process and formulation parametrs for inhalable rifampicin-PLGA micropaticle through design of experiment (DOE).
3. Identify a design space of spray drying method to get the inhalable rifampicin-PLGA microparticles.

REFERENCES

- Altan, S., Bergum, J., Pfahler, L., Senderak, E., Sethuraman, S. and Vukovinsky, K. E. (2010) 'Statistical Considerations in Design Space Development (Part II of III)', *Pharmaceutical Technology*, 34(8), 52 - 60.
- Bezerraa, M. A., Santelli, R. E., Oliveiraa, E. P., Villar, L. S. and Escaleira, L. A. I. (2008) 'Response surface methodology (RSM) as a tool for optimization in analytical chemistry', *Talanta*, 76, 965-977.
- Bosquillon, C., Lombry, C., Pré'at, V. r. and Vanbever, R. (2001) 'Influence of formulation excipients and physical characteristics of inhalation dry powders on their aerosolization performance', *Journal of Controlled Release*, 70, 329-339.
- BÜCHI Labortechnik AG *Training Papers Spray Drying*, English version B ed.
- Calleja, I., Blanco-Pr'ieto, M. 1. J., Ruz, N., Renedo, M. 1. J. and Dios-Viéitez, M. 1. C. (2004) 'High-performance liquid–chromatographic determination of rifampicin in plasma and tissues', *Journal of Chromatography A*, 1031, 289-294.
- Chan, H.-K., Clark, A., Gonda, I., Mumenthaler, M. and Hsu, C. (1997) 'Spray dried powders and powder blends of recombinant human deoxyribonuclease (rhDNase) for aerosol delivery', *Pharmaceutical Research*, 14(4), 431-427.
- Chen, D. H., Batychy, R. P., Johnston, L. and Mintzes, J. (2005) *Control of process humidity to produce large, porous particles.*,
- Chougule, M. B., Padhi, B. K., Jinturkar, K. A. and M, A. (2007) 'Development of Dry Powder Inhalers', *Recent Patents on Drug Delivery & Formulation*, 1, 11-21.
- Chow, A. H. L., Tong, H. H. Y., Chattopadhyay, P. and Shekunov3, B. Y. (2007) 'Particle Engineering for Pulmonary Drug Delivery', *Pharmaceutical Research*, 24(3), 411-437.
- Cook, R. O., Pannu, R. K. and Kellaway, I. W. (2005) 'Novel sustained release microspheres for pulmonary drug delivery', *Journal of Controlled Release*, 104, 79-90.

- Davies, N. M. and Feddah, M. R. (2003) 'A novel method for assessing dissolution of aerosol inhaler products', *International Journal of Pharmaceutics*, 255, 175-187.
- Elversson, J. and Fureby., A. M. (2005) 'Particle size and density in spray drying – effects of carbohydrate properties.', *Journal of pharmaceutical sciences*, 94, 2049-2060.
- Ferreira, S. L. C., Bruns, R. E., Silva, E. G. a. P. d., Santos, W. N. L. d., Quintella, C. M., David, J. M., Andrade, J. B. d., Breikreitz, M. C., Jardim, I. C. S. F. and Neto, B. B. (2007) 'Statistical designs and response surface techniques for the optimization of chromatographic systems', *Journal of Chromatography A*, 1158, 2-14.
- Florea, C. and Leucuta, S. E. (2008) 'Design Space Evaluation for Clarithromycin Film Coated Tablets by Experimental Design', *Farmacia*, 56(3), 300-310.
- Gilani, K., Najafabadi, A. R., Barghi, M. and Rafiee-Tehrani, M. (2005) 'The Effect of Water to Ethanol Feed Ratio on Physical Properties and Aerosolization Behavior of Spray Dried Cromolyn Sodium Particles', *Journal of pharmaceutical sciences*, 94(5), 1048-1059.
- Hickey, A. J., ed. (2004) *Pharmaceutical Inhalation Aerosol Technology*, Second edition ed., The United States of America: Marcel Dekker, Inc.
- 'ICH Pharmaceutical Development Q8(R2)', (2009)
- Learoyd, T. P., Burrows, J. L., French, E. and Seville, P. C. (2008) 'Chitosan-based spray-dried respirable powders for sustained delivery of terbutaline sulfate', *European Journal of Pharmaceutics and Biopharmaceutics*, 68, 224–234.
- Lebrun, P., Govaerts, B., Debrus, B., Ceccato, A., Caliaro, G., Hubert, P. and Boulanger, B. (2008) 'Development of a new predictive modelling technique to find with confidence equivalence zone and design space of chromatographic analytical methods', *Chemometrics and Intelligent Laboratory Systems*, 91(1), 4-16.
- Lewis, G. A., Mathieu, D. and Phan-Tan-Luu, R. (1999) *Drugs and the Pharmaceutical Sciences, Pharmaceutica Experimental Design*, The United States of America: Marcel Dekker.

- Lucas, P., Anderson, K., Potter, U. J. and Staniforth, J. N. (1999) 'Enhancement of small particle size dry powder aerosol formulations using an ultra low density additive', *Pharmaceutical Research*, 16(10), 1643-1647.
- Lundstedt, T. r., Seifert, E., Abramo, L., Thelin, B., Nystroöm, A. s., Pettersen, J. and Bergman, R. (1998) 'Experimental design and optimization', *Chemometrics and Intelligent Laboratory Systems*, 42, 3-40.
- Maltesen, M. J., Bjerregaard, S., Hovgaard, L., Havelund, S. and van de Weert, M. (2008) 'Quality by design - Spray drying of insulin intended for inhalation', *European Journal of Pharmaceutics and Biopharmaceutics*, 70(3), 828-838.
- Montgomery, D. C. (2009) *Design and Analysis of Experiments, International Student Version*, 7th Edition ed.
- O'Hara, P. and Hickey, A. J. (2000) 'Respirable PLGA Microspheres Containing Rifampicin for the Treatment of Tuberculosis: Manufacture and Characterization', *Pharmaceutical Research*, 17(8), 955-961.
- Global Tuberculosis Control: a short update to the 2009 report*, (2009) World Health Organization.
- Rabbani, N. R. and Se, P. C. (2005) 'The influence of formulation components on the aerosolisation properties of spray-dried powders', *Journal of Controlled Release*, 110, 130-140.
- Shama, J. O.-H., Zhang, Y., Finlay, W. H., Roa, W. H. and Löbenberg, R. (2004) 'Formulation and characterization of spray-dried powders containing nanoparticles for aerosol delivery to the lung', *International Journal of Pharmaceutics*, 269, 457-467.
- Stat-Ease, Inc. (2006) 'Design-Expert® Help file'.
- Suarez, S., O'Hara, P., Kazantseva, M., Newcomer, C. E., Hopfer, R., McMurray, D. N. and Hickey, A. J. (2001a) 'Airways delivery of rifampicin microparticles for the treatment of tuberculosis', *Journal of Antimicrobial Chemotherapy*, 48, 431-434.
- Suarez, S., O'Hara, P., Kazantseva, M., Newcomer, C. E., Hopfer, R., McMurray, D. N. and Hickey, A. J. (2001b) 'Respirable PLGA Microspheres Containing Rifampicin for the Treatment of Tuberculosis Screening in an Infectious Disease Model', *Pharmaceutical Research*, 18(9), 1315-1319.

- Sundaram, J., Hsu, C. C., Shay, Y.-H. M. and Sane, S. U. (2010) 'Design Space Development for Lyophilization Using DOE and Process Modeling', *BioPharm International*, 23(9).
- Takashima, Y., Saito, R., Nakajima, A., Oda, M., Kimura, A., Kanazawa, T. and Okada, H. (2007) 'Spray-drying preparation of microparticles containing cationic PLGA nanospheres as gene carriers for avoiding aggregation of nanospheres', *International Journal of Pharmaceutics*, 343, 262–269.
- Tomoda, K. and Makino, K. (2007) 'Effects of lung surfactants on rifampicin release rate from monodisperse rifampicin-loaded PLGA microspheres', *Colloids and Surfaces B: Biointerfaces*, 55, 115-124.
- Tomoda, K., Ohkoshi, T., Kawai, Y., Nishiwaki, M., Nakajima, T. and Makino, K. (2008) 'Preparation and properties of inhalable nanocomposite particles: Effects of the temperature at a spray-dryer inlet upon the properties of particles', *Colloids and Surfaces B: Biointerfaces*, 61(2), 138-144.
- USP 33/NF 28, (2010) *Validation of compendial procedures <1225>*, 1st Supplement ed., USA.
- Vanbever, R., Mintzea, J. D., Wang, J., Nice, J., Chen, D., Batycky, R., Langer, R. and Edwards, D. A. (1999) 'Formulation and physical characterization of large porous particles for inhalation', *Pharmaceutical Research*, 16(11), 1735-1742.
- Zidan, A. S., Sammour, O. A., Hammad, M. A., Megrab, N. A., Habib, M. J. and Khan, M. A. (2007) 'Quality by design: Understanding the formulation variables of a cyclosporine A self-nanoemulsified drug delivery systems by Box–Behnken design and desirability function', *International Journal of Pharmaceutics*, 332, 55-63.



APPENDICES

ศูนย์วิทยทรัพยากร
จุฬาลงกรณ์มหาวิทยาลัย

APPENDIX A

Validation of HPLC method for entrapment efficiency

The HPLC method was used to determine the rifampicin content in rifampicin-PLGA microparticles. The validation of HPLC methods used was presented as follows:

1. Specificity

The specificity of an analytical method is the ability to assess the peak of drug from the sample without interfered by other components, presented in the sample. To determine the specificity of the method, the placebo solution and the rifampicin solution has only drug dissolved in the same solvent. Both solutions were injected on column after filtration through 0.45 μm nylon filter and peak responses were recorded. The chromatogram of placebo was compared with the chromatogram of the drug solution.

Figure 46 revealed that standard solution of rifampicin was eluted at 3.8 min. Figures 47 showed the chromatogram of poly(DL-lactide-co-glycolide) in chloroform. It indicated that the PLGA solution did not interfered the peaks of drugs.

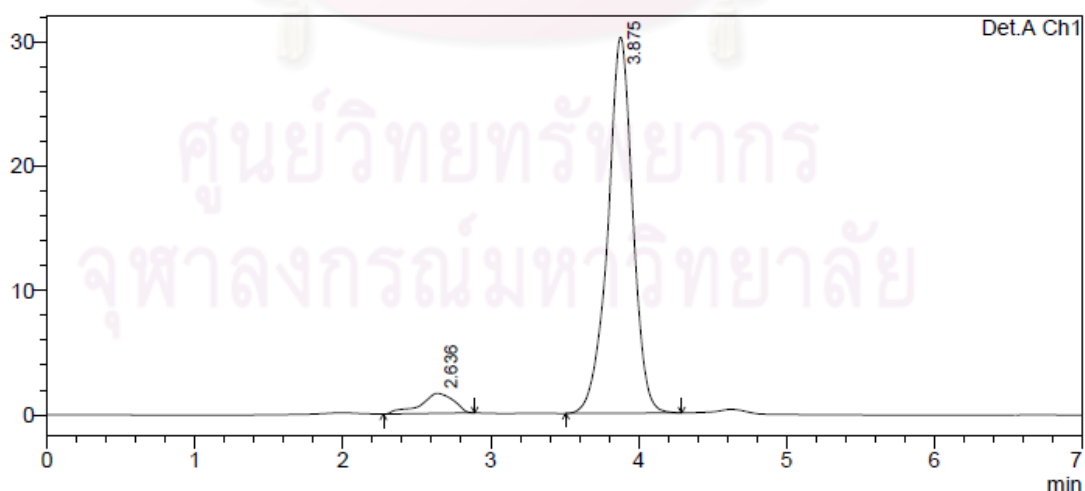


Figure 46 The chromatogram of standard rifampicin in entrapment efficiency

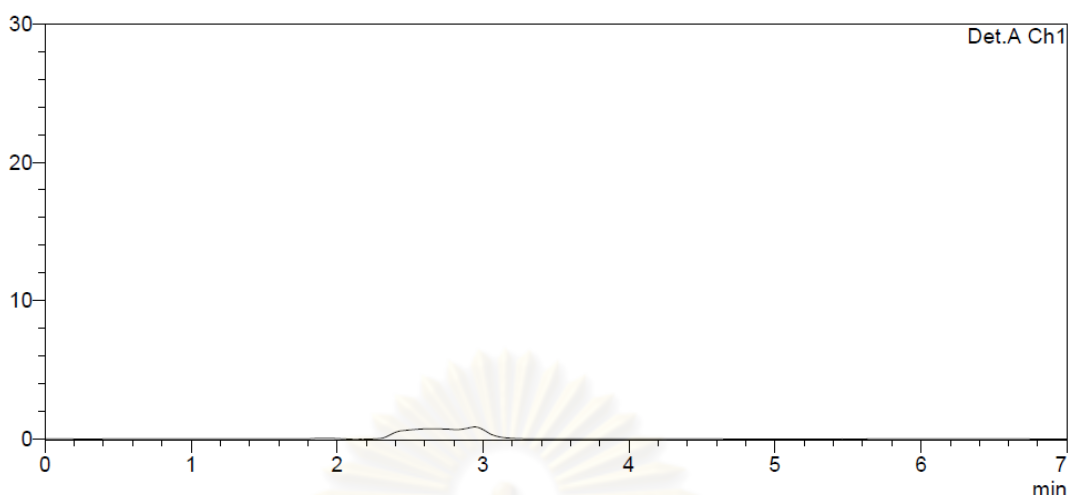


Figure 47 The chromatogram of PLGA in chloroform

2. Accuracy

The accuracy of an analytical method is the closeness of the test results obtained by that method to the true value. Three concentration levels of drug solution spiked in the placebo solution consisted of 0.08 % (w/v) PLGA dissolved in chloroform:methanol (1:9) were injected on column after filtration through 0.45 μm nylon filter and peak responses were recorded. Accuracy was calculated as the percentage of recovery of each drug solution. The mean percentage of recovery of 95-105% with percent of coefficient of variation (%RSD) < 2.00% indicates the high accuracy of the method.

Tables 29 showed the percentage of analytical recovery of rifampicin. The mean percentage of analytical recovery complied to the range of 95-105 % with low % RSD (<2.00 %) indicated the high accuracy of this method.

จุฬาลงกรณ์มหาวิทยาลัย

Table 29 Accuracy data of percentage of analytical recovery of rifampicin in entrapment efficiency

Accuracy set	Peak area	Concentration (ug/ml)		% Recovery	Average	SD	% RSD
		Actual	Calculated				
I (3.5 ml)	1139222		93.5365	102.5508			
	1136334	91.2100	93.2684	102.2567	102.1571	0.4517	0.4422
	1130511		92.7276	101.6639			
	1183386		97.6376	101.8862			
	1193005	95.8300	98.5308	102.8183	102.0076	0.7574	0.7425
	1177524		97.0932	101.3182			
	1189449		98.2006	100.7806			
	1207717	97.4400	99.8969	102.5215	102.1373	1.2113	1.1859
	1213892		100.4703	103.1099			
II (4.0 ml)	1282096		106.8037	102.4594			
	1293559	104.2400	107.8681	103.4806	103.2054	0.6535	0.6332
	1295757		108.0722	103.6764			
	1326191		110.8983	101.2585			
	1336878	109.5200	111.8907	102.1646	101.9570	0.6213	0.6094
	1340219		112.2009	102.4479			
	1325321		110.8175	99.5129			
	1318886	111.3600	110.2200	98.9763	99.3368	0.3123	0.3143
	1325422		110.8269	99.5213			
III (4.5 ml)	1422783		119.8678	102.2152			
	1444723	117.2700	121.9051	103.9525	103.4586	1.0843	1.0481
	1447950		122.2048	104.2080			
	1466352		123.9135	100.5710			
	1484970	123.2100	125.6424	101.9742	100.7130	1.1965	1.1880
	1453387		122.7096	99.5939			
	1433712		120.8826	96.4900			
	1431485	125.2800	120.6758	96.3249	97.2584	1.4762	1.5179
	1467041		123.9775	98.9604			

3. Precision

The precision of an analytical method is the degree of agreement among individual test results when the procedure is applied repeatedly to multiple samplings of homogenous sample. The percentage of coefficient of variation (%CV) or relative standard deviation (%RSD) values of peak area of standard solutions both within run and between run less than 2.00% which indicates that HPLC methods can be used to determine the amount of rifampicin over period of time studied.

Within run precision

The within run precision was determined by analyzing the standard solution at 100% of the three test concentrations (87.5, 100 and 112.5 µg/ml). Repeatability was assessed using a minimum of six determinations. The percentage of relative standard deviation (%RSD) value of peak area of rifampicin was determined.

Table 30 Precision data of rifampicin in entrapment efficiency

Concentration	Number	Day			Average (SD)	%CV
		1	2	3		
1	1	636139	626994	775398	687996.889 (68241.4011)	9.9189
	2	638048	637752	782683		
	3	643884	649793	778183		
	4	644667	641567	785873		
	5	642975	651144	788203		
	6	642891	639420	778330		
	Average	641420	639158	779800		
	SD	3477.1925	8828.1164	4974.3436		
%CV	0.5421	1.3812	0.6379			
2	1	942327	923669	946966	959941.222 (15620.4741)	1.6272
	2	933467	963474	960097		
	3	963863	968307	981824		
	4	972368	947448	975421		
	5	968571	953632	972275		
	6	967382	964302	973549		
	Average	957798	955250	968568		
	SD	16050.5021	16504.1759	12644.1309		
%CV	1.6758	1.7277	1.3054			
3	1	1269798	1236467	1270907	1281698.78 (18107.1709)	1.4127
	2	1243853	1280877	1276925		
	3	1284283	1306413	1298264		
	4	1296880	1279560	1295321		
	5	1289753	1282575	1294261		
	6	1280284	1297583	1286574		
	Average	1275897	1283081	1285761		
	SD	18819.7655	24114.3580	11040.8335		
%CV	1.4750	1.8794	0.8587			

Between run precision

The between run precision was determined by analyzing the standard solution at 100% of the same three test concentrations which prepared and injected on different days. The percentage of relative standard deviation (%RSD) value of peak area of rifampicin was determined.

Data of within run precision and between run precision of rifampicin analyzed by HPLC method are shown in table 30. The percentages of coefficient of variation (%CV) values of peak area in within run and between run were low (< 2.00 % and < 15%, respectively) which indicated that HPLC methods could determine the amount of the drugs over period of time studied.

4. Linearity

The linearity of an analytical method is the ability to obtain test results that are directly proportional to the concentration of drugs in samples within a given range. A general linearity acceptance criterion is that the correlation coefficient (r) of the linear regression is not less than 0.9999. Triplicate of each concentration of standard solutions in various concentrations range from 25 to 125 $\mu\text{g/ml}$ were analyzed. The linear regression analysis of the area under curve versus the concentrations was calculated.

Figures 48 showed the relationship between peak area and drug concentrations was linear ($R^2 = 0.9999$). This result indicated that HPLC method was acceptable for quantitative analysis of nicotine drug in the range studied.

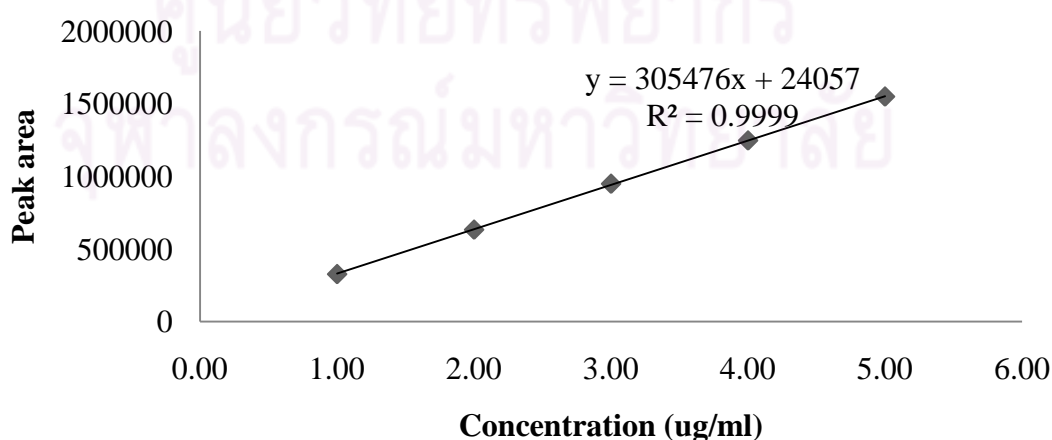


Figure 48 Calibration curve for entrapment efficiency condition

APPENDIX B

Validation of HPLC method for dissolution

The HPLC method was used to determine the rifampicin content in rifampicin-PLGA microparticles. The validation of HPLC methods used was presented as follows:

1. Specificity

The specificity of an analytical method is the ability to assess the peak of drug from the sample without interfered by other components, presented in the sample. To determine the specificity of the method, phosphate buffer saline pH 7.4 and rifampicin standard solution were injected on column after filtration through 0.45 μm nylon filter and peak responses were recorded. The chromatogram of phosphate buffer saline pH 7.4 was compared with the chromatogram of the drug solution.

Figure 49 revealed that standard solution of rifampicin was eluted at 3.8 min. Figures 50 showed the chromatogram of phosphate buffer saline pH 7.4 (PBS). It indicated that the PBS did not interfered the peaks of drugs.

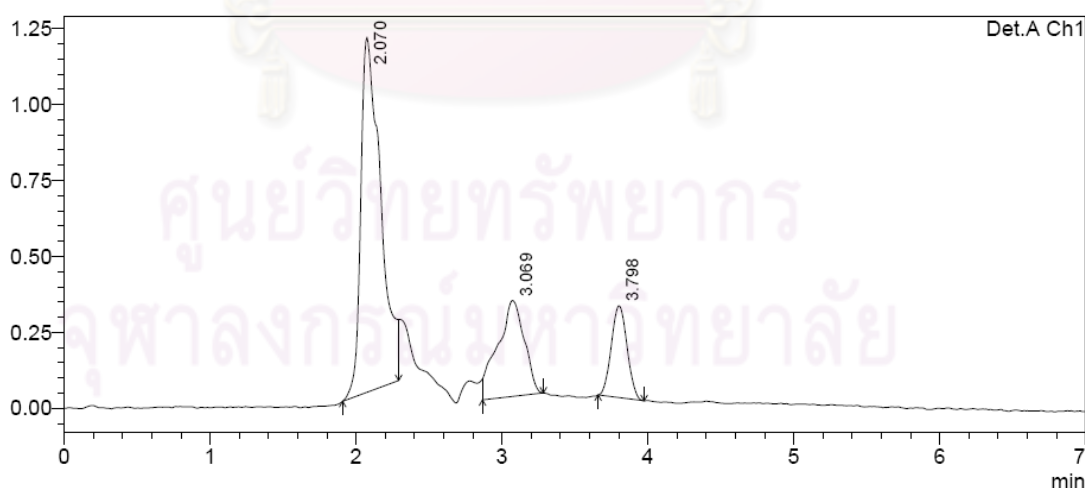


Figure 49 The chromatogram of standard rifampicin in dissolution condition

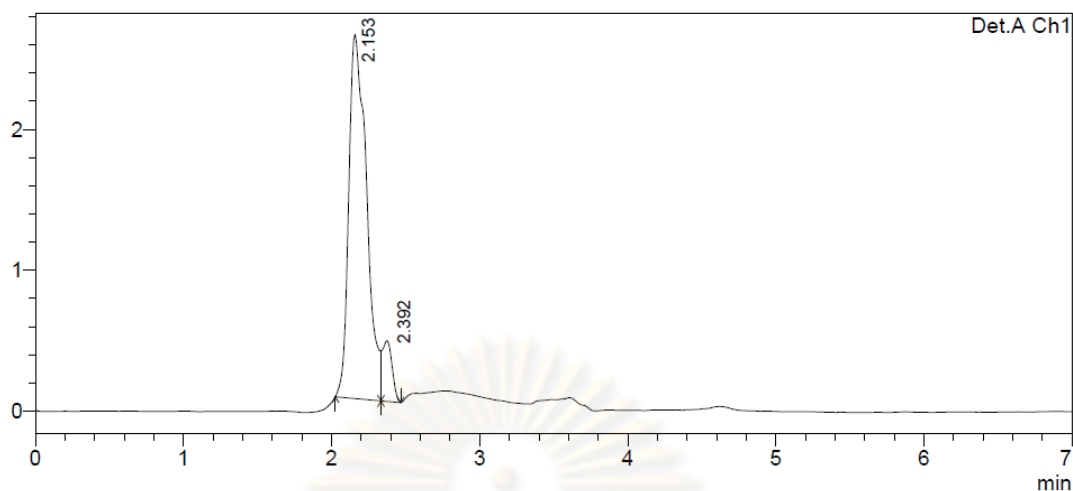


Figure 50 The chromatogram of phosphate buffer saline pH 7.4

2. Accuracy

The accuracy of an analytical method is the closeness of the test results obtained by that method to the true value. Three concentration levels of drug solution (80, 100 and 120% of assay concentration) spiked in phosphate buffer saline pH 7.4 were injected on column after filtration through 0.45 μm nylon filter and peak responses were recorded. Accuracy was calculated as the percentage of recovery of each drug solution. The mean percentage of recovery of 95-105% with percent of coefficient of variation (%RSD) < 2.00% indicates the high accuracy of the method.

Tables 31 showed the percentage of analytical recovery of rifampicin in dissolution condition. The mean percentage of analytical recovery complied to the range of 95-105 % with low % RSD (<2.00 %) indicated the high accuracy of this method.

Table 31 Accuracy data of percentage of analytical recovery of rifampicin in dissolution condition

Accuracy set	Peak area	Concentration (ug/ml)		% Recovery	Average	SD	% RSD
		Actual	Calculated				
I (1 ml)	55853		0.4865	103.5161			
	54901	0.47	0.4786	101.8197	102.2765	1.0858	1.0617
	54718		0.4770	101.4937			
	49944		0.4370	101.6369			
	48806	0.43	0.4275	99.4205	100.5566	1.1093	1.1031
	49418		0.4326	100.6124			
	55853		0.4865	101.3595			
	54901	0.48	0.4786	99.6985	100.1457	1.0632	1.0617
	54718		0.4770	99.3792			
II (5 ml)	286431		2.4176	102.8759			
	281778	2.35	2.3786	101.2177	102.5916	1.2562	1.2244
	288691		2.4365	103.6813			
	256431		2.1663	100.7599			
	250729	2.15	2.1186	98.5388	99.5700	1.1190	1.1238
	252969		2.1373	99.4114			
	289452		2.4429	101.7868			
	290502	2.40	2.4517	102.1532	101.9844	0.1849	0.1813
	290100		2.4483	102.0130			
III (10 ml)	574767		4.8324	102.8161			
	579678	4.70	4.8735	103.6912	102.7731	0.9403	0.9150
	569132		4.7852	101.8120			
	526557		4.4286	102.9908			
	526800	4.30	4.4306	103.0381	103.1135	0.1732	0.1679
	528204		4.4424	103.3116			
	580927		4.8839	101.7489			
	587484	4.80	4.9389	102.8929	102.5274	0.6746	0.6580
	587756		4.9411	102.9404			

3. Precision

The precision of an analytical method is the degree of agreement among individual test results when the procedure is applied repeatedly to multiple samplings of homogenous sample. The percentage of coefficient of variation (%CV) or relative standard deviation (%RSD) values of peak area of standard solutions both within run

and between run less than 2.00% which indicates that HPLC methods can be used to determine the amount of rifampicin over period of time studied.

Table 32 Precision data of rifampicin in dissolution condition

Concentration	Number	Day			Average (SD)	%RSD
		1	2	3		
1	1	65067	68321	65876	66879.7 (1940.42)	2.9013
	2	65291	69944	69381		
	3	64672	68806	68886		
	4	65621	69418	67772		
	5	65494	67645	64898		
	6	64800	67648	64294		
	Average	65157.5	68630.33	66851.2		
	SD	378.8386	938.9936	2130.42		
	RSD	0.58142	1.36819	3.18681		
2	1	207947	200310	239452	213549 (18987.85)	8.8915
	2	207170	197729	240502		
	3	205228	192969	240100		
	4	203639	199813	239495		
	5	199238	197835	237389		
	6	199701	197310	238059		
	Average	203820.5	197661	239166		
	SD	3694.069	2600.818	1202.54		
	RSD	1.812413	1.315797	0.5028		
3	1	435140	395954	420927	422554 (20974.65)	4.9637
	2	444659	403202	425693		
	3	441908	394696	437484		
	4	444593	393189	426974		
	5	442254	391566	437756		
	6	443342	393142	433488		
	Average	441982.7	395291.5	430387		
	SD	3541.911	4154.269	6891.44		
	RSD	0.801369	1.050938	1.60122		

Within run precision

The within run precision was determined by analyzing the standard solution at 100% of the three test concentrations (0.4, 2 and 4 µg/ml). Repeatability was assessed using a minimum of six determinations. The percentage of relative standard deviation (%RSD) value of peak area of rifampicin was determined.

Between run precision

The between run precision was determined by analyzing the standard solution at 100% of the same three test concentrations which prepared and injected on different days. The percentage of relative standard deviation (%RSD) value of peak area of rifampicin was determined.

Data of within run precision and between run precision of rifampicin analyzed by HPLC method are shown in table 32. The percentage of coefficient of variation (%CV) values of peak area both within run and between run were low (<2.00 % and < 15%, respectively) which indicated that HPLC methods could determine the amount of the drugs over period of time studied.

4. Linearity

The linearity of an analytical method is the ability to obtain test results that are directly proportional to the concentration of drugs in samples within a given range. A general linearity acceptance criterion is that the correlation coefficient (r) of the linear regression is not less than 0.9999. Triplicate of each concentration of standard solutions in various concentrations range from 0.04 to 8 $\mu\text{g/ml}$ were analyzed. The linear regression analysis of the area under curve versus the concentrations was calculated.

Figure 51 shows the relationship between peak area and drug concentrations is linear ($R^2 = 1.0000$). This result indicated that HPLC method was acceptable for quantitative analysis of nicotine drug in the range studied.

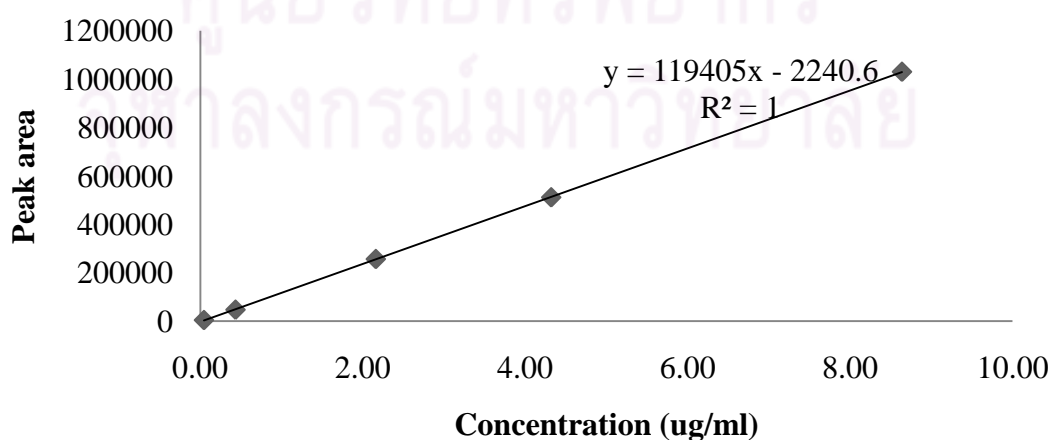


Figure 51 Calibration curve for dissolution condition

APPENDIX C

The description of spray drying parameters (BÜCHI Labortechnik AG)

1. Inlet drying temperature

Inlet drying temperature is the temperature of the heated drying air which is sucked or blown in over a heated by the aspirator. The heated air temperature is measured prior to flowing into the drying chamber. The solvent is removed by vaporization when spray drying a solution, emulsion or dispersion.

The temperature of the air flow does not have to be higher than the boiling point of water to evaporate the individual drops during the short residence time. The gradient between wet surface and not saturated gas leads to an evaporation at low temperatures. The final product is separated and has no further thermal load.

2. Aspirator

The drying air is sucked or blown through the device by the aspirator motor creating under pressure conditions. By the regular speed, the amount of heated drying air can be increased or decreased. If the system is running in the sucking mode, a slight underpressure will take effect in the spray dryer. Because the amount of energy available for vaporization changes when the amount of drying air is increased or decreased, the aspirator speed setting has a significant effect on the drying performance of the device.

The optimum setting must be determined experimentally using the flowing guidelines: high aspirator speed will increase degree of separation in the cyclone in the other hand low aspirator speed will decrease degree of separation.

3. Pump performance

The peristaltic pump feeds the spray solution to the nozzle. The pump rate directly corresponds to the inlet mass. The higher the throughput of solution, the more energy is needed to evaporate the droplet to particles. The limitation of the pump is when the particles are not dry enough resulting in sticky product or wet walls in the cylinder. The pump throughput is also dependent upon various factors such as the viscosity of the spray solution and tubing diameter. The following guidelines can be

derived from the facts described above as they relate to the pump rate: reducing the pump rate while holding the inlet temperature and aspirator flow rate constant increases the dry content of the final product.

4. Spray flow

The spray flow rate is the amount of compressed air needed to disperse the solution, emulsion or suspension. A gas other than compressed air can be used. The spray flow rate can be set to between 300 and 800 l/h on the device. A rotameter indicated the spray flow throughput. The table 33 gives a correlation of the flow meter and the gas throughput. The particle size of the final product can be influenced by the spray flow setting. The guidelines of spray flow setting are following: the higher the spray flow rate, the smaller the size of the particles in the final product.

Table 33 The correlation of the flow meter and the gas throughput

Height of flow meter (mm)	Gas throughput (Normlitre/hour)
5	84
10	138
15	192
20	246
25	301
30	357
35	414
40	473
45	536
50	601
55	670
60	742
65	819

APPENDIX D

The description of Desirability function, Weight and Importance

(Stat-Ease, 2006)

1. Desirability function

Desirability function is an objective function, $D(X)$, that ranges from zero to one. It reflects the desirable ranges for each response (d_i). The simultaneous objective function is a geometric mean of all transformed responses:

$$D = (d_1 \times d_2 \times \dots \times d_n)^{\frac{1}{n}} = (\prod_{i=1}^n d_i)^{\frac{1}{n}} \quad (16)$$

where n is the number of responses in the design. If any of the responses or factors fall outside their desirability range, the overall function becomes zero.

For simultaneous optimization, each response must have a low and high value assigned to each goal. On Design-Expert®, the goal field for responses must be one of five choices: none, maximum, minimum, target or in range. Factors will always be included in the optimization, at their design range, or as a maximum, minimum of target goal.

The meanings of the goal parameters are following:

Maximum

$d_i = 0$ if response less than low value

$0 \leq d_i \leq 1$ as response varies from low to high

$d_i = 1$ if response more than high values

Minimum

$d_i = 1$ if response less than low value

$0 \geq d_i \geq 1$ as response varies from low to high

$d_i = 0$ if response more than high values

Target

$d_i = 0$ if response less than low value

$0 \leq d_i \leq 1$ as response varies from low to target

$1 \geq d_i \geq 0$ as response varies from target to high

$d_i = 0$ if response more than high values

Range

$d_i = 0$ if response less than low value

$d_i = 1$ as response varies from low to high

$d_i = 0$ if response more than high values

The d_i for “in range” are included in the product of the desirability function “ D ”, but are not counted in determining “ n ”:

$$D = (\prod d_i)^{\frac{1}{n}} \quad (17)$$

If the goal is none, the response will not be used for the optimization.

The numerical optimization finds a point that maximizes the desirability function. The characteristics of a goal may be altered by adjusting the weight or importance. For several responses and factors, all goals get combined into one desirability function.

2. Weigh

The shape of the desirability of each goal can change by changing the weight field. Weights are used to give added emphasis to the upper/lower bounds, or to emphasize the target value. With a weight of 1, the d_i will vary from 0 to 1 in a linear fashion. Weights greater than 1 (maximum weight is 10), give more emphasis to the goal. Weights less than 1 (minimum weight is 0.1), give less emphasis to the goal. The formulas and outcomes for various options can be seen in figure 52 – 55.

The weight criterion is bounded by the limits 0.1 to 10.0. The default value (from Design-Expert®) of 1.0 produces a desirability that ramps in a linear fashion from the area of zero desirability to the area where desirability equals one.

Values less than one put less emphasis on getting to the goal and values greater than one put more emphasis on achieving the exact goal.

For goal of maximum, the desirability will be defined by the following formulas:

$$\begin{aligned}
 d_i &= 0, & Y_i &\leq \text{Low}_i \\
 d_i &= \left[\frac{Y_i - \text{Low}_i}{\text{High}_i - \text{Low}_i} \right]^{wt_i}, & \text{Low}_i &< Y_i < \text{High}_i \\
 d_i &= 1, & Y_i &\geq \text{High}_i
 \end{aligned}$$

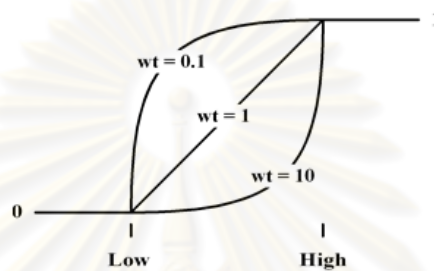


Figure 52 Formulas and desirability curves for goal is maximum

For goal of minimum, the desirability will be defined by the following formulas:

$$\begin{aligned}
 d_i &= 1, & Y_i &\leq \text{Low}_i \\
 d_i &= \left[\frac{\text{High}_i - Y_i}{\text{High}_i - \text{Low}_i} \right]^{wt_i}, & \text{Low}_i &< Y_i < \text{High}_i \\
 d_i &= 0, & Y_i &\geq \text{High}_i
 \end{aligned}$$

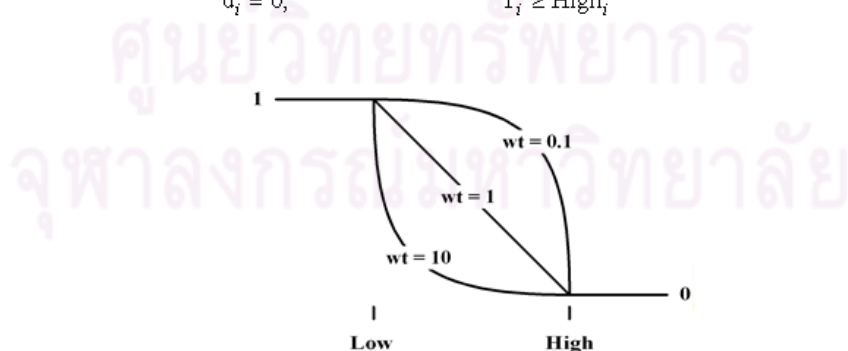


Figure 53 Formulas and desirability curves for goal is minimum

For goal as a target, the desirability will be defined by the following formulas:

$$\begin{aligned}
 d_i &= 0, & Y_i &\leq \text{Low}_i \\
 d_i &= \left[\frac{Y_i - \text{Low}_i}{T_i - \text{Low}_i} \right]^{wt_1}, & \text{Low}_i &< Y_i < T_i \\
 d_i &= 1, & Y_i &= T_i \\
 d_i &= \left[\frac{\text{High}_i - Y_i}{\text{High}_i - T_i} \right]^{wt_2}, & T_i &< Y_i < \text{High}_i \\
 d_i &= 0, & Y_i &\geq \text{High}_i
 \end{aligned}$$

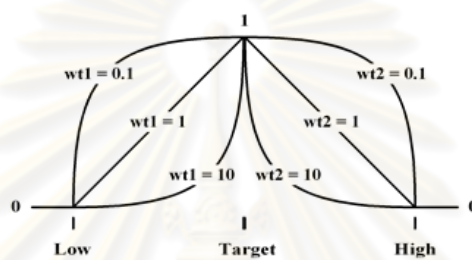


Figure 54 Formulas and desirability curves for goal is target

For goal within range (a constraint), the desirability will be defined by the following formulas:

$$\begin{aligned}
 d_i &= 0, & Y_i &\leq \text{Low}_i \\
 d_i &= 1, & \text{Low}_i &< Y_i < \text{High}_i \\
 d_i &= 0, & Y_i &\geq \text{High}_i
 \end{aligned}$$

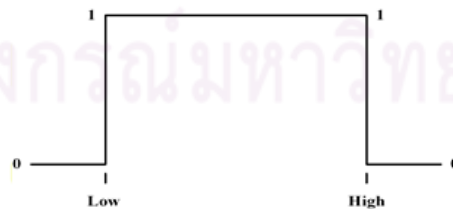


Figure 55 Formulas and desirability curves for goal as range

3. Importance

In desirability objective function $D(X)$, each response can be assigned as importance relative to the other responses. Importance (r_i) varies from the least important (+) a value of 1, to most important (+++++) a value of 5. If varying degrees of importance are assigned to the different responses, the objective function is:

$$D = (d_1^{r_1} \times d_2^{r_2} \times \dots \times d_n^{r_n})^{\frac{1}{\sum r_i}} = (\prod_{i=1}^n d_i^{r_i})^{\frac{1}{\sum r_i}} \quad (18)$$

where n is the number of responses in the measure. If all the importance values are the same, the simultaneous objective function reduces to the normal form for desirability.



คุรุวิทยาลัย
จุฬาลงกรณ์มหาวิทยาลัย

BIOGRAPHY

Miss Phennapha Saokham was born on May 24th, 1983. She received her bachelor of Pharmacy degree in 2005 from Faculty of Pharmacy, Chiangmai University, Chiangmai, Thailand. After graduation, she intended to study the Master's degree program in industrial pharmacy at Chulalongkorn University.

During her study at Chulalongkorn University, she had a presentation and publication on the topic of “The effect of process variables on the physical properties of spray dried poly(d,l-lactide-co-glycolide) (PLGA) microparticles loaded with rifampicin for inhalation” at The 36th Congress on Science and Technology of Thailand (STT 36), Bangkok International Trade & exhibition Center (BITEC) on October 26th – 28th, 2010.



ศูนย์วิทยทรัพยากร
จุฬาลงกรณ์มหาวิทยาลัย